

The University of Southern Queensland



***DEVELOPMENT OF AUTOMATED TURF
TESTING EQUIPMENT FOR PLAYING
SURFACES.***

A Dissertation submitted by

Leslie Charles Zeller

A.D.Eng (DDIAE)

B.App.Sc (CQU)

For the award

Master of Engineering

December 2008

Abstract

Research has shown that a significant percentage of sporting injuries can be attributed to the sporting surface. The most serious of these injuries require surgery, for example, to correct knee ligament damage, a condition which involves expensive procedures and lengthy post-operative rehabilitation. The responsibility for meeting the costs of these injuries is not restricted to the player or the team; there is an unnecessary burden on society in terms of overtaxing an already encumbered health system.

A correlation between knee injuries and the traction properties of the sporting surface has been identified by Dr John Orchard, a recognised expert in Australia for sporting injuries. Turf traction referred to in this thesis is a term relating to the shoe and sporting surface interface and reflects the maximum amount of torque a studded sporting shoe can impart on the surface before the integrity of the surface is compromised. Current equipment to measure turf traction properties has limited accuracy and repeatability. This thesis reports the development of a device which measures turf traction with improved accuracy, repeatability and operator safety in comparison with existing commercially-available equipment.

The design described in this thesis comprises a rotating ground-engaging 'foot' driven by a DC motor to provide the required torque for traction measurement, and this torque is continuously monitored using a load cell via an idler sprocket in the drive train. A digital load indicator displays and transmits torque data, and a programmable controller automates the test sequence. A permanently-installed laptop computer analyses, displays and records the traction data. The mechanical design includes a chassis which provides convenient movement across a playing surface and also convenient transport between sporting surfaces.

The design automates only those measurement processes that require a high degree of accuracy and repeatability. Non-critical actions are operated manually to maximise simplicity and minimise development costs. Commercially available technology is used wherever possible within the design to eliminate specialist maintenance skills or knowledge. Software was developed to analyse, display and record the traction data and produce a traction profile which is unique for this type of equipment. A full patent has been granted on the device (encompassing function, design and performance) to facilitate commercial development by the Queensland Department of Primary Industries and Fisheries.

An evaluation of the accuracy and repeatability of this machine is described and several experiments were undertaken to analyse its ability to compare and differentiate turf species from the traction results. For torque measurements within the expected operating range of 50 to 100 Nm a maximum error of $\pm 1.28\%$ has been established.

It is demonstrated that the device meets the design objectives of accuracy, repeatability and operational safety. It has been used within a national Horticulture Australia project to determine best practices for sustainable and safe playing surface of Australian Football League sports fields.

Certification of Dissertation

I certify that the ideas, designs and experimental work, results, analyses and conclusions set out in this dissertation are entirely my own effort, except where otherwise indicated and acknowledged.

I further certify that the work is original and has not been previously submitted for assessment in any other course or institution, except where specifically stated.

Leslie Charles Zeller

Student Number: 0012000951

Signature of Candidate Date

ENDORSEMENT

Signature of Supervisor/s Date

Acknowledgments

I would like to thank the turf research group of the DPI&F for providing the funding, in particular Dr Don Loch, Matt Roche and Larry Cooper for providing background information and data. I would also like to acknowledge Toowoomba DPI&F staff, Greg McLean, for his assistance in developing the software for data capture and analysis, Troy Jensen for his assistance with ArcView software, Erin Gallagher for her assistance with Surfer[®] software and John McAlpine for their assistance providing engineering and workshop support. Thanks also to my wife Vicki for her patience and encouragement and my sons Karl and Mark for their support during the process of completing this dissertation.

The guidance and assistance of my supervisors, Nigel Hancock and Selvan Pather, is much appreciated.

Les Zeller
December 2008

TABLE OF CONTENTS

1.INTRODUCTION.....	1
1.1 INTRODUCTION.....	1
1.2 AIMS OF THE PROJECT / OBJECTIVES	2
1.3 METHODOLOGY	3
1.4 THESIS OVERVIEW	3
1.5 PUBLICATIONS	5
2. BACKGROUND	6
2.1 INTRODUCTION.....	6
2.2 SURFACE PROPERTIES	6
2.2.1 <i>Ball Rebound Resilience</i>	6
2.2.2 <i>Rolling resistance</i>	8
2.2.3 <i>Hardness</i>	9
2.2.4 <i>Friction</i>	11
2.2.5 <i>Traction</i>	11
2.3 TURF BOTANICAL STRUCTURE	13
2.4 ANATOMY OF THE HUMAN KNEE	15
2.5 RECENT TURF AND INJURY RESEARCH.....	19
2.6 CONCLUSION	20
3. EQUIPMENT REVIEW	21
3.1 INTRODUCTION.....	21
3.2 CURRENT STANDARDS FOR TRACTION MEASUREMENT	21
3.3 CURRENT TRACTION MEASUREMENT EQUIPMENT	21
3.3.1 <i>Canaway Device</i>	22
3.3.2 <i>Review of Canaway Device</i>	23
3.3.3 <i>McNitt Device</i>	25
3.3.4 <i>Review of McNitt Device</i>	25
3.4 PATENT SEARCH RESULTS.....	30
3.5 CONCLUSION.....	32
4. CONCEPT DESIGN.....	34
4.1 INTRODUCTION.....	34
4.2 SYSTEM FUNCTIONALITY	34
4.2.1 <i>Portability</i>	34
4.2.2 <i>Traction measurement</i>	35
4.2.3 <i>Data acquisition/analysis</i>	35
4.3 SYSTEM SPECIFICATIONS	36
4.4 SYSTEM OPERATIONAL CONSIDERATIONS	37
4.4.1 <i>Manual option</i>	37
4.4.2 <i>Semi-automated option</i>	37
4.4.3 <i>Fully automated option</i>	38
4.5 SYSTEM DESIGN REQUIREMENTS	38
4.5.1 <i>Portability and transport options</i>	38
4.5.2 <i>Application of shear force</i>	39
4.5.2.1 Options for applying the shear force	39
4.5.3 <i>Traction transducer</i>	40
4.5.3.1 Traction transducer options	41
4.5.4 <i>Measurement options for rotation</i>	44

4.5.5	<i>Instrumentation, data recording and analysis</i>	44
4.5.5.1	Instrumentation options	45
4.5.5.2	Data recording options.....	46
4.5.5.3	Data analysis options	46
4.6	DESIGN DECISIONS.....	46
4.6.1	<i>Portability selection</i>	47
4.6.2	<i>Type of traction measurement system, automatic versus manual</i>	47
4.6.3	<i>Transducer selection</i>	47
4.6.4	<i>Instrumentation selection</i>	48
4.6.5	<i>Data recording and analysis method selection</i>	49
5.	FINAL DESIGN AND PROTOTYPE DEVELOPMENT	50
5.1	INTRODUCTION.....	50
5.1.1	<i>Measurement Requirement</i>	50
5.2	MECHANICAL DESIGN.....	51
5.2.1	<i>Detachable ground engaging foot and weight system</i>	51
5.2.2	<i>Lifting mechanism</i>	53
5.2.3	<i>Frictionless drop</i>	57
5.2.4	<i>Traction Loading System</i>	61
5.2.5	<i>Trolley</i>	66
5.3	CONTROLLER AND INSTRUMENTATION	67
5.3.1	<i>Control system</i>	68
5.3.1.1	Alpha Controller	68
5.3.1.2	Control Sequence	69
5.3.1.3	Relay and Limit Switches.....	73
5.3.2	<i>Instrumentation</i>	73
5.4	DATA PROCESSING AND STORAGE	76
5.4.1	<i>File management</i>	76
5.4.2	<i>Serial port management</i>	78
5.4.3	<i>Data presentation and storage</i>	78
5.4.4	<i>Realtime data analysis</i>	79
5.5	CONCLUSION	80
6.	ERROR ANALYSIS AND CALIBRATION.....	82
6.1	INTRODUCTION.....	82
6.2	SOURCES OF ERRORS AND ERROR ANALYSIS PROCEDURES	82
6.3	LOAD CELL AND INSTRUMENTATION ERRORS.....	83
6.4	SYSTEMATIC ERRORS	84
6.5	CALIBRATION.....	85
6.6	CONCLUSION	89
7.	EVALUATION AND PERFORMANCE TESTING	90
7.1	INTRODUCTION.....	90
7.2	PERFORMANCE OBJECTIVES	90
7.3	EVALUATION WITH RESPECT TO DETECTING VARIATIONS IN TRACTION LEVELS (PERFORMANCE OBJECTIVE A).....	90
7.3.1	<i>Results</i>	91
7.3.2	<i>Discussion</i>	91
7.3.3	<i>Conclusion (Performance Objective A)</i>	93
7.4	EVALUATION WITH RESPECT TO DETECTING TURF VARIETIES (PERFORMANCE OBJECTIVE B).....	93
7.4.1	<i>Rationale</i>	93
7.4.2	<i>Method</i>	94
7.4.3	<i>Results</i>	95
7.4.4	<i>Discussion</i>	97

7.4.5	<i>Conclusion (Performance Objective B)</i>	97
7.5	EVALUATION WITH RESPECT TO MEASURING VARIABILITY WITHIN AND BETWEEN SPORTING FIELDS (PERFORMANCE OBJECTIVE C)	98
7.5.1	<i>Method</i>	98
7.5.2	<i>Results</i>	99
7.5.3	<i>Discussion</i>	104
7.5.4	CONCLUSION (PERFORMANCE OBJECTIVE C)	106
8.	CONCLUSION	107
8.1	PROJECT CONCLUSIONS	107
8.2	FURTHER WORK & ENHANCEMENTS.....	109
8.3	MECHANICAL OPTIMIZATION	109
8.4	INCORPORATED CALIBRATION FACILITY	110
8.5	SPATIAL MAPPING FACILITY	110
8.6	CONCLUSION	110
	REFERENCES:	111
	APPENDIX A	115
	APPENDIX B	119
	APPENDIX C	120
	APPENDIX D	121

LIST OF FIGURES

<i>Figure 2.1 Basic rolling resistance method using a stimpmeter.....</i>	<i>10</i>
<i>Figure 2.2 (a) Original Clegg Hammer (1976) with analogue meter to indicate hardness, (b) Current model of Clegg Hammer.....</i>	<i>10</i>
<i>Figure 2.3 Manual traction measuring device sold in Australia.....</i>	<i>12</i>
<i>Figure 2.4 Turf grass botanical structure</i>	<i>13</i>
<i>Figure 2.5 The knee showing the synovial joint (a) The synovial membrane and fluid (b) lateral view showing meniscus and patella</i>	<i>16</i>
<i>Figure 2.6 Ligaments of the knee.....</i>	<i>17</i>
<i>Figure 2.7 Failure points for high collagen and high elastin ligaments</i>	<i>18</i>
<i>Figure 3.1 Canaway traction measurement device.....</i>	<i>23</i>
<i>Figure 3.2 McNitt’s “Pennfoot” device for measuring traction.....</i>	<i>26</i>
<i>Figure 3.3 Pennfoot linear operation</i>	<i>26</i>
<i>Figure 3.4 Pennfoot rotational operation.....</i>	<i>27</i>
<i>Figure 3.5 Diagram showing plan view of strike plate and applied forces in mechanism illustrated in Figure 3.4 of McNitt device.....</i>	<i>27</i>
<i>Figure 3.6 Error evaluation of the McNitt device during rotation.</i>	<i>29</i>
<i>Figure 5.1 Areas of development of the automated turf traction tester.</i>	<i>50</i>
<i>Figure 5.2 Weights assembly</i>	<i>52</i>
<i>Figure 5.3 Ground engaging foot</i>	<i>52</i>
<i>Figure 5.4 Original lifting mechanism</i>	<i>54</i>
<i>Figure 5.5 Main drive shaft</i>	<i>54</i>
<i>Figure 5.6 Improved lifting mechanism.....</i>	<i>55</i>
<i>Figure 5.7 Roll pin guides and slots</i>	<i>55</i>
<i>Figure 5.8 Lifting operation using lever and parallelogram.</i>	<i>56</i>
<i>Figure 5.9 (a) Dog clutch operation – the outer cylinder rotating the main drive shaft with small lugs to initiate drop (b) Frictionless drop with no contact between outer cylinder and main drive shaft.....</i>	<i>58</i>
<i>Figure 5.10 Lug positions in dog clutch.....</i>	<i>59</i>
<i>Figure 5.11 Outer cylinder of dog clutch, main drive sprocket and bearing mount.....</i>	<i>60</i>
<i>Figure 5.12 Shaft upper position retaining roll pin</i>	<i>60</i>
<i>Figure 5.13 Drive sprockets and chains configuration.....</i>	<i>64</i>
<i>Figure 5.14 Drive sprockets and chains with scale.....</i>	<i>64</i>
<i>Figure 5.15 Motor chain tension adjustment set screw</i>	<i>65</i>
<i>Figure 5.16 Main sprocket chain tension adjustment and locking screw.....</i>	<i>65</i>
<i>Figure 5.17 Three wheeled trolley.....</i>	<i>67</i>
<i>Figure 5.18 Controller and Instrumentation.....</i>	<i>68</i>
<i>Figure 5.19 Controller hardware</i>	<i>69</i>
<i>Figure 5.20 Alpha program motor control flowchart</i>	<i>70</i>
<i>Figure 5.21 Visual Logic Software screen capture</i>	<i>71</i>
<i>Figure 5.22 Main drive Cam limit switch.....</i>	<i>72</i>
<i>Figure 5.23 Lift limit switch.....</i>	<i>72</i>
<i>Figure 5.24 Load Cell mounting and idler sprocket.....</i>	<i>74</i>
<i>Figure 5.25 Vector diagram for loading the loadcell</i>	<i>75</i>
<i>Figure 5.26 Data profiles of three turf species using Microsoft Excel.....</i>	<i>76</i>
<i>Figure 5.27 Main program window.....</i>	<i>77</i>
<i>Figure 5.28 Change serial interface parameters window.....</i>	<i>79</i>
<i>Figure 5.29 Automated Turf Traction Testing Machine</i>	<i>81</i>
<i>Figure 6.1 Vector diagram of forces showing angle variation of vectors at maximum load</i>	<i>86</i>

<i>Figure 6.2 Determination of angle change by measuring angle between tangents for change in idler sprocket position.</i>	<i>86</i>
<i>Figure 6.3 Calibration weight and loading arm</i>	<i>87</i>
<i>Figure 6.4 Calibration loading nut.....</i>	<i>88</i>
<i>Figure 6.5 Calibration loading arm attachment</i>	<i>88</i>
<i>Figure 7.1 Turf traction tests for 5 turf varieties.....</i>	<i>92</i>
<i>Figure 7.2 Maximum traction results for different turf varieties.....</i>	<i>92</i>
<i>Figure 7.3 Turf traction comparison of 3 turf varieties.</i>	<i>95</i>
<i>Figure 7.4 Boxplot showing comparason of 3 turf varieties.....</i>	<i>95</i>
<i>Figure 7.5 Turf traction results from Suncorp and ANZ Stadiums.....</i>	<i>100</i>
<i>Figure 7.6 Boxplot of data from ANZ and Suncorp Stadiums</i>	<i>100</i>
<i>Figure 7.7 Field traction variability of Suncorp Stadium.....</i>	<i>101</i>
<i>Figure 7.8 Maximum traction data from ANZ Stadium</i>	<i>102</i>
<i>Figure 7.9 Aerial images of northern end of ANZ Stadium</i>	<i>103</i>
<i>Figure 7.10 Effect of shade on traction at Suncorp Stadium.....</i>	<i>104</i>

LIST OF TABLES

<i>Table 3.1 Workplace Health and Safety Load Handling Recommendations.....</i>	<i>24</i>
<i>Table 7.1 GenStat® analysis of variance output for turf variety discrimination</i>	<i>96</i>
<i>Table 7.2 Summary of maximum traction data from Suncorp and ANZ.....</i>	<i>99</i>
<i>Table 7.3 Analysis of shading effect on traction from Suncorp Stadium.....</i>	<i>104</i>
<i>Table B1. Specifications for Load Cell.....</i>	<i>119</i>
<i>Table B2. Dimensions of Load Cell.....</i>	<i>119</i>
<i>Table C1. Specifications for Ranger 2100 Digital Indicator</i>	<i>120</i>

GLOSSARY

ACL	—	Anterior cruciate ligament
AFL	—	Australian Football League
AFLMOA		AFL Medical Officers' Association
ANOVA	—	Analysis of Variance
ASCII	—	American Standard Code for Information Interchange
ASTM	—	American Society for Testing and Materials
BSC	—	Bearing Service Centre
CRF	—	Coefficient of rolling friction
DPI&F	—	Department of Primary Industries and Fisheries
EEPROM	—	Electrically Erasable Programmable Read Only Memory
GPS	—	Global Positioning System
ISO	—	International Organization for Standardization
IV	—	Impact Value
MAT	—	Maximum Available Traction
MMH	—	Modern Material Handling
NIOSH	—	National Institute for Occupational Safety and Health
PC	—	Personal computer
PCB	—	Printed circuit board
PCL	—	Posterior cruciate ligament
PLC	—	Programmable Logic Controller
RAM	—	Random Access Memory
RS232	—	Recommended Standard 232
STRI	—	Sports Turf Research Institute
UEFA	—	Union of European Football Associations
USB	—	Universal Serial Bus

Chapter 1

INTRODUCTION

1.1 Introduction

Injuries are inevitable in all sporting activities as players push their bodies to the limit to achieve optimum results. These injuries may result from inadequate physical training or preparation, contact with other players/equipment or interaction between the player and the sporting surface. Australian Rules football injury data, collected by Dr John Orchard between 1997 and 2002, shows that 47% of the most notable injury categories can be attributed to the playing surface (Orchard, et al. 2002). Dr John Orchard is recognised in Australia as an expert on sports injuries having collected and published a number of papers and reports relating sports injuries to surface characteristics.

Knee anterior cruciate ligament (ACL) injuries are commonly occurring in all codes of football. Dr Orchard has shown in the Australian Football League (AFL) injury report 2002 (Orchard, 2003) that there is not a strong correlation between ground hardness and the incidence of ACL injuries but implies these injuries are more likely to be attributed to the amount of traction the surface provides. The ability to accurately measure traction would allow Dr Orchard's hypothesis to be tested by relating sports injuries directly to traction measurements.

There is a need to utilise and further develop instruments to measure ground conditions. Current instruments used to measure the traction of turf sporting surfaces have limited accuracy and repeatability which limit their usability for field or species comparison research. The greatest need is for a portable, readily available, inexpensive device that can measure a value for Maximum

Available Traction (MAT) on a given field at a given time (Dunn et al. 1994; McNitt, et al. 1997). This thesis describes the development of such a turf traction measuring device.

1.2 Aims of the Project / Objectives

The aim of this project was to develop a low cost turf traction measuring instrument to meet the following objectives.

Objective 1: Develop a device which measures the traction of turf surfaces with better accuracy than commercially available systems to a level of approximately $\pm 1\%$.

Objective 2: Develop a device which measures the traction of turf surfaces with high repeatability.

Objective 3: Develop a device which improves the operational safety for turf traction measurements.

The design of this device will allow:

- the comparison of turf varieties to assist in the selection of the most appropriate species for sporting fields in Queensland;
- benchmarking of existing elite and amenity sports fields with a view to establishing a standard;
- monitoring of sports fields for maintenance scheduling.

1.3 Methodology

The process involved in developing an automated turf traction tester includes the following steps:

- to review the equipment currently used to measure the traction of turf grasses and determine any limitations or deficiencies in their design;
- research possible transducers to measure traction and associated mechanisms required for automation of the data acquisition process;
- consider design options and determine an optimal design;
- construct a prototype;
- field test the prototype and evaluate its performance; and
- review results and propose improvements.

1.4 Thesis Overview

This thesis consists of the following chapters:

Chapter 2: Background – This chapter describes:

- the properties that characterise the playing quality of a sporting surface;
- the turf structure and how it relates to the playing surface;
- the mechanics and functionality of the knee and discusses injuries of the knee that relate to the interaction between the player and the sporting surface; and

- current research relating sporting surface and injuries.

Chapter 3: Equipment Review – This chapter discusses the limitations and deficiencies in the design or operation of equipment currently used to measure traction of natural turf sporting surfaces. A review of other devices that measure traction/friction/slip for other surfaces is also covered in this chapter.

Chapter 4: Concept Designs – A number of options to measure traction and possible methods to automate these measurements are proposed in this chapter.

Chapter 5: Final Design and Prototype Development – This chapter describes the equipment and materials used in the design and development of a prototype turf traction testing machine.

Chapter 6: Calibration and Error Analysis – This chapter describes the calibration procedure and analyses any errors evident in the prototype turf traction testing machine.

Chapter 7: Evaluation – This chapter describes the objectives, methodologies and results for the evaluation of the turf traction tester.

Chapter 8: Testing and Analysis of Results – A description of the testing procedure, calibration process and data validation is undertaken in this chapter. Also covered in this chapter is a discussion on how the results can be used in the maintenance and management of sporting fields.

Chapter 9: Conclusion and Further Work – This chapter provides an overview of the work that has been described in the foregoing chapters highlighting the important conclusions. It then discusses any future improvements which could be made to further develop this turf testing machine.

1.5 Publications

- Roche, M.B., Loch, D.S., Poulter, R.E. and Zeller, L.C. 2008. Measuring the traction profile on sportsfields: Equipment development and testing. *Acta Hort. (ISHS)* 783:399-414
http://www.actahort.org/books/783/783_42.htm
- Roche, M., Zeller, L. and Loch, D. (2006). Putting science behind traction measurement. *Australian Turfgrass Management* 8(5) 40-44.
- Zeller, L.C. (inventor) (2007) *An apparatus and method for measuring surface properties*. IP Australia Patent 2004270767, filed 11 September 2003; published 31 May 2007; expiry 10 September 2024.
- Zeller, L.C. (inventor) (2008) *An apparatus and method for measuring surface properties*. New Zealand Patent application 545705; accepted 11 July 2008.

BACKGROUND

2.1 Introduction

Almost 50% of Australian Football League (AFL) sporting injuries have been attributed to the playing surface (Orchard, et al. 2002). This chapter describes the playing surface properties which have been identified by Baker and Canaway as affecting the playing quality and player safety (Baker & Canaway 1993). The physical structure of turf grasses and the components that affect friction and traction are identified. The anatomy of the knee is examined and Anterior Cruciate Ligament (ACL) injuries are investigated as these proved to be the most severe AFL injury type for the period of 1997 to 2002 (Orchard, et al. 2002). Dr John Orchard's hypothesis is that there is a correlation between the traction the playing surface provides and the number of ACL injuries. Improving the measurement of traction will enable research to quantify safety limits for traction for Australian sporting surfaces.

2.2 Surface properties

The ideal amenity sports field is one which is hard wearing and requires low maintenance while maximising the player's enjoyment of the game and minimising the risk of injury. The physical properties of the playing surface that affect the player's enjoyment of the game are ball rebound resilience, rolling resistance, hardness, friction and traction (Baker & Canaway 1993). These properties are described in turn:

2.2.1 Ball Rebound Resilience

Ball rebound resilience is the ratio of ball bounce height to ball drop height. For example if a ball bounces to a height of two metres after being dropped

from a height of five metres the ball rebound resilience would be expressed as 0.4 or 40%.

Another commonly used parameter is Coefficient of Restitution (McCutchen, 2002). The coefficient of restitution is a measure of the elasticity of the collision between a ball and the surface. Elasticity is a measure of how much of the initial kinetic energy of two colliding objects remains as kinetic energy after a collision. For an inelastic collision, some kinetic energy is transformed into other forms of energy, for example, the production of heat and sound or is used in deforming the material, and therefore does not contribute to moving the object.

The coefficient of restitution is always in the range between zero and one. A totally elastic collision has a coefficient of restitution of 1. Two diamonds bouncing off each other is a good example of an elastic collision. Conversely a plastic collision is one where the objects do not bounce but stick together. Two lumps of clay colliding is an example of a plastic or inelastic collision.

The coefficient of restitution is the ratio of the differences in velocities of colliding objects before and after the collision.

$$c = \frac{v_{2a} - v_{1a}}{v_{1b} - v_{2b}} \quad (2.1)$$

where c = coefficient of restitution

v_{1b} = linear velocity of object 1 before impact

v_{2b} = linear velocity of object 2 before impact (will be negative if opposite direction to object 1)

v_{1a} = linear velocity of object 1 after impact

v_{2a} = linear velocity of object 2 after impact

A ball of mass m dropped from a height h will reach the ground with kinetic energy equal to the potential energy which is determined by the drop height, i.e.

$$\frac{mv^2}{2} = mgh \quad (2.2)$$

where \mathbf{g} is acceleration due to gravity.

Therefore

$$v = \sqrt{2gh}$$

The velocity after rebounding v_1 due to the coefficient of restitution c is

$$v_1 = cv = c\sqrt{2gh}$$

and the ball will reach a rebound height h_1 of

$$h_1 = \frac{v_1^2}{2g} = \frac{c^2(2gh)}{2g} = c^2h \quad (2.3)$$

resulting in the equation

$$c = \sqrt{\frac{h_1}{h}} \quad (2.4)$$

Therefore: ***ball rebound resilience = (coefficient of restitution)²***

2.2.2 Rolling resistance

Rolling resistance relates to the speed of the surface. It can be considered as a force, opposing and retarding the rolling motion and acting in the direction opposite to travel. The methods for measuring rolling resistance include:

- releasing a ball down a 20° incline from a standard height and measuring the total distance the ball rolls. A resulting turf speed is calculated by averaging at least six distance readings, three in each direction. The incline method uses a device called a stimpeter. Figure 2.1 shows this method for determining the rolling resistance for a turf surface on a golf green.; and

- a technique for bowls (Bell & Holmes 1988) by releasing an unbiased bowl from a height of 0.5m down a standard incline of 30° and measuring the distance travelled, D and the time taken for the bowl to stop, T and calculating a green speed by:

$$\text{Greenspeed} = \sqrt{\frac{27.4}{D/T^2}} \quad (2.5)$$

where Greenspeed is the value representing the rolling resistance,
 D is the distance the bowl travels, and
 T is the time taken for the bowl to come to rest.

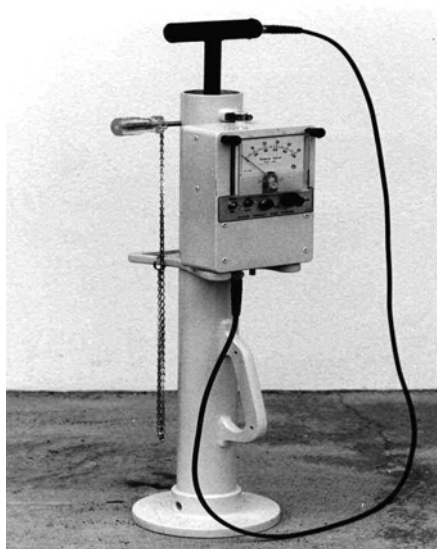
2.2.3 Hardness

The hardness relates to the interaction between a player and the surface e.g. running, falling and injury potential. Players perceive that the surface has two physical properties, stiffness and resilience. Stiffness is the ratio of the applied force to the amount of deflection and resilience is the proportion of energy returned to the player compared to the amount of energy applied to the surface.

An instrument commonly used to measure ground hardness is a Clegg Hammer. This device consists of a compaction hammer operating within a vertical guide tube. When the hammer is released from a fixed height it falls through the tube and strikes the surface under test, decelerating at a rate determined by the stiffness of the material within the region of impact. A precision accelerometer mounted on the hammer feeds its output to a hand held digital readout unit which registers the deceleration in units of Impact Value (IV). Figure 2.2 shows the original device and the current commercially available Clegg Hammer.



Figure 2.1 Basic rolling resistance method using a stimpmeter
(from <http://turf.uark.edu/research/overview.html>, accession date 24/02/2008)



(a)



(b)

Figure 2.2 (a) Original Clegg Hammer (1976) with analogue meter to indicate hardness, (b) Current model of Clegg Hammer.
(images from <http://www.clegg.com.au/photos.asp>, accession date 11/02/2008)

2.2.4 Friction

Friction and traction are the surface properties that reflect the player's ability to perform running and cutting manoeuvres without excessive slipping or falling (Baker & Canaway 1993). Friction applies to the interaction between smooth-soled footwear and the turf surface. The friction is a measure of the resistance the surface provides where the physical structure of the turf does not fail. The friction is defined as

$$F = \mu N \quad (2.6)$$

where μ is the coefficient of friction, and

N is the normal force (the force applied at 90° to the frictional force).

Friction can be determined by measuring the force required to slide an object with a standard surface property and of a known mass across a horizontal surface. To eliminate the effect of the turf leaf structure and the fact that the surface may not be exactly horizontal readings should be taken in opposing directions and averaged.

2.2.5 Traction

Traction is similar to friction in that it indicates the resistance the surface provides through the shoe and surface interface, but represents the maximum shear strength of a combination of turf thatch, root system and soil. Traction also differs from friction in that the footwear has studs, cleats or spikes to provide extra grip. The studs penetrate the surface and use the structural strength of the surface to increase the resistive forces. Traction is dependent on the depth of penetration of the stud or cleat and is a measurement of the maximum torque before the turf structure fails. Traction is expressed by a maximum torque value and also differs from friction as it relates to the turfs structural characteristics rather than the turf leaf characteristics.



**Figure 2.3 Manual traction measuring device sold in Australia
(Henderson et al. 2004)**

Current commercially available equipment to measure traction uses the Canaway model (section 3.3.1) but uses a standard torque wrench (see Figure 2.3). Therefore the maximum torque must exceed the torque wrench setting before a reading can be recorded. This proves to be an inefficient method of measuring traction because:

- if the torque wrench setting is not reached during a test will only indicate that the traction was less than the setting; and
- if the torque wrench setting is reached during a test will only indicate that the traction was greater than the setting.

Therefore a number of tests must be made before a value of traction can be determined.

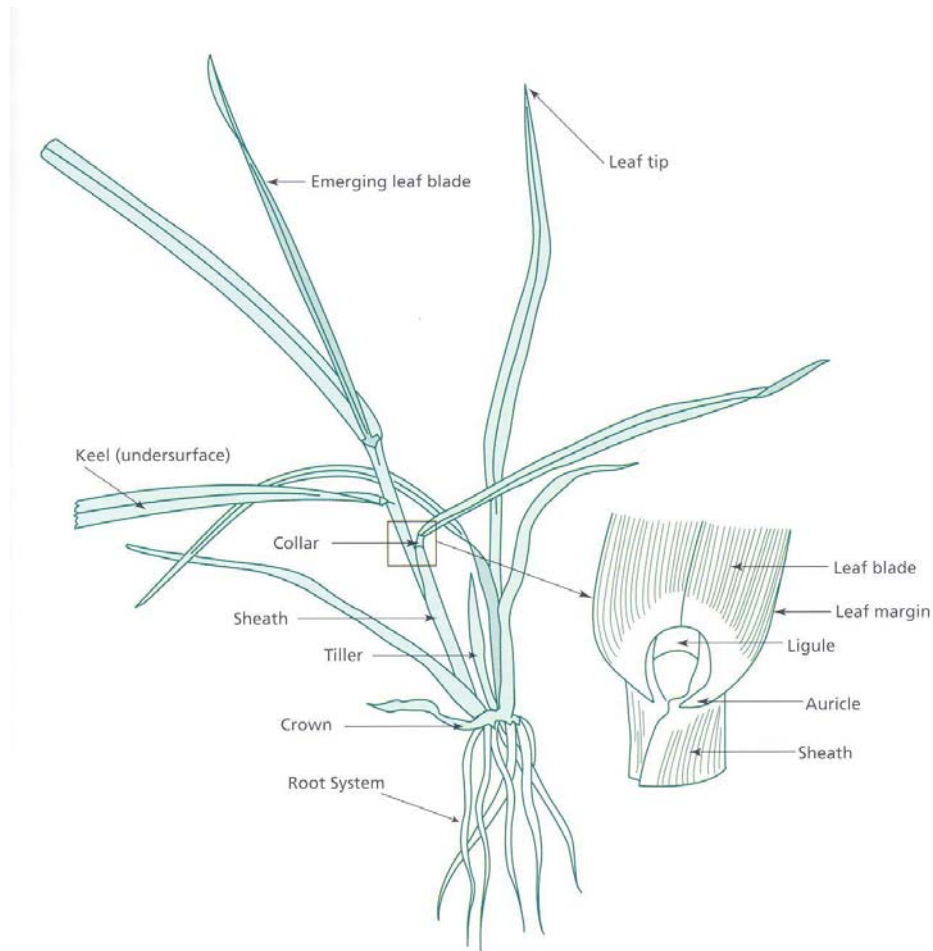


**Figure 2.4 Turf grass botanical structure
(reproduced from: Aldous & Chivers, 2002)**

2.3 Turf Botanical Structure

The turf plant consists of components shown in Figure 2.4 i.e. the below ground root system and above ground components growing from the crown, namely, the tiller, sheath, collar and leaf.

The turf provides a barrier between the player and the soil material. Not only does it form a cushioning layer, it also minimises dust and provides a reasonably homogeneous playing surface.

The components of the turf grass that affect ball rebound resilience, hardness and rolling resistance are a combination of the above-ground and below-ground structures as well as ground moisture.

The parts of the turf grass plant relevant to a sporting surface friction are the above-ground components, which are the leaf matter, sheath, collar, crown & tiller. As there are a number of components that make up the surface contact area and assuming the normal force to be evenly distributed over the sole of the shoe, the friction will be most affected by the component of the turf with the predominant surface contact with the sole of the shoe. Therefore we can assume in most cases the friction will depend largely on the physical attributes of the leaf blade.

Traction on the other hand is reliant on the shape and length of studs or cleats and their interaction with the sporting surface. As this is a combination of above and below ground structures, for example, the root system, its connection with the soil and the soil shear strength have a large affect on the available traction of the surface.

Traction is highly positively correlated with grass root density and a number of surface characteristics such as ground hardness, grass type and density, and negatively correlated with soil moisture content (Holmes & Bell 1986; McNitt, et al. 1997; Orchard, 2002). Surface hardness is mainly controlled by moisture content (Baker, 1991). Softening the surface by altering irrigation management practices may reduce hardness, traction and ACL injury incidence (Orchard, et al. 1999; Orchard & Finch 2002). Watering tends to slow down ball roll, however, for low angle impacts watering can cause the ball to skid, giving the impression of a faster playing surface. Watering also tends to reduce ball rebound (Holmes & Bell 1986).

Grass type, density and root density do not vary greatly from game to game (Baker, 1991). Warm season, stoloniferous grasses such as couch grass (*Cynodon dactylon*) have been the predominantly used grasses on northern Australian sports turf fields. They provide higher surface traction than tufted

grasses like cool-season, perennial ryegrass (*Lolium perenne*). Using these perennial ryegrasses may play a significant role in reducing ACL injuries in AFL (Orchard, et al. 1999). Couch grasses are already over sown with perennial ryegrass on all premier and affluent non-premier AFL sportsgrounds.

Reducing the height of mowing cut (Mooney & Baker 2000) and removing verdure (Rogers & Waddington 1989) can significantly affect traction and may be a means of altering traction properties from week to week. All of the playing surface properties are affected by cutting height as the larger the amount of biomass the softer the surface but the stud penetration depth into the turf root system may be reduced. Cutting height, rolling and watering are management operations used to modify the playing surface.

2.4 Anatomy of the human knee

The knee is a large synovial joint with three articulations. The term synovial describes the joint as being lubricated by a viscous fluid. A synovial joint (Figure 2.5) exists where the bone ends are covered with cartilage that is lubricated and nourished by synovial fluid. Synovial joints have an outer layer composed of strong, fibrous (collagen) tissue that looks like a sleeve. This sleeve is comprised of ligaments (Figure 2.6) that provide the primary stability of the joint.

The synovial fluid is produced by the synovium on the inner lining of the sleeve. Some synovial joints have a washer-like structure between bone ends called the meniscus. Its purpose is to absorb shock, to stabilize the joint, and to spread synovial fluid.

The junction between the femur and the tibia (tibiofemoral joint) form two condylar articulations while the patella and femur (patellofemoral joint) form the third.

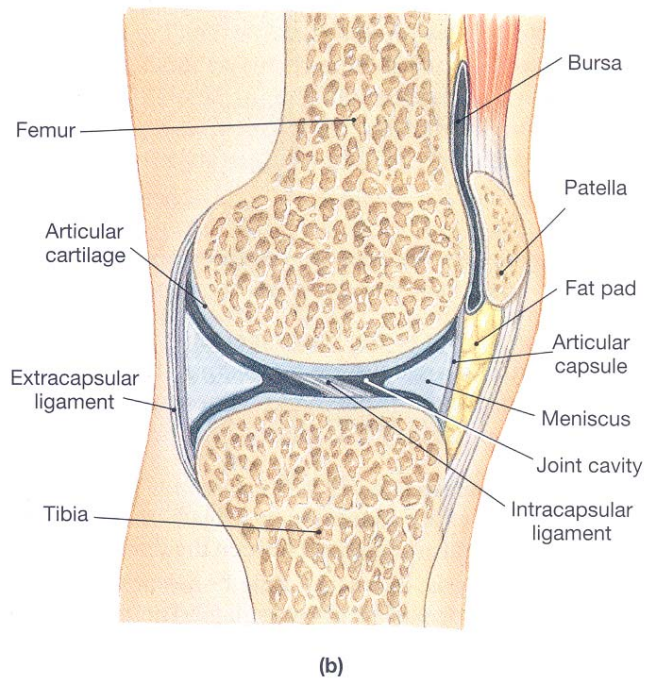
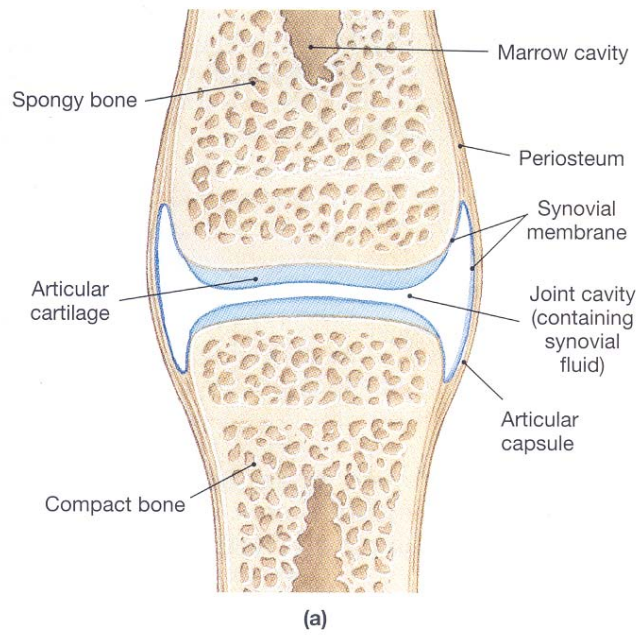
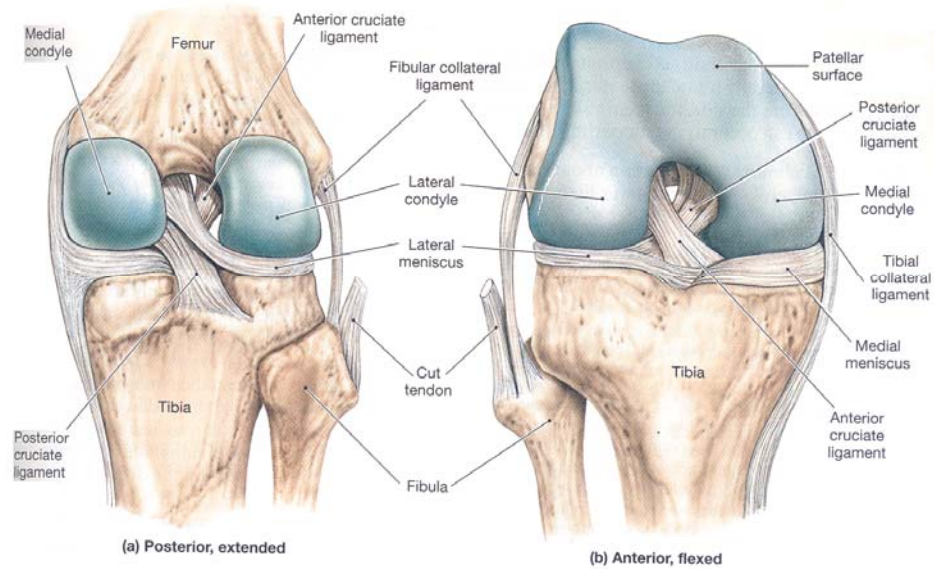


Figure 2.5 The knee showing the synovial joint (a) The synovial membrane and fluid (b) lateral view showing meniscus and patella (reproduced from Martini, 1989).



**Figure 2.6 Ligaments of the knee
(reproduced from Martini, 1989).**

The femur is the large bone between the hip and the knee, the tibia is the larger of two bones between the knee and ankle and the patella is commonly referred to as the knee cap.

The knee functions predominantly as a hinge joint with some lateral and rotational motions allowed. The many ligaments of the knee allow movement and provide stability (Figure 2.6).

The ACL injuries are a common and severe sporting injury in all codes of football. The anterior and posterior cruciate ligaments (Figure 2.6) limit the forward and backward sliding of the femur on the tibia plateaus during knee flexion and extension. These ligaments also limit knee hyperextension.

Figure 2.7 shows the stress/strain comparison of ligaments with high collagen eg. cruciate ligaments as compared to ligaments with high elastin. This demonstrates that the cruciate ligaments provide stability through minimal

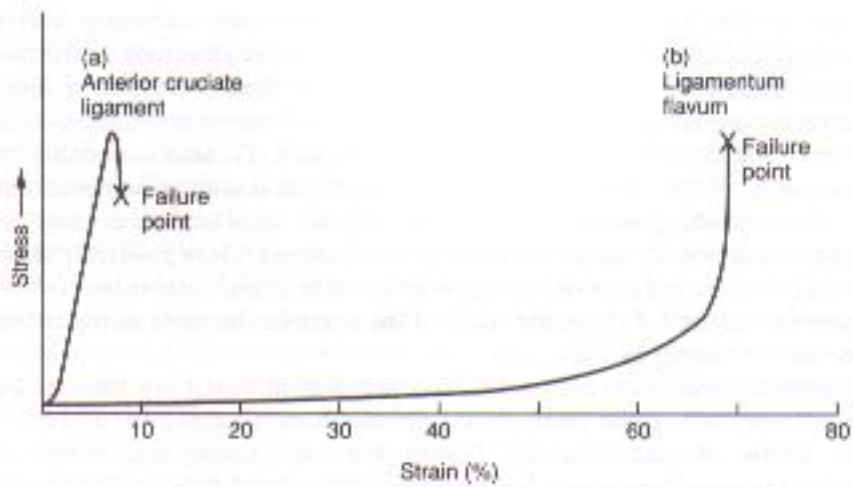


Figure 2.7 Failure points for high collagen and high elastin ligaments (reproduced from Low & Reed 1996).

elongation under high stress situations. The collagen tissue is elastic for 3-4% of its elongation with final rupture occurring at 7-8%.

With regard to injuries of the cruciate ligaments, forces sustained from the anterior direction (front) strain or rupture the posterior cruciate ligament (PCL) and conversely forces directed from the posterior of the knee damage the ACL. However injuries to the cruciate ligaments most often occur as a result from a combination of forces. For the ACL, the most dangerous loading situation will occur when the knee is fully extended, weight bearing and an anteriorly directed tibial force is combined with an internal tibial torque. This could occur after the player's body is travelling forward through the air and lands while he or she is trying to change direction. Where traction values are high and limited energy absorption by the sporting surface, large forces are transferred to the knee joint resulting in an increased risk of ligament injuries.

2.5 Recent Turf and Injury Research

There has been much research conducted on the type, frequency and severity of sporting injuries for various sporting activities. Numerous studies have been conducted and publications produced about injury data by Dr John Orchard relating to Australian Rules football. The Queensland Department of Primary Industries and Fisheries has a turf research group based at Redlands Research Station. Their research has evolved from pasture research to turf grasses for amenity horticulture and initially involved a comparative study of turf varieties developed in the past decade. The emphasis of this research was to test varieties which had not been tested previously under Queensland's climatic conditions.

A research project funded by Horticulture Australia (TU02007), and AFL Queensland was initiated to review and monitor non-elite sporting fields and to establish standard criteria for sporting surfaces that minimize the players' risk of injury due to player-surface interactions while providing a surface that enhances the quality of the game. This research involves quantifying the characteristics of sporting playing surfaces.

The importance of traction to the ongoing playability of non-elite fields is of high priority because high-traction, warm season grasses are used on non-elite AFL fields. These grounds are frequently relatively hard which also increases their inherent traction and the risk of injury. In Australian conditions, on natural/landfill construction fields, it would be rare to encounter too little traction and therefore the priority is to establish upper field traction limits and ensure values are within them.

There is evidence to show that certain injuries are directly related to the quality of the playing surface, for example, up to 24% of soccer injuries correlate directly with the playing surface (DPI 2004; Ekstrand 1982; Nigg &

Yeadon 1987). A major problem with elite football players returning from injury is that their fitness is tested playing in reserve or minor grade matches. These matches are generally played on amenity sports fields that are not of the high standard of elite fields. A concern of AFL Queensland is that playing on the lesser quality fields may be detrimental to the player's recovery. Players returning from ACL injury, for example, are 10-times more likely of recurrence of the same knee injury and are 4-times more likely to injure the opposite knee ACL during the following months after their return. (Orchard, et al. 2002).

2.6 Conclusion

This chapter has described:

- the surface properties that relate to a sporting field of arena and how these are measured or quantified;
- the structure of the turf grass and how the individual components affect the surface properties;
- the anatomy of the knee and potential anterior and posterior cruciate ligaments injuries and their causes; and
- recent injury related turf research conducted by Queensland DPI&F, and established a link between the traction property of turf sporting surfaces, management practises and ACL sporting injuries.

EQUIPMENT REVIEW

3.1 Introduction

High traction levels provided by the playing surface have been identified as a major contributor to sporting injuries. The traction of turf surfaces is currently determined using a manually operated device developed in 1986 and more recently a hydraulically operated machine. Investigations of these devices reveal potential measurement errors. The limitations and operational errors of these devices motivated the development of a more accurate and repeatable machine.

3.2 Current Standards for Traction Measurement

At present the traction of natural turf surfaces can be measured by using a commercially available manually operated device similar to equipment developed at the Sports Turf Research Institute (STRI), Bingley, West Yorkshire (Canaway & Bell 1986) from which the British Standard (BS 7044 1990) and the STRI Standard Testing Procedure #200798 were created (2008, pers. Comm., 9 December). A hydraulically operated machine “Pennfoot” (McNitt, et al. 1996) was developed at Pennsylvania State University, and a proposed American Society for Testing and Materials (ASTM) traction standard WK486 is based on this work.

3.3 Current Traction Measurement Equipment

The traction measurement principle is defined as a measurement of the force required to initiate rotational movement of a studded disc which is contact with the turf surface (reproduced from the STRI Standard Testing Procedure

#200798) (Canaway & Bell 1986) or shoe (McNitt, et al. 1996). This torque is a representation of the force acting at a known distance from the axis of rotation.

3.3.1 Canaway Device

The manually operated device developed by Canaway and Bell (Canaway & Bell 1986) and illustrated in Figure 3.1, reproduced from the STRI Standard Operating Procedure #200798 is comprised of:

- a mild steel disc 145 ± 1 mm in diameter and 12 ± 2 mm thick with 6 football studs 15 ± 1 mm long equi-spaced at a radius of 46 ± 1 mm from the centre of the disc;
- an 800 ± 25 mm long shaft with attached lifting handles and threaded into the centre of the studded disc;
- a set of lifting weights positioned centrally via a thrust bearing on the studded disc; and
- a two-handed torque wrench with a dial indicator and a scale with a maximum value of 80 Nm.

The total mass of the disc, shaft, weights and torque wrench should be within the range of 46 ± 2 kg. The device is dropped from 60 ± 10 mm onto the test surface to ensure penetration of the football studs and uses a two-handed torque wrench to measure a maximum traction value while the device is rotated through 180° .

Canaway used a trolley to transport the device between test sites and to create a constant drop height (Canaway & Bell 1986). A similar device is commercially available (Figure 2.3) and is being used by curators of elite sporting stadiums, for example Suncorp Stadium in Queensland, to monitor surface characteristics.

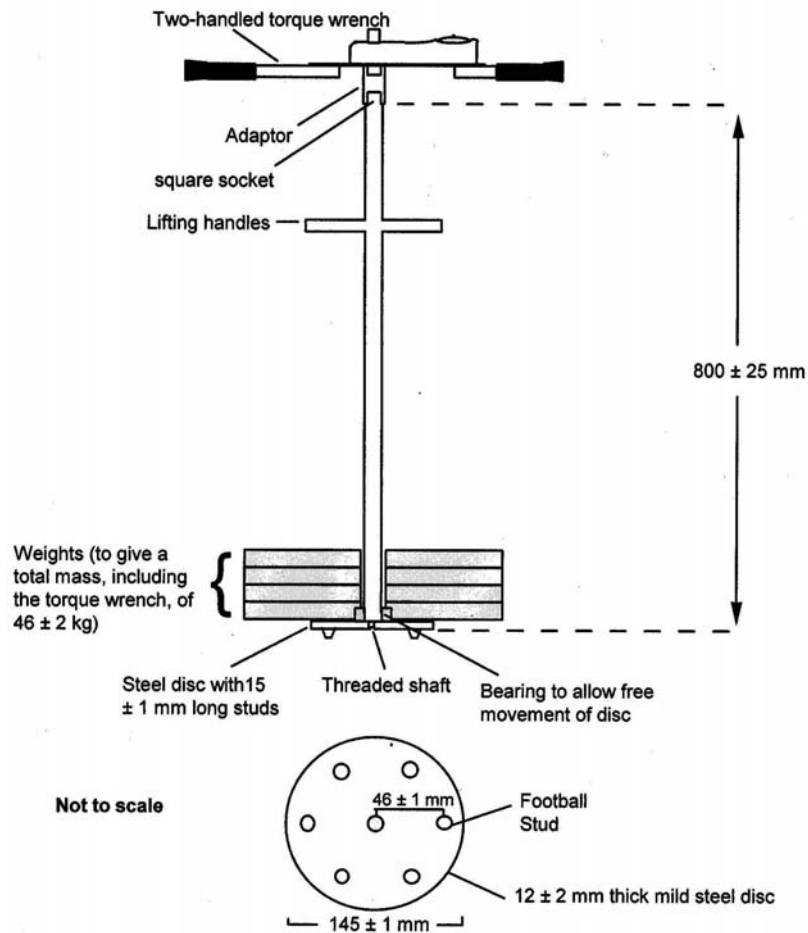


Figure 3.1 Canaway traction measurement device reproduced from: STRI Standard Testing Procedure #200798.

3.3.2 Review of Canaway Device

The manually operated device by Canaway uses a torque wrench to quantify a value of traction. The principle is sound but the accuracy is limited by the resolution of the dial gauge and the repeatability is subject to operational variability. For example, the manufactures specification for rated measurement accuracy for the torque wrench described in the standard operating procedure is $\pm 3\%$. The measurement accuracy also depends on operating technique as the device can pivot causing it to rotate around one

stud rather than the central axis (McNitt, et al. 1997). This operational variability affects the repeatability. Other issues which affect repeatability include:

- stud penetration depth;
- the effect that variation of rotational speed may have on traction measurement; and
- the resulting errors due to variations in vertical forces applied by the operator during testing.

This device also highlights a workplace health and safety issue requiring the single operator to manually lift a mass of approximately 46kg after each test. The Workplace Health and Safety Act 1995 does not stipulate weight limits for manually handling loads as there are many factors to be considered. However the following standards are used as a guide in determining safe maximum lifting limits (Table 3.1).

- International Organization for Standardization (ISO) Standard 11228-1 (ISO, 2003)
- Modern Material Handling (MMH) (Mital, et al. 1997)
- National Institute for Occupational Safety and Health (NIOSH) (Water, et al. 1993)

Table 3.1 Workplace Health and Safety Load Handling Recommendations

Maximum load weight under optimal conditions		
Standard*	maximum load weight (kg)	Comments
ISO 11228-1	25	Load can be handled by 95 % of men and 70 % of women.
MMH	27	Load can be handled by 90 % of men. Maximum load for women is 20 kg.
NIOSH	23	Load can be handled by 90 % of the population (men and women).

3.3.3 McNitt Device

The McNitt device (Figure 3.2) makes both linear and rotational measurements. It has a sports shoe as the interface with the surface and uses one hydraulic ram for linear movement (Figure 3.3) and two hydraulic rams acting on a strike plate (Figure 3.4) for rotational movement. Linear tractional force is calculated from the hydraulic pressure measurement multiplied by the effective surface area in the ram. Rotational traction is calculated using the hydraulic pressure measurement to determine the force similar to the linear measurement, which is further multiplied by the length of the lever arm (the distance from the axis of rotation to the point the ram acts on the strike plate) (McNitt, et al. 1997). The device description on the web page (McNitt & Petrunak 2003) uses a hydraulic pump and a pressure transducer connected to a computer to measure traction.

3.3.4 Review of McNitt Device

The principle of measuring hydraulic pressure to quantify linear and rotational traction measurements using McNitt's "Pennfoot" is sound if unloaded frictional effects are compensated for in the calibration. The method McNitt uses to rotate the ground engaging foot involves two rams acting on a strike plate (Figure 3.4). This, however, introduces errors as rotation occurs due to changes in length of the moment arm and changes in direction of the applied force which does not remain perpendicular to the strike plate (Figure 3.5).

Figure 3.5 shows that the relative direction of the applied force with respect to the strike plate changes as the angle of rotation, θ increases. The distance, d from the applied force to the axis of rotation also changes during rotation. Both these parameters affect the calculation of torque but publications regarding this device do not indicate the use of rotation angle or changes in moment length for the determination of torque.



Figure 3.2 McNitt's "Pennfoot" device for measuring traction.
(from <http://cropsoil.psu.edu/mcnitt/Infill6.html>, accession date 19/02/08)



Figure 3.3 Pennfoot linear operation
(from <http://cropsoil.psu.edu/mcnitt/Infill6.html>, accession date 19/02/08).

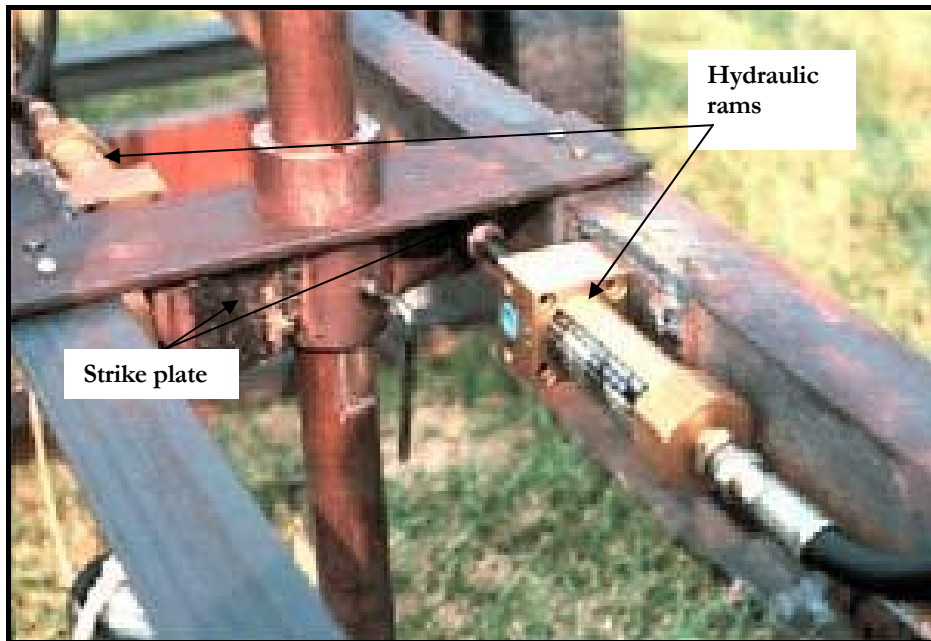


Figure 3.4 Pennfoot rotational operation.
 (from <http://cropsoil.psu.edu/mcnitt/Infill6.html>, accession date 19/02/08)

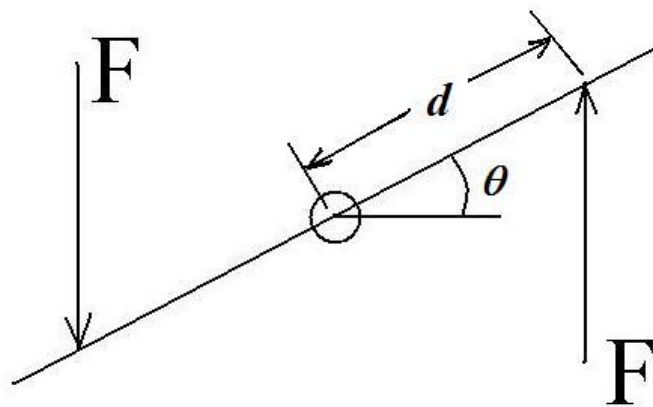


Figure 3.5 Diagram showing plan view of strike plate and applied forces in mechanism illustrated in Figure 3.4 of McNitt device.

An email to Andrew McNitt (2004, pers. Comm., 24 July) confirmed that rotational angle is not accounted for in determining a torque value. Analysis of the equipment design suggests that a maximum potential error e will exist if the rotational angle and change in moment arm are not accounted for in the determination of a torque or traction value.

As the angle θ increases during rotation the component of the ram's force that is perpendicular to the moment arm decreases. Therefore the ram is required to produce more force for an equivalent torque, resulting in a positive error (Figure 3.6).

From Figure 3.5 the percentage error due to direction of applied force e_1 is

$$e_1 = 100 \times (1 - \cos \theta) \% \quad (3.1)$$

where θ is rotational angle (Figure 3.5)

The distance, d changes during rotation because the rams are fixed to the frame and operate parallel to the frame and each other while pushing on the strike plate. Upon initial rotation the position of the applied force moves from the centre axis of the ram to the inside edge of the 16mm collar attached to the end of the piston rod. This effectively changes the length of the moment arm d , from 81mm to 73mm. From this point, the moment arm length d continues to increase as the angle θ increases until maximum rotation is reached and the test is completed. As this length d increases the ram is required to produce less force for an equivalent torque, therefore the error is positive for values of d less than 81mm, and negative for values greater than 81mm (Figure 3.6).

The percentage error due to change in the moment arm length e_2 is

$$e_2 = 100 \times \left(1 - \frac{d}{81}\right) \% \quad (3.2)$$

where d is the moment arm length (Figure 3.5)

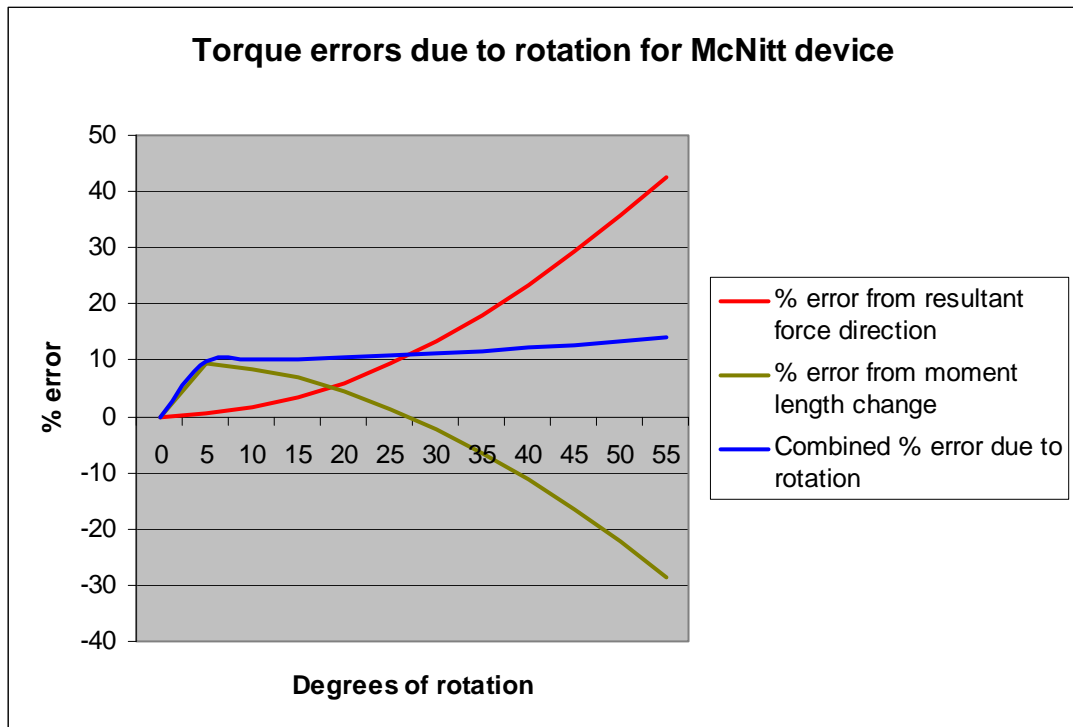


Figure 3.6 Error evaluation of the McNitt device during rotation.

Hence the total error e due to rotation for the McNitt device is given by:

$$e = e_1 + e_2 = 100 \times \left(2 - \cos \theta - \frac{d}{81} \right) \% \quad (3.3)$$

McNitt calculates torque using a moment arm of 81mm, which only occurs at two points during a rotation between 0 and 40° (at 0° and 27° with the moment arm varying between approximately 73mm and 90mm). The resultant force due to a change in angle of 40° of rotation equates to an error of 23%, however compensating for the respective change in the moment arm length reduces the combined error to 12.2% (Figure 3.5).

Published data (McNitt, et al. 1997) indicates that under typical operating conditions angles of maximum torque values are in the range of 30 to 50

degrees of rotation. Hence evaluation of the McNitt device (Figure 3.2) shows potential errors of 11 to 13.5% over the expected range.

3.4 Patent Search Results

An International Patent search was conducted in July 2004 and identified seven existing patents potentially relevant to the present study. These are:

US 4712418 A (Augustin), 15 December 1987.

This patent discloses an apparatus that measures surface friction, in particular, of surfaces designed for traffic such as road surfaces, floor coverings and similar surfaces. This device is an electric motor attached to a frame by a pressure torque cell with the rotor shaft also attached to the frame by bearings. The bottom of the rotor has a base plate which supports the contact members. The friction of the surface is determined from the torque cell resisting the motor from turning when loaded by the friction of the surface.

FR 2751748 A1 (Societe Labosport Societe a Responsabilite Limitee), 30 January 1998.

This device uses a rotating shaft driven by a motor and measures the rotational force generated by the friction between a contact pad and a synthetic sporting surface. The contact pad is offset from the axis of the motor and is attached by two arms forming a right angle triangle. The arm that forms the hypotenuse is spring loaded and adjustable in length allowing the normal force to be varied and allows measurement of uneven surfaces.

US 005920005 A (Moss), 6 July 1999.

This device is a cylindrical direct shear apparatus to engage multiple layers of geosynthetic, geotechnical, or both types of materials for evaluating interface friction.

WO 2002/063279 A1 (Ten Cate Nicolon B.V.), 15 August 2002.

This patent discloses a device for measuring the static and/or dynamic friction coefficient of artificial grass for sporting surfaces. This device has an anchoring body and a vertical bar with a ground engagement device, such as a football boot attached at the lower end. This vertical bar is connected to the anchoring body by means of two horizontal bars. The lower bar provides a pivot point for the vertical bar and provides adjustment of vertical loading. An electric actuator drives the upper bar horizontally to apply a horizontal movement to the ground engagement device. Strain gauges attached to the vertical bar measure the bending moment caused by the resistance of the surface to determine the coefficient of friction.

WO 2002/097401 (Eastman Chemical Company), 5 December 2002.

This invention relates to an apparatus for measuring the frictional characteristics of plastic articles having non-planar, irregular surfaces such as thermoplastic bottles.

US 2003/0101793 A1 (Evans), 5 June 2003.

The equipment described in this patent is a machine for testing wear, wear preventative and friction properties of lubricants and other materials eg. oils, grease, dry film lubricants and other lubricants. This invention is a new and improved "four ball test machine" adapted to provide enhanced load control accuracy and repeatability compared to existing four ball test machines.

WO 2004/051239 A1 (Ten Cate Nicolon B.V.), 17 June 2004.

This describes a device for measuring static and/or dynamic friction of natural and artificial grass surfaces. It employs a rotatable shaft with a ground engaging foot attached at the lower end. The ball of this foot is the ground contact point and is positioned directly below the axis of the shaft. The applied vertical force (normal force) is adjustable by removable weights at the top of the shaft.

3.5 Conclusion

The measurement of the physical properties of sporting fields prior to large sporting events is becoming commonplace to protect sporting bodies from liability if injuries occur. The Department of Primary Industries & Fisheries in Queensland is establishing benchmarks for the management of sporting arenas to minimise the risk of injuries.

Traction is currently measured with equipment similar to Canaway and Bell's design from 1986. In addition to the shortcomings already discussed (section 3.2.2) commercial units available in Australia differ from the design specifications of the testing procedure described in section 3.3.1. The torque wrench with a dial indicator has been replaced with a standard torque wrench commonly found in mechanics workshop which relies on the operator exceeding the torque setting to register. To obtain a reading the operator performs a number of tests increasing the setting until this torque level is exceeded. This approach limits the accuracy and increases the number of tests to determine a reading. Also in commercial units the standard 46kg mass used to ensure stud penetration has been replaced with a 20kg mass to conform to the National Standard for Manual Handling. As there is no trolley or supporting structure the drop height is random and will vary from test to test because it is controlled only by the operator's estimation. This non-standard approach affects the measurement consistency and the ability for comparative research.

The patent search disclosed one relevant machine (patent WO 2004/051239) for friction testing of artificial and natural turf surfaces. However this device was designed to measure the friction rather than traction of artificial turf and therefore is not equipped to engage or measure the strength of the turf root system.

The accuracy limitations and potential errors and Workplace Health and Safety issues highlighted for the Canaway and McNitt equipment demonstrated the need for the development of a more accurate and repeatable research tool for traction measurement of turf surfaces.

CONCEPT DESIGN

4.1 Introduction

The issues described thus far have highlighted the need for an improved method for measuring traction on sporting surfaces. The shortcomings of current equipment described in chapter 3 include accuracy, repeatability and operator safety issues. For an improved and effective design the operational features and criteria need to be established. To achieve this, the functionality of the device can be divided into three specific areas. This chapter describes these areas and the conceptual ideas and methods evaluated during the design process.

4.2 System functionality

The overall traction measurement system should include at least the following functionality.

- Portability – The ability to transport the device between measurement sites.
- Traction measurement – A method of accurate and repeatable application of a force or torque to the surface to measure its tractional properties.
- Data acquisition/analysis – The ability to display and record data.

4.2.1 Portability

The device will be required to test a number of sites on a playing surface and be capable of being transported between sporting fields. The method of transportation will play a major part in the physical design and therefore the dimensions of the resulting device. The measurement process itself is not

affected by the portability but is largely dependent on it. For example, the process of traction measurements will require a physical structure capable of repeated operation over the full traction range without failure or affecting the accuracy of the measurement process. This structure will have physical properties such as mass, size and shape which will directly affect the method of transportation.

4.2.2 Traction measurement

The traction measurement is effectively a representation of the shear strength of a combination of turf thatch, root system and soil. A standard measurement method should be established to allow comparative measurements which represent the traction experienced by a player. Most field-type sporting footwear contains lugs or replaceable studs, cleats or spikes. Therefore a device to measure traction to establish a safe sporting surface should provide similar penetration through the thatch and into the root system as current sports footwear.

A value of maximum traction can only be determined from a force or torque measurement to the point of failure of the root system. Therefore the device must apply and measure a shear force to the root system of the turf grass. Published data from DPI&F research (Loch 2003) collected using a device similar to the Canaway design shows the expected maximum traction value for all natural turf sporting surfaces to be less than 100 Nm.

4.2.3 Data acquisition/analysis

For the device to be useful the traction measurement must be presented to the operator for manual recording and interpretation or automatically recorded into non-volatile memory for future analysis.

4.3 System specifications

The specifications for a new device to measure traction are dependent on the user's requirements for the data or the information it generates. For example if the intention is to measure turf traction characteristics for turf variety selection, the research will be carried out on experimental plots where other parameters such as soil characteristics are known or controlled. For this application the measurement accuracy and repeatability should be as good as possible and not a limiting factor. Current equipment provides one data point per test which limits the possible analysis. Therefore a device that produces a profile of traction with respect to displacement will provide more information about the turf root structure and the way it fails.

With these factors in mind the specifications for the instrument were formulated to include the abilities:

- to measure traction to an accuracy better than existing equipment by at least a factor of 2, giving a required maximum inaccuracy of $\pm 1.5\%$;
- to be repeatable and allow for comparative measurements for research;
- to produce a traction profile relative to angular rotation or linear movement; and
- to be portable and meet national Workplace Health and Safety standards.

After meetings with potential customers for such a device it is envisaged that this equipment may be used as a maintenance tool for sporting clubs, schools and local councils throughout Australia to ensure their responsibilities are met for providing a safe environment for sport. As most sporting authorities have limited budgets, minimising the cost of such equipment is also a priority and therefore a major consideration for the prototype design.

4.4 System Operational Considerations

There are three options with regard to the operation.

- The device is operated manually
- The device is semi-automated
- The device is fully automated

4.4.1 Manual option

A manually operated device implies that all of the operation and measurement is performed manually. Therefore the operator exerts a force to apply a shear action or torque to the turf structure until failure occurs. This can be through mechanical advantage for example a lever or a screw device. The measurement and recording of data is also a manual process, therefore the instrumentation would be required to display the maximum value and the angle or displacement to achieve this traction value. This would not provide a traction profile but would provide more information than is currently available. Again the sensing element and the instrumentation can provide the necessary accuracy but systematic errors through manual measurement may be introduced. The Canaway design is an example of a manual design but lacks the ability to produce a data profile as there is no provision for measuring angle. This would be a painstaking process to perform manually if angle or displacement measurements were included in the design.

4.4.2 Semi-automated option

A semi-automated design would allow the device to have functions that are controlled within the device, for example using some automation would allow data collection and storage be performed at high rates and a capability of producing a data profile. The application of any required torque can also be automated providing the required repeatability. Being semi-automated has the disadvantage that an operator is still required for each measurement.

However if problems occur direct visual feedback allows intervention by the operator.

4.4.3 Fully automated option

A fully automated design can vary from a system where a single traction test or a multiple of tests is performed without intervention by an operator. The main difference between the two systems is the addition of automating the movement of the device between test sites within a sporting field.

4.5 System design requirements

The system design requirements can be divided into sections, for example:

- a method of transporting the device from site to site;
- a method of applying the shear force;
- a method to measure traction; and
- an instrumentation and data recording system.

4.5.1 Portability and transport options

The device can be transported between test sites within a sporting field by one or more of the following means.

- Carried – If the device is to be carried it must meet workplace health and safety standards, for example it should contain lifting handles and have minimal mass so that the operator is at no risk of injury in the course of using or transporting the equipment.
- Towed – For towing the device should track effectively behind a vehicle and have no effect on the operation or safety of the vehicle operator or bystanders and have minimal effect on the playing surface.
- Pulled or pushed – If the device is to be manually pulled or pushed to and from test sites it should provide sufficiently low resistance during movement to enable efficient data collection by a single operator.

- Driven or flown – Implies that the device is self propelled with an onboard engine or powering system. It may also operate autonomously, be remotely or manually controlled. Again safeguards must be in place to ensure safety to the operator, bystanders or property.

4.5.2 Application of shear force

As traction refers to the maximum resistance a surface can provide to a sports shoe with studs, spikes or cleats when a horizontal force is applied, it is largely dependent on the penetration depth of the stud and the normal or downward force applied. Other factors, for example mowing height will also affect traction measurements as excess grass leaf matter will limit penetration depth. Therefore the device should meet standard criteria regarding these parameters to allow for comparative testing:

- between turf varieties for turf selection for areas which have different climatic conditions; or
- for monitoring field variability for management strategies.

4.5.2.1 Options for applying the shear force

A manual system of applying this force is demonstrated by the Canaway system using a studded footplate. The stud penetration depth is achieved by dropping the 46 ± 2 kg mass (of lifting weights) together with the footplate and handle from a predetermined height. The 46 kg mass also acts to ensure full stud penetration depth remains throughout the test. A maximum of six studs are used to apply the shear force to the turf root system. The “T” handle used to apply a rotational movement utilises mechanical advantage produced by a moment arm determined from the length of the handles. Other options to obtain a mechanical advantage are a mechanical screw, a gearbox, a hydraulic or pneumatic system utilising a hand or foot pump. A

shear vane that is forced laterally or rotated is also an option for use in a manual system.

A semi-automated or a fully automated method for engaging the root system and applying the shear force could use hydraulics (as in McNitt's "Pennfoot"), pneumatics or electrics. A hydraulic system using rams or motors would have the advantage of being able to provide high torque and high power but would require a pump, oil storage and a power unit to provide the pressure and flow required.

A pneumatic system could provide a similar solution with the option of a gas storage cylinder to provide the required power. This would reduce the weight of the device by not requiring a power unit/pump as part of the system. For repeatability, i.e. motor speed, the design would need to include pressure regulators to compensate for changes in supply pressure as the air is used. Another issue that could affect the performance is the fact that air is compressible and therefore motor speed could also be affected by variations in the load. Similarly, an electric system could use a motor and generator or battery and/or solar panel as the power source with the same issues regarding size and weight.

4.5.3 Traction transducer

Traction, as described in section 2.2.5, is determined by measurement of a torque. Torque is the moment of a force and is represented in units of Newton metres (Nm). Torque is quantified by the product of the force tending to cause rotation about an axis and the distance from the point this force is acting from the axis. The force is applied at a point tangential to an arc with a radius length or moment arm equal to this distance. Therefore the torque is determined by multiplying the force by this distance. For example:

$$\mathbf{\textit{Torque = Force} \times \mathbf{\textit{Distance}}} \tag{4.1}$$

In this work “Traction” is defined as being the maximum torque applied by the standard testing machine to the turf surface and sub-surface.

The transducer must be capable of measuring up to the maximum expected torque value while meeting the required accuracy. This maximum traction value has been specified from previous research (Loch 2003) and quantified to be 100 Nm. Therefore the transducer and method of using the transducer must allow measurements of up to 100 Nm without failure or affecting the accuracy or performance of future tests.

Other considerations for the selection of a transducer are the input and output specifications, non-linearity, repeatability, creep or drift and the effect of temperature variations. The transducer selection is also dependant on the instrumentation and the desired method of recording the traction data.

4.5.3.1 Traction transducer options

The transducer selected for the prototype should not affect the measurement by providing any additional torque or should provide a torque which can be characterised or predicted for the measurement range of this device.

Torque transducers are commercially available that utilize magneto-elastic technology to provide accurate torque and angle measurements. The costs of these transducers start at approximately USD2000 (Magna-Lastic Devices, Inc.).

As torque is quantified in Newton metres (Nm) and represents a rotational force at a defined distance (moment), a cheaper alternative is to design a system such that the moment length remains constant and therefore the torque value can be determined by measuring only a force.

Force can be determined:

- directly using a load cell that utilizes strain gauges glued to a piece of machined steel or aluminium, and wired together into a Wheatstone Bridge (Cooper 1978) configuration. Load cells are commercially available and start in price from approximately AUD200 depending on quality and capacity;
- by measuring the pressure in a hydraulic system, as in the McNitt device (McNitt, et al. 1997). Pressure sensors are also commercially available at similar pricing to load cells but require a hydraulic system including rams and plumbing; or
- by measuring the compression or extension of a spring using a displacement sensor. There are numerous methods for measuring displacement for example:
 - ◆ using an LVDT (Linear Variable Differential Transformer) which is an electromagnetic sensor. The LVDT principle of measurement is based on differential magnetic coupling developed by the position of the moveable magnetic core relative to the central primary and the two inversely-connected secondary coils;
 - ◆ using a Hall-effect sensor that measures displacement from a Hall voltage which is proportional to variations in the flux density as the sensor is moved within a magnetic field;
 - ◆ using an inductive (variable reluctance) transducers which utilizes the change in inductance of a coil (inductor) as the distance from a ferromagnetic material changes (Wobschall 1987);
 - ◆ using a capacitive displacement transducer which is based on the principle that capacitance is dependant on the area of the capacitive plates, the distance between the plates and the dielectric between the plates. Therefore varying any of these

relative to displacement produces a measurable change in capacitance;

- ◆ using an ultrasonic SONAR transducer, used for the measurement of distance (primarily underwater), uses a piezoelectric element emitting pulses of ultrasonic (e.g. >20 kHz) acoustic energy directed to the target, which is a small area on the object. The signal reflected from the target travels back to the transducer, generating electrical pulses in the element. The time between transmitting and receiving the pulses is a measure of the distance between the transducer and the target. In this sonic radar, a separate or the same element can be used for generating and receiving the signals;
- ◆ using a piezoelectric transducer which uses the principle that a voltage is developed across certain crystals when they are strained;
- ◆ using a brush-type encoder which contains a disk or strip with digital code markings of contacting and non-contacting segments. A pick-off brush in contact with the segments closes or opens an electrical circuit, providing a digital signal in response to the displacement of moving parts;
- ◆ using an optical linear encoder which uses a grating on film to interrupt light between a light emitting diode and photodiode or phototransistor to indicate changes in displacement; or
- ◆ using an optical distance sensor that utilizes a laser diode to reflect a spot of light of the object in question onto a linear phototransistor array and using triangulation determines a measurement for distance.

All these techniques are potentially applicable options to measure traction in the design of the required machine.

4.5.4 Measurement options for rotation

To produce a data profile of traction with respect to angular rotation a method is needed to determine the angle of rotation for each traction measurement. This can be achieved using a transducer that indicates the instantaneous angular displacement and referencing this measurement with the torque measurement for the same instant in time. Transducers that measure angular displacement are:

- Absolute digital displacement encoders use the same technique using a grating on film to interrupt light between light emitting diodes and photodiodes or phototransistors to indicate changes in displacement. By using a binary encoding strip the rotation is represented by a binary code and an instantaneous angular displacement can be measured (Wobschall 1987).
- Potentiometers give a change in resistance with the rotation of the input shaft and can be used as an angular displacement transducer.
- Resolvers and inductosyn transducers use phase relationships between a motor-generator pair to measure angular displacement (Wobschall 1987).

4.5.5 Instrumentation, data recording and analysis

Like the method of transportation, the instrumentation system can vary from manually recording to computer controlled data acquisition. The options will depend on the output specifications of the transducer and the type of storage media selected.

4.5.5.1 Instrumentation options

The instrumentation is the equipment that converts the outputs from the transducers into a usable format. This can be as basic as a dial indicator on a torque wrench as used in the Canaway device or a computerised data acquisition system. For the dial indicator the data is read, interpreted and recorded manually whereas a computerised system can record in the order of 100,000 readings per second with a measurement resolution of 0.025% of full scale. The instrumentation system specifications are determined by the transducers selected and the required data output format.

To electronically record analogue traction data in a computer the signal must first be converted into an appropriate format for the computer to interpret. If the data is recorded automatically the output signal from the transducer is digitised using an analogue to digital, voltage to frequency or similar converter and processed using computer technology and stored into non-volatile memory of some kind. The computer system may vary from a low cost, low power 8-bit microprocessor circuit on a single board to an off the shelf portable personal computer (PC). As the PC is generally used for office work it does not have the necessary input specifications to measure analogue signals over the range or with the required accuracy of approximately $\pm 1\%$. There are a number of analogue to digital data acquisition boards/modules that interface to a computer system. These vary from internal printed circuit boards (PCBs) that connect directly to the data bus; external devices which connect via the Recommended Standard 232 (RS232) port or via the Universal Serial Bus (USB). Both are recommended standard interfaces for connecting serial devices approved by the Electronic Industries Alliance (EIA).

4.5.5.2 Data recording options

The options vary from:

- data being manually collected and recorded in a laboratory log book, processed manually or typed into a computer program eg. spreadsheet for analysis and presentation; or
- data being automatically collected by a computer based system and recorded electronically and stored in non-volatile memory, for example:
 - battery backed random access memory (RAM);
 - electrically erasable programmable read only memory (EEPROM) which can be programmed a byte at a time;
 - ‘flash memory’ which is similar to EEPROM but is programmed and erased in large blocks and is found in USB memory devices;
 - on hard or floppy disks which use magnetic medium for data storage; or
 - optical disk which uses laser technology to read and write data.

The type of data storage will depend on the computer system and whether the data analysis is real-time or post-processed.

4.5.5.3 Data analysis options

Data can be analysed manually or entered into a database where statistical methods or mathematical functions can be performed. This proves to be an efficient way to perform repeated processing to multiple sets of data. An alternative is to develop software specific to the processing and output requirements.

4.6 Design Decisions

This section discusses the options selected for the prototype turf traction measuring device to meet the specifications defined in section 4.3.

4.6.1 Portability selection

A requirement for the device was to be easily transported between sporting fields. The ability for it to fit in a station wagon and be moved and used by a single operator was desirable as this maximises the transport options. This criterion plays a major factor in determining the physical size and weight of individual components. Designing the device around a small trolley similar to that used by Canaway (Canaway & Bell 1986) achieves this.

4.6.2 Type of traction measurement system, automatic versus manual

As previously stated the main focus for the design was to develop a machine to efficiently and effectively measure the traction properties of sporting surfaces. The repeatability and accuracy specifications defined in section 4.3 are addressed by automating the measurement process. Therefore the design would incorporate automation for all aspects that affect the accuracy and efficiency of data collection.

However, as an operator would be present during testing, the processes which do not affect the efficiency of data collection would be operated manually, for example moving the device between test sites, resetting and initiating each test. This reduces the design cost and complexity, which in turn improves the systems potential reliability. Therefore the resulting prototype design incorporates both automatic and manual processes.

4.6.3 Transducer selection

The high price and limited Australian availability of a torque transducer prompted a search for a less expensive alternative. By using a chain drive to rotate a foot and produce the torque, a measurement of the tension force in the chain will directly correlate with the applied torque. This tension force

multiplied by the radius of the main sprocket attached to the ground engaging foot will represent torque and therefore traction.

The factors affecting the transducer selection included:

- The accuracy of measuring tension in a chain using a force transducer is largely dependant on the geometry of the measuring system remaining constant. Using the displacement of a spring was not adopted because changes in spring length change the chain geometry and therefore the direction of force vectors.
- The cost and maintenance of hydraulic rams, plumbing and a pressure sensor eliminated it as a viable option as the transducer.
- The load cell option provided easy installation, more accurate and predictable results with minimal deflection over the measurement range and therefore minimal effect on the geometry of the force vectors.

A load cell measuring the normal force acting on an idler sprocket within the main drive chain proved to be the most accurate and cost effective solution to measure chain tension.

4.6.4 Instrumentation selection

An instrumentation system that utilises commercially available technology provides an efficient and cost-effective solution to meet the resolution and accuracy requirements defined in the specifications in section 4.3. Using a digital load indicator with programmable range and offset adjustment and having a serial data output provides both manual and automatic data acquisition options with minimal development time.

4.6.5 Data recording and analysis method selection

A laptop personal computer was selected for both the storage and analysis of traction data. As the instrumentation provided serial traction data the simplest and cost effective solution was to utilise existing computer equipment to record and analyse the data. The laptop provides three options for data storage, for example:

- the computer hard drive;
- a 3.5 inch floppy disk;
- an optical disk; or
- a USB memory stick.

A laptop computer also provides standard terminal software to capture and record the traction data and standard spreadsheet software for analysis. However, it was considered preferable to develop custom software to display, analyse and record the traction data. This decision greatly enhanced the user-friendliness of the machine and, importantly, minimised the possibility of operator error.

FINAL DESIGN AND PROTOTYPE DEVELOPMENT

5.1 Introduction

This chapter describes the design and development of the automated turf traction tester. The development incorporates three discrete areas (shown in Figure 5.1), the mechanical design, the electronic control and instrumentation and the data processing and analysis which make up the overall design of the turf traction tester.

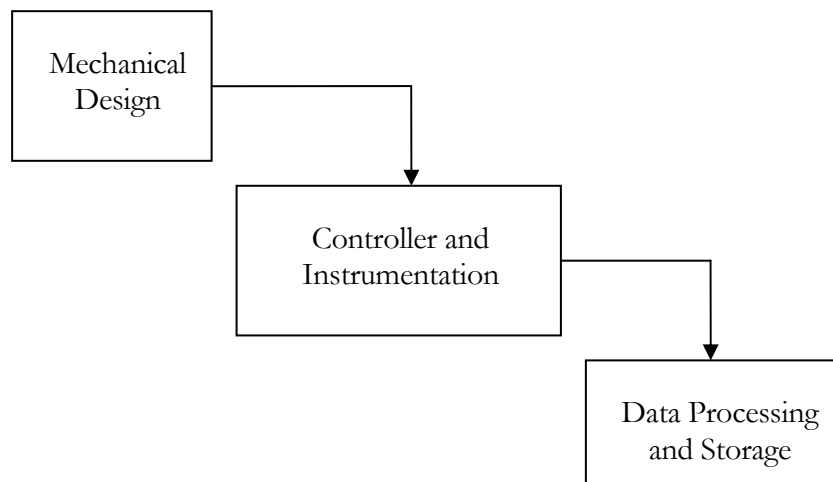


Figure 5.1 Areas of development of the automated turf traction tester.

5.1.1 Measurement Requirement

To produce a traction profile for a turf surface a number of angle and torque measurements must be taken simultaneously while the rotating force is being applied.

The torque delivered to the turf under test is determined from a force transducer located in the drive train (described in section 5.3.2). The angle associated with each maximum torque measurement is computed as a proportion of the number of data readings to reach maximum torque to the total number of data readings multiplied by the angle of maximum rotation (150° which is preset by a limit switch).

5.2 Mechanical Design

The mechanical design has been developed in line with meeting the system requirements and functionality. The main components within the mechanical design include the detachable ground engaging foot and weights system, the lifting mechanism, the frictionless drop, traction loading system, and the trolley.

5.2.1 Detachable ground engaging foot and weight system

As traction relates directly to the interface between the players footwear and the playing surface a standard foot plate was constructed based on the Canaway design (Canaway 1986). By utilising this standard, all future traction measurements can be compared with past research.

A modular system was designed to enable a single operator to use and transport the device. To minimise the component mass required to be lifted during transportation, the 40 kg of loading weights and ground engaging foot were designed to be removed and disassembled. The drive shaft was threaded to allow removal of the ground engaging foot (Figures 5.2 & 5.3) from the main drive shaft.

The body building lifting weights were machined to fit together to form a single mass with all central holes aligned. A thrust bearing inserted in the bottom lifting weight allows the ground engaging foot to turn independent to the weights and



Figure 5.2 Weights assembly



Figure 5.3 Ground engaging foot

eliminate any friction effect between the weights and the turf. The thrust bearing also ensured that the combined 40kg mass was concentric about the central main drive shaft eliminating the possibility of friction due to contact with the shaft during rotation. The footplate was drilled and tapped to allow testing of different stud configurations e.g. size, shape and pattern. Figure 5.2

shows the complete ground engaging foot assembly with Figure 5.3 showing the studded footplate.

5.2.2 Lifting mechanism

Also required within the system is the ability to lift the foot and mass of approximately 46 kg to the start position after each test. During preliminary testing of the turf traction tester a basic lever arm was utilised to lift the 46 kg of mass. The mechanical advantage of the lever system reduced the force required to lift the mass to approximately 110 N or 11 kg of force. This force is applied vertically down eliminating lifting and utilising the mass of the operator to operate the lever. This was achieved using a pivoted arm with a two pronged fork (Figure 5.4) which contacted the bottom face of a disc that was welded to the main drive shaft (Figure 5.5). A 6 mm bolt acted as a fulcrum (Figure 5.4) for the pivot arm which provided the mechanical advantage required for a single operator to use the automated turf traction Tester. This lifting arm had a hinged section which folds forward for compactness.

This lifting system was subsequently modified because the forks experienced wear during initial testing. An improved lifting method utilising a parallelogram and nylon wear pads (Figure 5.6) was designed to reduce friction. Also, the four nylon guides used to align the roll pin during lifting were also experiencing wear and were replaced with two steel guides. During the lifting process the guides rotate the main drive shaft and align the roll pin with the slots in the support plate (Figure 5.7). This system provided a vertical lift with the surface of the wear pads remaining parallel to the lifting disk throughout the lift. A lever arm with similar mechanical advantage to the previous version pushes on a roller attached to the bottom section of the parallelogram. A roller adjusts for the differences in centres of rotation of the lifting arm about the fulcrum and the vertical arm of the parallelogram as it rotates about its upper pivot points. A compression spring (figure 5.6) is

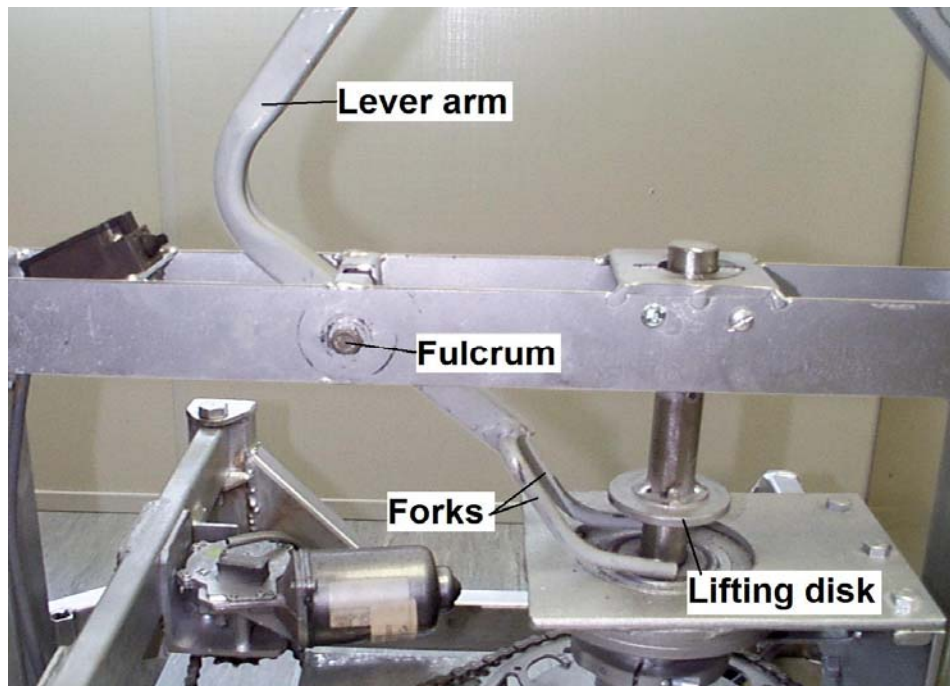


Figure 5.4 Original lifting mechanism

included to ensure the parallelogram returns to the lower position after operation. Operation of the lifting system is shown in Figure 5.8.

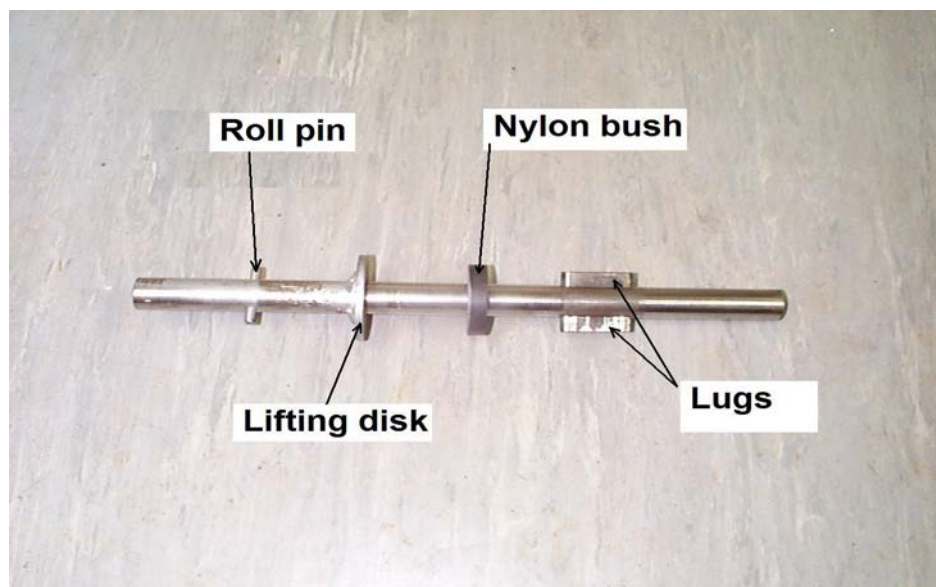


Figure 5.5 Main drive shaft

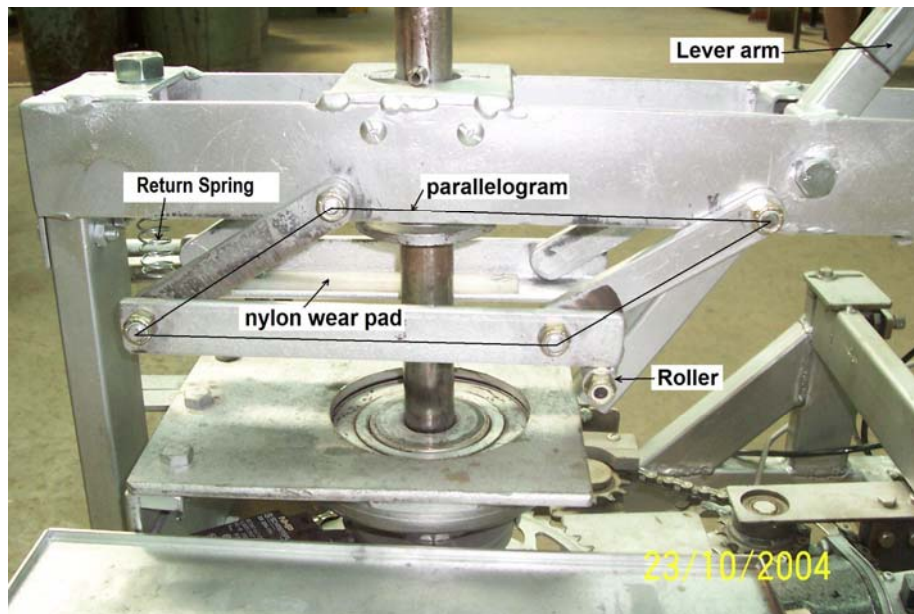


Figure 5.6 Improved lifting mechanism

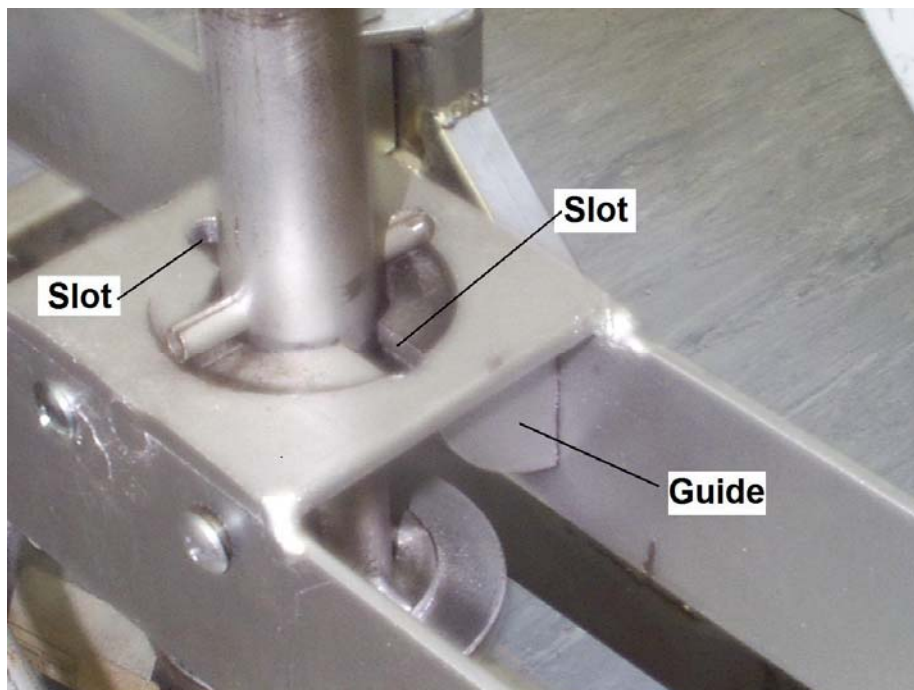


Figure 5.7 Roll pin guides and slots



Figure 5.8 Lifting operation using lever and parallelogram.

5.2.3 Frictionless drop

To meet the criteria of repeatability the system needed to ensure penetration of football studs into the turf root system for each traction test. Dropping the ground engaging foot with a mass of approximately 46 kg from a height of 60 mm is the standard used for the manual Canaway device. This method was adopted for this design as it remains repeatable if:

- the mass remains constant;
- the drop height remains constant; and
- there is no friction during the drop.

The mass is made up of four 10 kg cast iron lifting weights and will experience little or no corrosion or damage and therefore the mass will remain constant. The drop height is set and remains constant for each test by the physical structure of the machine, the use of solid wheels and the design of the drop mechanism. The roll pin (Figure 5.7) retains the main drive shaft and therefore ground engaging foot a constant height above the ground until the drop is initiated. The frictionless drop is achieved using a dog clutch (Figures 5.9 and 5.10) to isolate the main drive shaft and therefore the ground engaging foot from the motor, chain and sprocket drive system during the drop. The dog clutch re-engages the main drive shaft to the drive system to rotate the ground engaging foot during each traction test.

A dog clutch is a type of clutch that couples two rotating shafts or other rotating components by interference. The two parts of the clutch are designed such that one will push on the other, causing both to rotate at the same speed (Figure 5.9(a)). Dog clutches are used where slip must be avoided and they are not affected by wear in the same way as friction clutches.

The two rotating components within the dog clutch used in this machine are a 60 mm pipe section to form an outer cylinder and a 25 mm solid main drive shaft forms the inner rotating component. The main drive shaft has two lugs

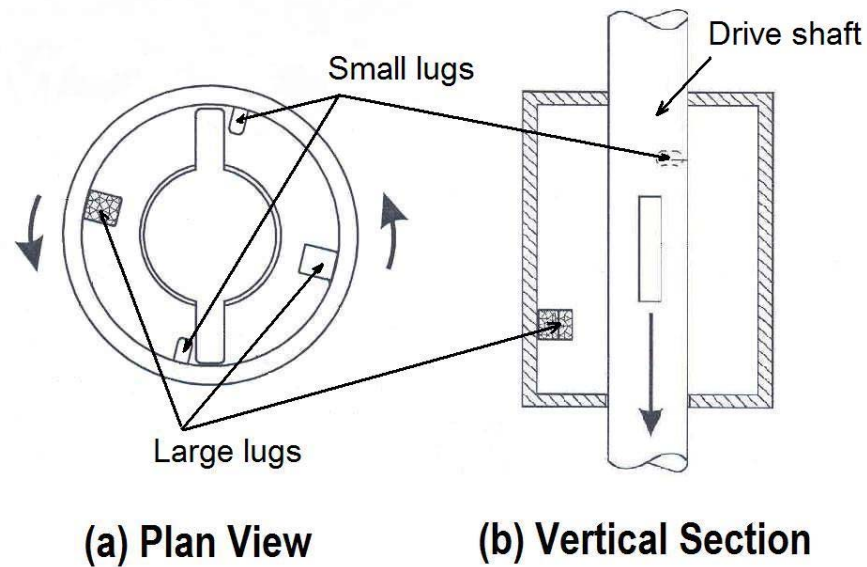


Figure 5.9 (a) Dog clutch operation – the outer cylinder rotating the main drive shaft with small lugs to initiate drop (b) Frictionless drop with no contact between outer cylinder and main drive shaft.

(Figures 5.5) which engage with four internal lugs attached to the inside of the outer cylinder (Figure 5.10). The two large lugs which are diametrically opposed at the bottom section of the outer cylinder transfer torque to the ground engaging foot during traction testing. The two smaller lugs offset by 90° to the larger lugs and also diametrically opposed in the top section of the outer cylinder are used to rotate the main drive shaft and initiate the drop at the start of each test.

The outer cylinder is attached to the main drive sprocket and is positively driven by the motor through the chain and sprocket system. It is supported by the machine structure using two single row radial bearings (Bearing Service Centre (BSC) part number BSC 6212) which allow it to rotate with minimal friction (Figure 5.11).

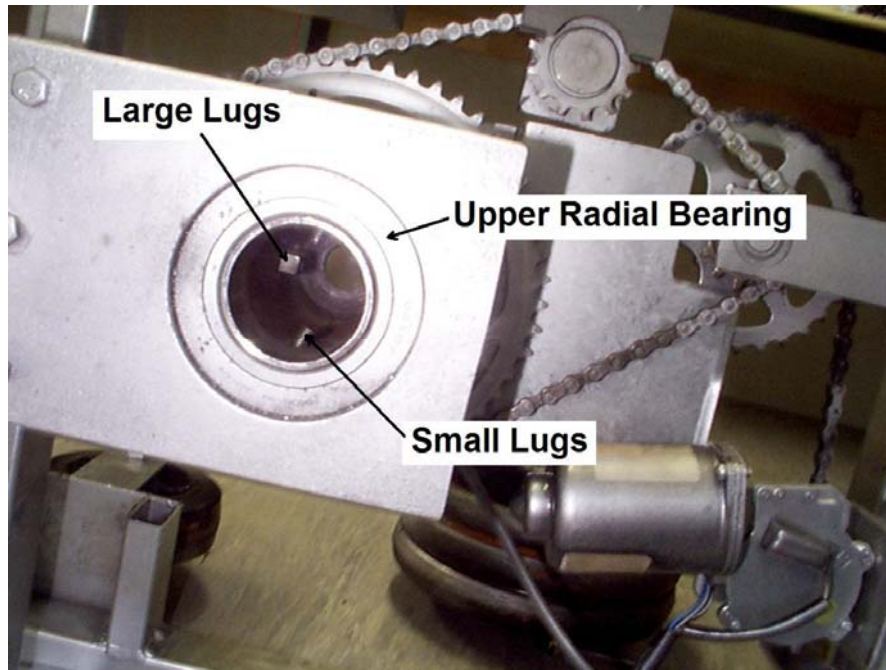


Figure 5.10 Lug positions in dog clutch

Prior to each test the main drive shaft and therefore ground engaging foot is suspended 60 mm above the ground by the roll pin and support plate (Figure 5.12). The two smaller lugs within the dog clutch are used to rotate the main drive shaft until the roll pin and slots in support plate align. At this point the main drive shaft drops freely due to gravity until the foot plate comes to rest on the ground surface. Oil impregnated nylon bushes are pressed into each end of this pipe section and act as a guide to centralise the main drive shaft on unlevel surfaces and ensure the dog clutch components are aligned concentrically for the application of power to the ground engaging foot. The motor continues to rotate the outer cylinder during this frictionless transition between the upper and lower positions of the main drive shaft (Figure 5.9(b)). The 90° offset between the smaller and larger lugs provide a period of time where the outer cylinder rotates approximately 75° with no traction load on the main drive shaft. This allows measurement of a zero reference for each subsequent traction reading and relates directly to frictional effects due to bearings etc. within the drive system rotating the outer cylinder.

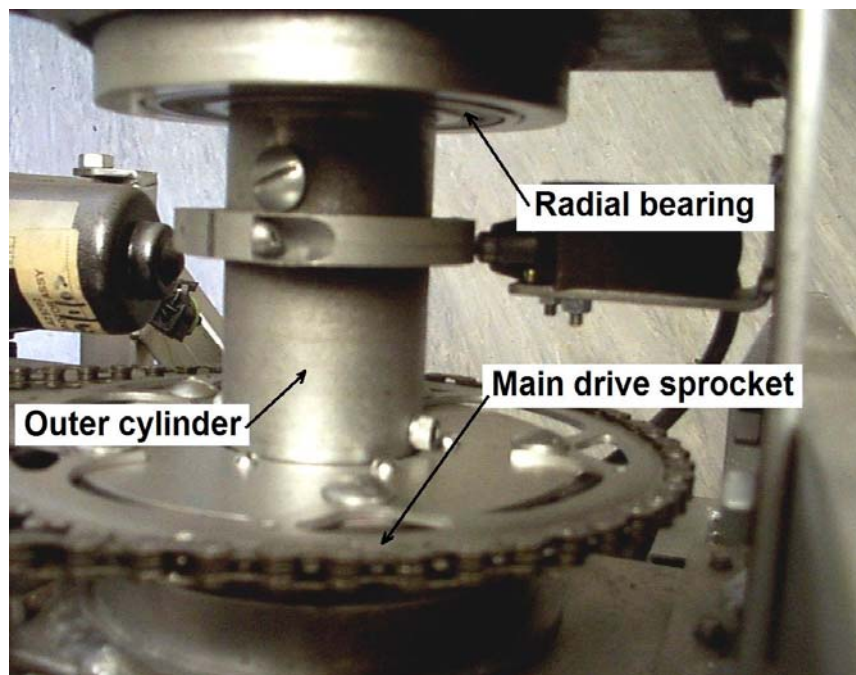


Figure 5.11 Outer cylinder of dog clutch, main drive sprocket and bearing mount.

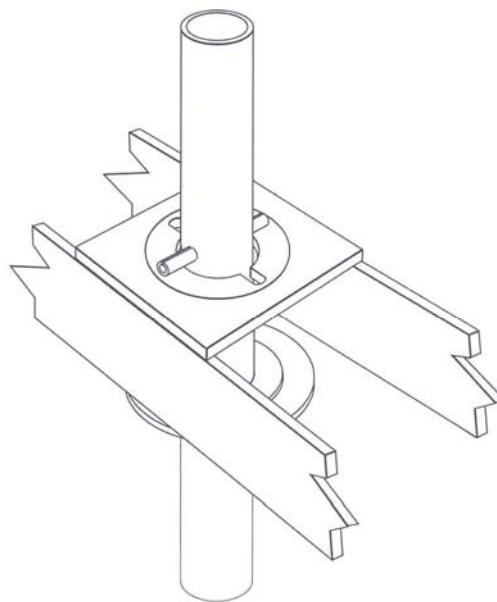


Figure 5.12 Shaft upper position retaining roll pin

After the drop the foot is engaged in the turf and the larger lugs are used to transfer torque between the motor and chain drive system and the ground engaging foot. The lugs on the main drive shaft are approximately 25 mm long and ensure correct clutch operation for small variations in drop distance. This variability could be due to variations in surface topography, thatch height or the effect of different stud configurations and sizes.

5.2.4 Traction Loading System

The degree of automation of the traction turf testing machine was principally determined by cost and simplicity while still meeting the accuracy and repeatability specifications for the device. Automating the rotation of the ground engaging foot improves the repeatability by providing a constant loading speed. Having a repeatable mechanised loading system also improves the accuracy by eliminating non-concentric or side loading which was found to be an issue with the Canaway device (McNitt, et al 1997).

Historical data and recent experimentation using a Canaway device (Loch 2003) showed the expected maximum torque to be 100 Nm for turf surfaces. To meet these load and operational specifications the mechanical loading mechanism is comprised of:

- a motor;
- sprockets and chains;
- chain adjustments; and
- a dog clutch.

The traction loading system uses a motor to rotate a ground engaging foot to measure the resistance provided by the turf. The motor controls the position and movement of the main drive shaft and therefore the ground engaging foot to enable the capture of traction data and also produce a profile of the torque relative to angular rotation. The criteria of portability dictated the use of a DC motor operating on battery power as mains power is not always

available in most measurement situations and a generator is neither practical nor cost effective.

A 24 volt, 32 Nm truck windscreen wiper motor with a further gear reduction using sprockets and chains was selected to develop the required torque. A major advantage of using this motor is that it incorporates a gearbox and therefore minimises the number of hardware components required to reduce the speed and therefore increase the torque. Also, utilising a 24 volt motor approximately halves the current drawn from the battery compared to a 12 volt equivalent motor for the same output power. This reduction in current increases the battery life while allowing the use of wiring with conductors having smaller cross sectional area.

Two 12 volt 7Ah batteries connected in series provide the required 24 volt DC power to operate the motor. Wiring has been included so the batteries can be charged in circuit or removed and charged using a suitable charger.

The motor is connected to the main drive shaft via four sprockets and two chains. The following three factors determined the selection and configuration of sprockets:

- the sampling speed of the instrumentation;
- the maximum torque requirement; and
- the availability of sprockets.

The gear ratios for the reduction from motor sprocket to intermediate sprockets and to the main drive sprocket are 14:30 and 13:52 respectively (Figure 5.13 and 5.14). The overall reduction ratio of 1:8.6 produces a drive shaft speed of approximately 6.4 revolutions per minute or 9.4 seconds per revolution. This sprocket ratio also increases the potential output torque of the main drive shaft to approximately 275 Nm or 2.75 times more than the specified maximum output torque. This gear reduction minimises the loading

effect on motor speed when the maximum expected output torque of 100 Nm is experienced.

Providing a constant motor speed, a chain drive system and utilising a dog clutch with no slip allows rotational angle of the drive shaft to correlate linearly with motor operation time. Therefore by sampling data at regular time intervals and having a constant total angle of rotation each traction data point is referenced to an angle of rotation. This correlation between torque and rotation angle is independent of small changes in motor speed due to battery voltage variations as the battery discharges over time.

Provision has been made for chain tension adjustment for both chains as shown in Figures 5.15 and 5.16. There is a screw adjustment for each ensuring that tightening the locking bolts does not affect the adjustment. The motor chain adjustment in Figure 5.15 uses a set screw to move the angle iron motor mounting bracket horizontally. Two slotted holes in the frame section supporting the bracket allow this movement. When the chain is adjusted, two fixing bolts secure the bracket to the frame.

The main sprocket chain is adjusted using the same frame section. This section of frame is hinged at one end and allows the bracket supporting the intermediate sprockets to move through an arc and therefore tension the chain. A slotted section of 40mm x 5mm is welded to the frame section and is used to secure the chain using the chain locking bolt when the adjustment using the chain tensioning set screw (Figure 5.16) is complete.

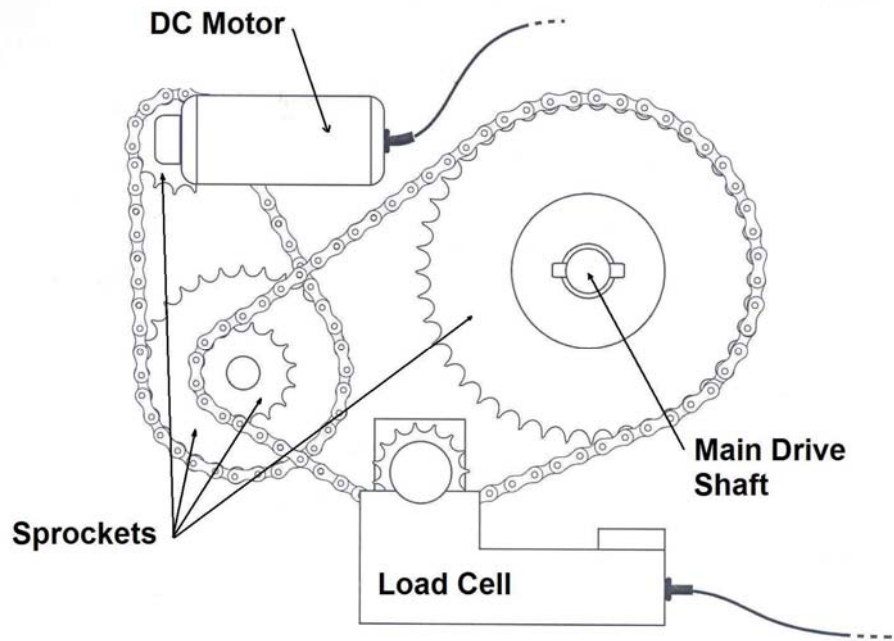


Figure 5.13 Drive sprockets and chains configuration

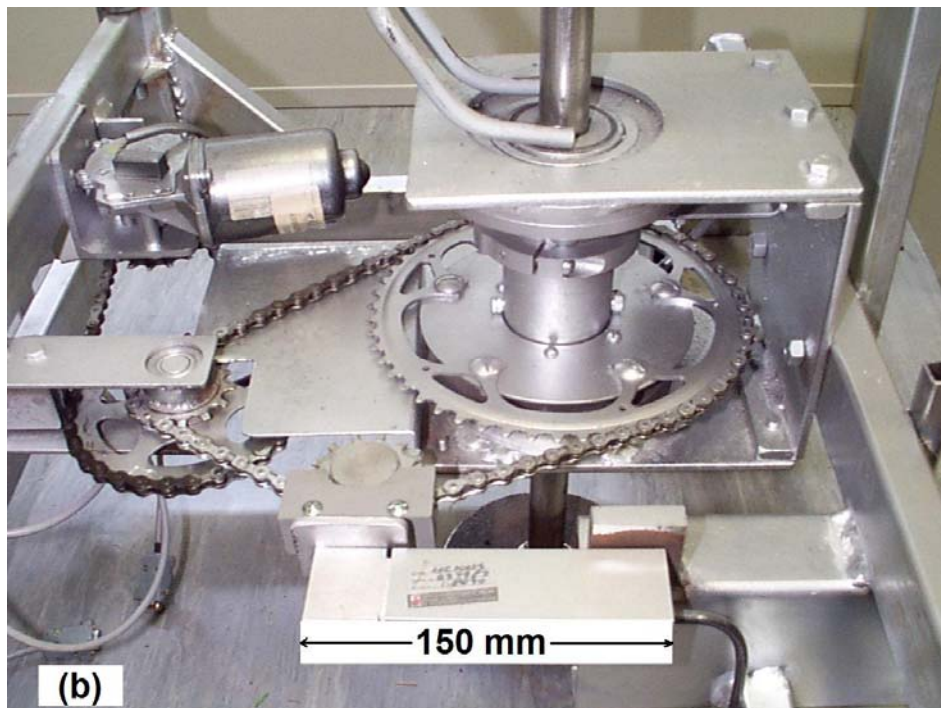


Figure 5.14 Drive sprockets and chains with scale.

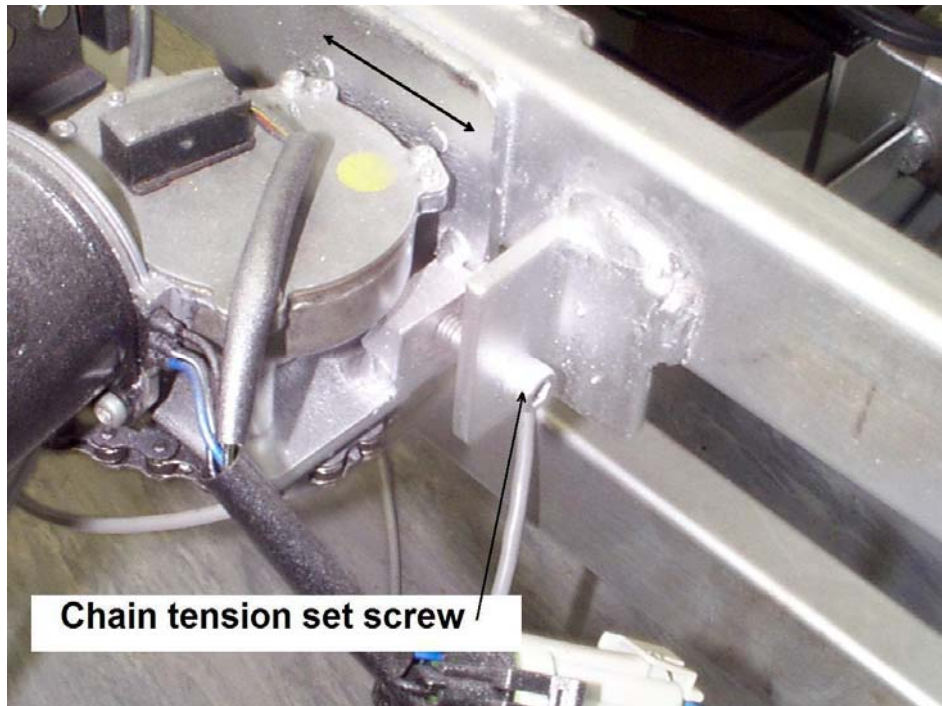


Figure 5.15 Motor chain tension adjustment set screw

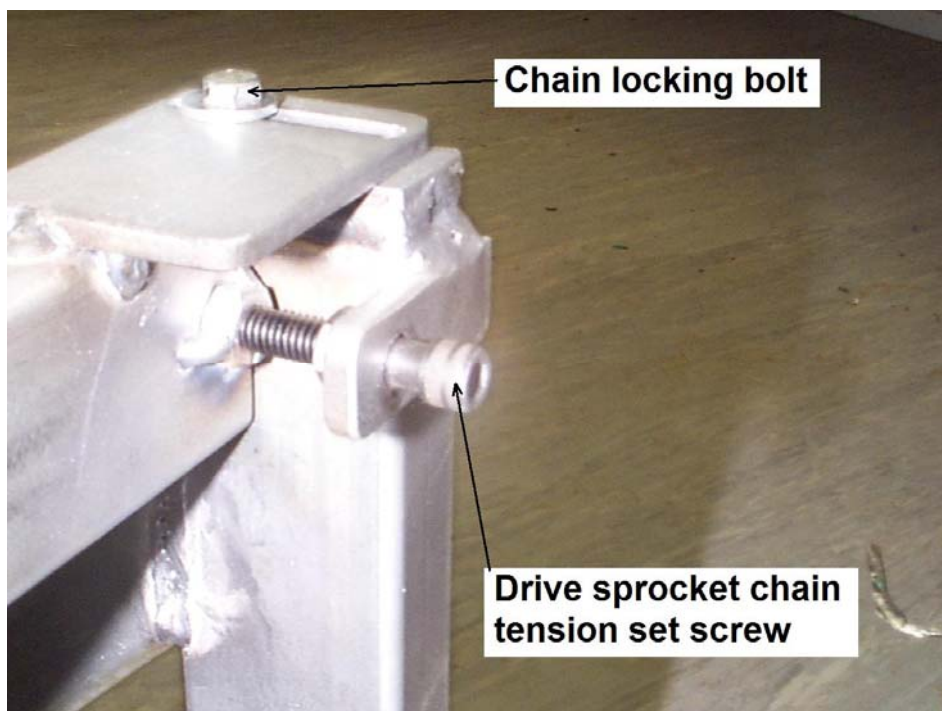


Figure 5.16 Main sprocket chain tension adjustment and locking screw

5.2.5 Trolley

To minimise costs and keep construction simple a three wheeled trolley with front wheel steering as shown in Figure 5.17 similar to both Canaway (Canaway & Bell 1986) and McNitt's (McNitt, et al. 1996) design (Figure 3.2).

The wheels were selected to meet the trolley mobility requirements. For example, the wheel diameter and width was selected to limit rolling resistance while providing a low cost solution allowing the trolley to be manoeuvred around the sporting field by a single operator. All three wheels are 150 mm in diameter and 50 mm wide and have solid nylon tyres. Solid wheels were used to minimise variations in machine height to ensure the drop height remained constant for each traction test. The two rear wheels are fixed castors with ball bearings. The front wheel is a swivel castor with the axle connected directly to the handle for towing and steering.

Two steel spikes driven into the ground fix the trolley's position and ensure stability during each test. This prevents rotation of the trolley while testing turf surfaces that require large amounts of torque.

The trolley frame was constructed from 20mm x 50mm x 2mm RHS steel which was selected due to availability (a plentiful supply in stock) and ease of welding (2 mm wall thickness allowed construction by welder with limited experience). The steel frame provided a compact, light weight and rigid platform for mounting the mechanical and electronic hardware.



Figure 5.17 Three wheeled trolley

5.3 Controller and Instrumentation

To ensure the repeatability and accuracy of the traction turf tester the mechanics of the measurement system has been automated. A commercially available programmable logic controller (PLC), digital load indicator and laptop computer are used for motor control and to measure and record the data (Figure 5.18). Automating the measurement system ensures that systematic errors which might be introduced by differing operator practices are minimised.

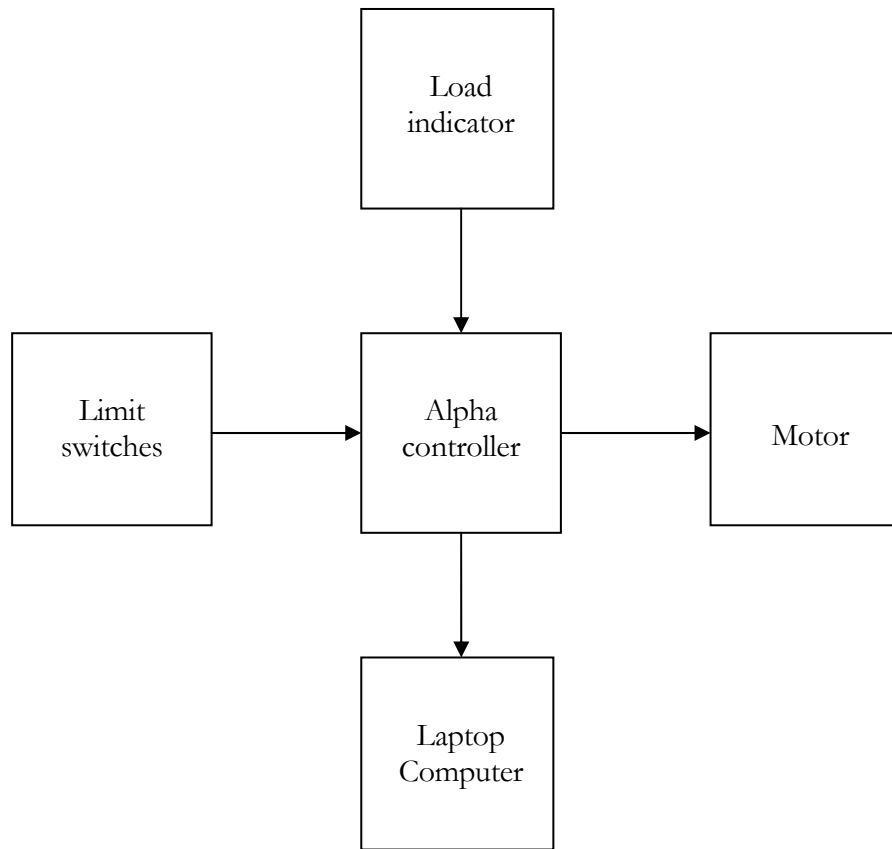


Figure 5.18 Controller and Instrumentation

5.3.1 Control system

The control system comprises of a Mitsubishi Alpha series controller AL-10MR-D, a Finder 55.32 type 24 volt relay with two change over contacts (Figure 5.19), two Schmersal ZR33611Z type limit switches and a single pole momentary push button switch.

5.3.1.1 Alpha Controller

The Alpha controller in Figure 5.19 is programmed using Visual Logic Software which has a graphical user interface in which logic gates and function blocks are linked on-screen to create a functional program.

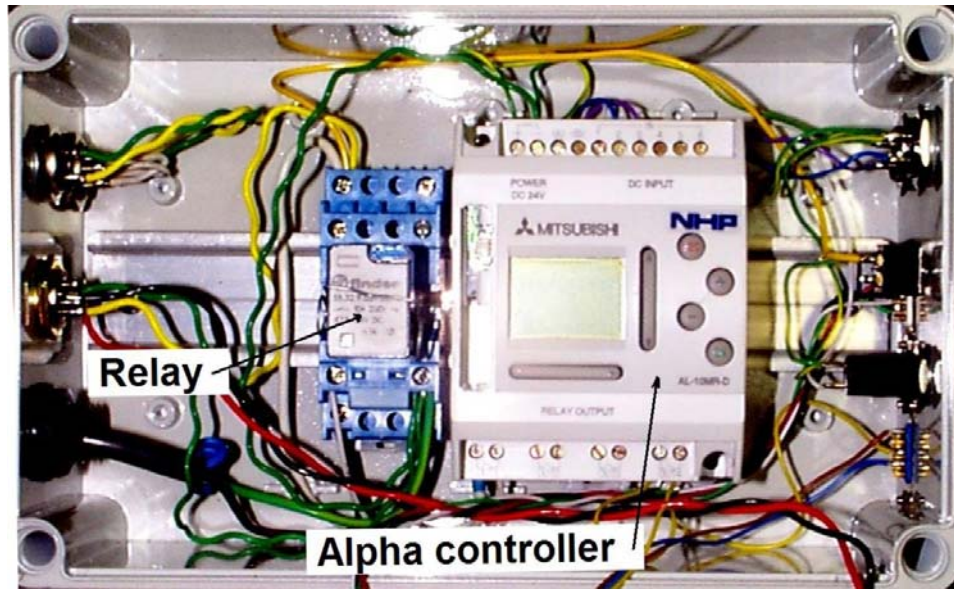


Figure 5.19 Controller hardware

The program is stored in non-volatile memory within the Alpha controller and runs whenever power is connected. Figure 5.20 is a flow chart of the turf traction tester program and Figure 5.21 is a screen capture of the program within the software development environment.

5.3.1.2 Control Sequence

The Alpha controller monitors the start button which is used to initiate each test. On activation of the start button an S-R Latch (block B03 in Figure 5.21) is set energising the finder relay via output 01 which provides power to the electric motor. A One Shot timer (B10), NOT gate (B12) and the AND gate (B11) provide a delay disabling the Cam limit switch until sufficient rotation has occurred to avoid false triggering from contact bounce. The S-R Latch (B03) also activates the data enable output after a short delay provided by an On-Delay function block (B13). The data enable output then connects the serial torque data (RS232 format) from the load cell instrumentation to the computer for storage and analysis.

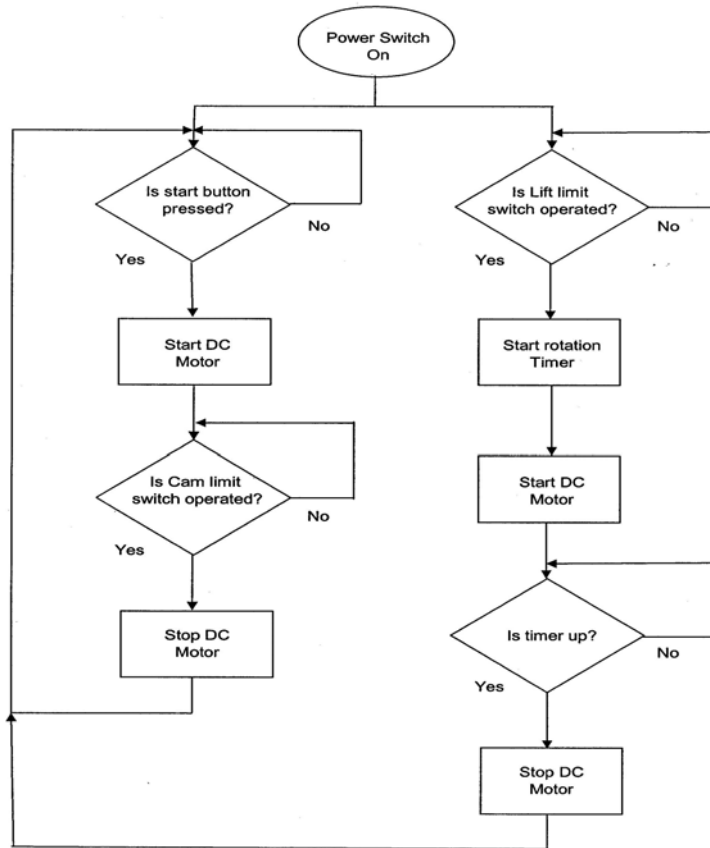


Figure 5.20 Alpha program motor control flowchart

The drive shaft then rotates until the Cam limit switch (Figure 5.22) is activated. This causes a low-to-high transition signal which initiates the Pulse function (B09) and resets the S-R Latch which disconnects power from the motor and terminates the data flow by deactivating the data enable output.

At the completion of data collection the ground engaging foot is manually raised using the lifting mechanism until the roll pin passes through the slots in the upper support plate. At this point the Lift limit switch (Figure 5.23) is activated causing the motor to be powered which rotates the main shaft for a

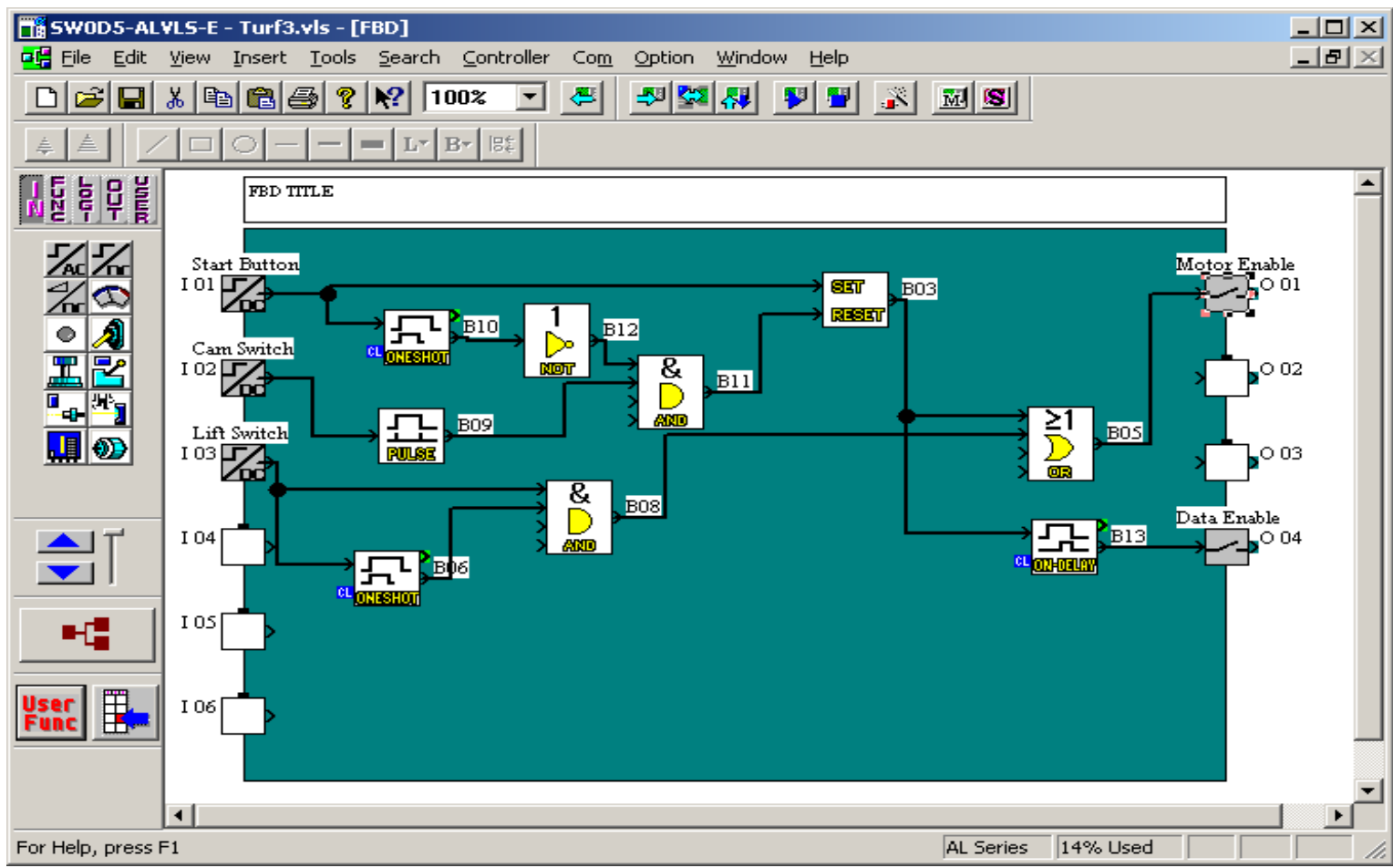


Figure 5.21 Visual Logic Software screen capture

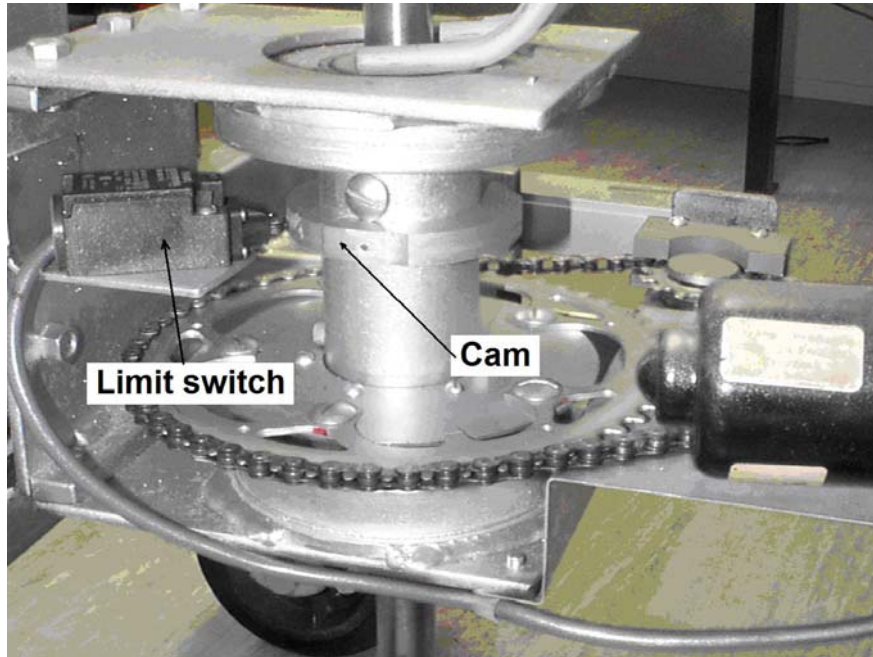


Figure 5.22 Main drive Cam limit switch

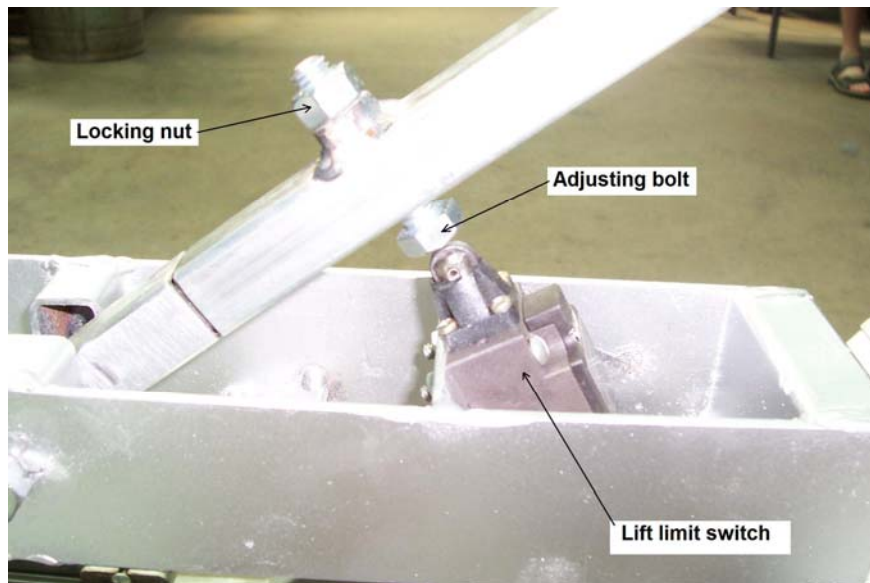


Figure 5.23 Lift limit switch

preset time period (One Shot B06) to return the main shaft to the start position ready for the next test.

5.3.1.3 Relay and Limit Switches

The relay (Figure 5.19) is included in the circuit to supply power to the electric motor to protect the Alpha controller's internal relay contacts from arcing when switching high current due to large loads or fault conditions.

The limit switch in Figure 5.22 is used to indicate when the main shaft, and therefore ground engaging foot, has rotated through approximately 150 degrees while in contact with the turf surface. At this point the controller disconnects power to the relay which in turn disconnects power from the motor.

The lift limit switch is activated when the roll pin on the main shaft is raised above the supporting plate. This height is adjusted using the bolt and locking nut shown in Figure 5.23. This limit switch provides the signal for the controller to supply power to the motor to rotate the main drive shaft to the start position.

5.3.2 Instrumentation

The electronic instrumentation consists of:

- a 100kg load cell;
- a commercially available digital indicator from Ranger Instruments;
- and
- a laptop computer.

The load cell (Figure 5.24) is attached to the frame and an idler sprocket within the main drive chain system. The torque required to rotate the ground engaging foot is translated directly into the tension in the chain. An increase in torque causes the chain to straighten. By positioning this idler sprocket relative to the fixed sprockets the vector sum of the tensional forces in the chain (Figure 5.25) is measured using the load cell as a cantilever. An

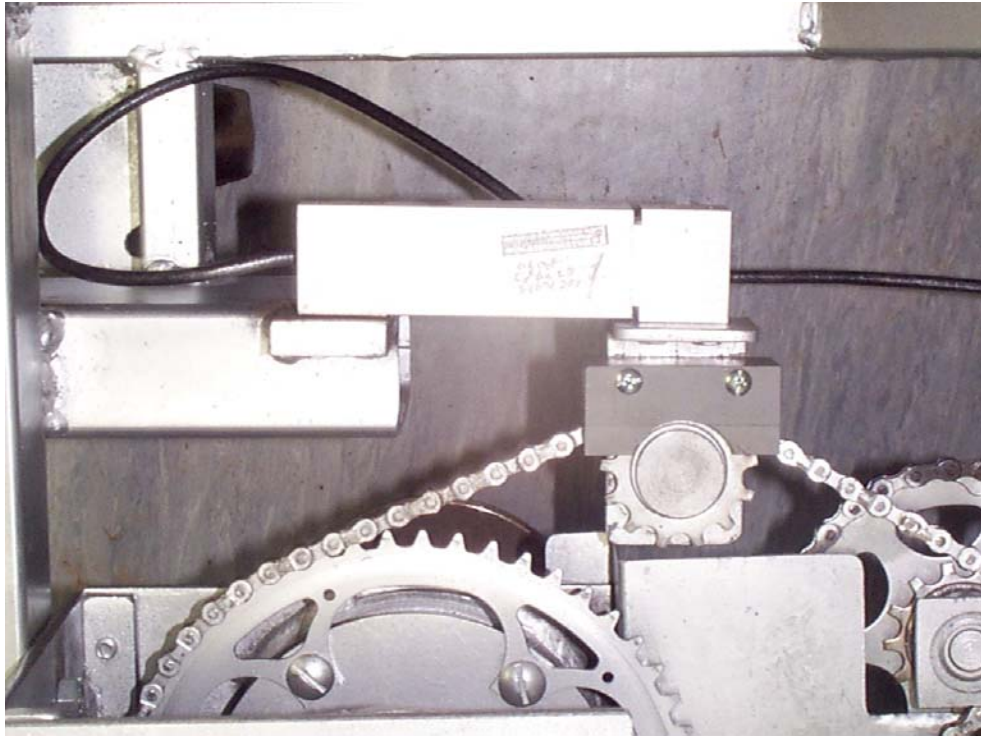


Figure 5.24 Load Cell mounting and idler sprocket

adjustable stop has been included (not shown in Figure 5.24) to limit bending and therefore protect the load cell in the event of jamming or excessive loads.

A torque value is determined from the radius of the large sprocket and the tension in the chain, i.e.

$$\text{Torque} = \text{Force (tension in chain)} \times \text{Distance (radius of drive sprocket)}$$

As there is a linear relationship between the force measured by the load cell and the torque required to rotate the drive shaft, the digital indicator is calibrated to display the torque value directly. Although the digital indicator has an option to display the maximum or peak value (allowing the unit to be used without a computer), the serial RS232 interface is utilised to capture a continuous stream of data. The serial data protocol is 4800 baud, 8 data bits, 1 stop bit and no parity.

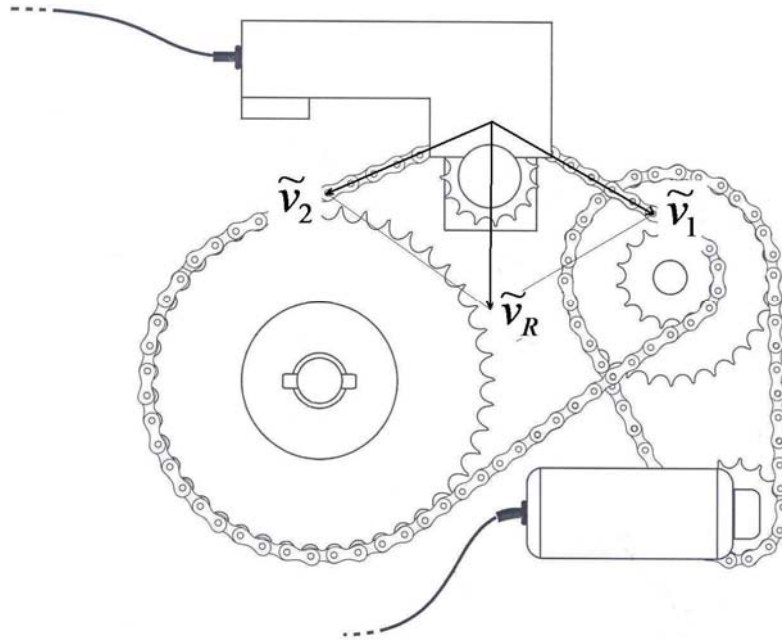


Figure 5.25 Vector diagram for loading the loadcell

The two serial data output options for the digital indicator include continuous data streaming at approximately 10 samples per second or by polling the instrument up to a maximum of 25 samples per second. The option selected was to output data continuously such that the serial data output combined with a computer allows continuous recording of data during the testing operation. This ensured a consistent data sampling rate and therefore a repeatable number of data points for each test which is independent of computer hardware and software. A computer program reads the serial data for each test, formats and records the data in a .csv file. A data profile for three different turf species was produced using Microsoft Excel is shown in Figure 5.26.

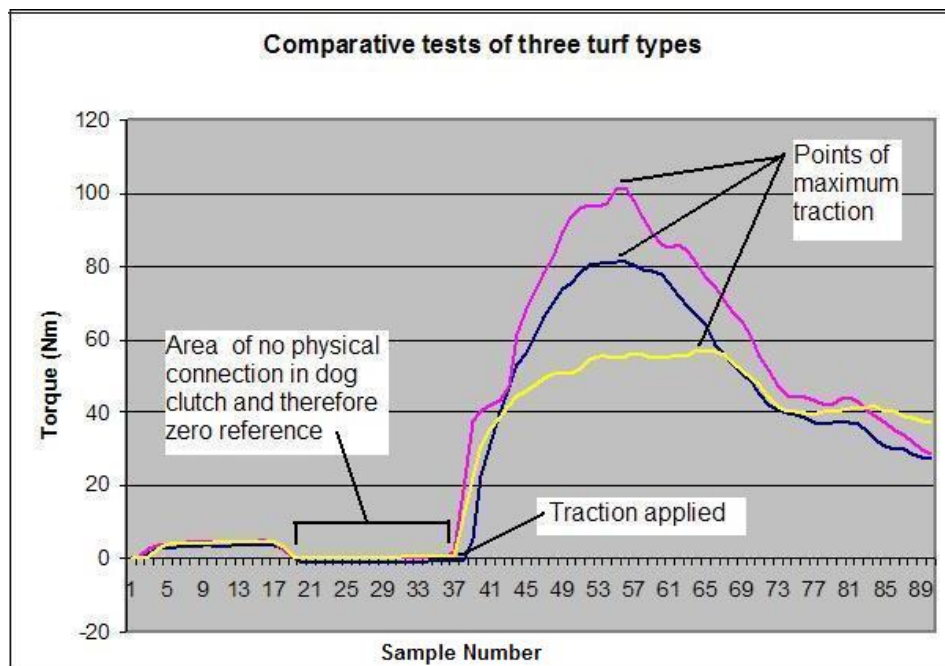


Figure 5.26 Data profiles of three turf species using Microsoft Excel

5.4 Data processing and storage

The software (Appendix A) was developed using Borland C++ Builder to capture, format and store serial data from the Ranger 2000 unit. The program is based on the windows environment (Figure 5.27) and consists of four parts namely:

- setting the filename and path for the .csv file
- opening and changing the serial port settings
- ASCII data and graphical representation and storage
- data analysis

5.4.1 File management

The ability to change or modify the data filename is built into the software. When the program is executed a default filename is created and all data will be stored in this file unless the filename is changed or the program is restarted. The data file will also be saved in the current directory unless changed.

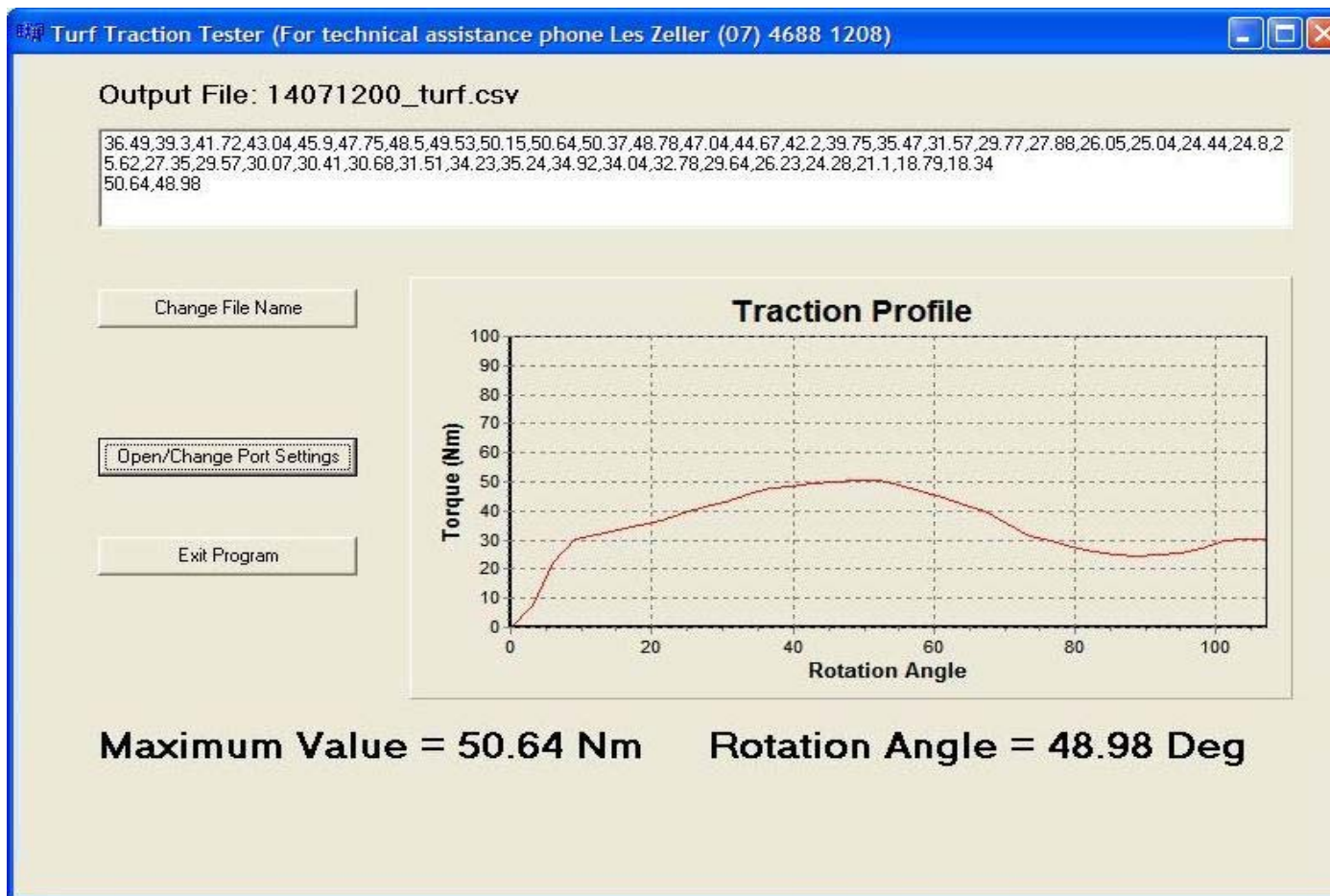


Figure 5.27 Main program window

A button on the main program window allows the user to change the output filename (Figure 5.27, *left hand side*), the default filename string is made up of the time and date that the program is executed followed by a descriptor to indicate a turf data file, i.e. in the form:

`ddmmhhnn_turf.csv`

where `dd` represents the day of the month 01 – 31

`mm` represents the month of the year 01 – 12

`hh` represents the hour of the day 00 – 23

and `nn` represents the minute of the day 00 – 59

5.4.2 Serial port management

The software also provides the ability to change the parameters associated with the data transfer between the Ranger Instruments 2100 and the computer (Figure 5.28). This allows the program to be run on computers with different hardware configurations eg. some newer computers have USB ports rather than an RS232 interface. This option also gives the ability to utilise Bluetooth if required.

5.4.3 Data presentation and storage

Data flow between the Ranger Instruments 2100 and the computer is managed by the Alpha controller and is enabled only during a traction test. The data is read into a buffer for temporary storage and then processed and saved in the output file at the completion of each test. A timer within the program acts like a retriggerable monostable (Floyd 1982) with each character received resetting the timer. This section of the software is used to determine the end of each data set by detecting when the data flow ceases. The data is displayed within the main program window in both ASCII characters and graphically displaying a traction value profile of torque in Newton metres with respect to rotational angle in degrees (Figure 5.27).

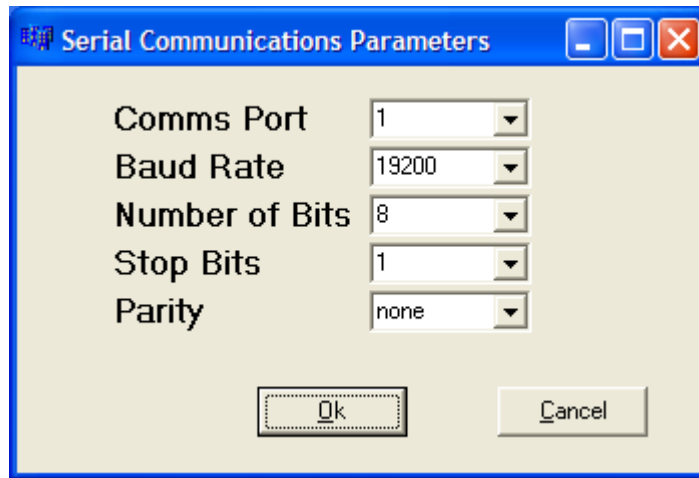


Figure 5.28 Change serial interface parameters window

5.4.4 Realtime data analysis

The maximum traction reading and its rotational angle for each test is displayed on the main program window (Figure 5.27). The maximum value is determined by:

- initially setting the maximum value to zero; and
- comparing each value in turn and updating maximum value if the current value is greater.

The method for determining the rotational angle to maximum is based on the following:

- the maximum rotation of the ground engaging foot while in contact with the turf is 150 degrees; and
- the speed of rotation remains constant within the maximum range of turf traction testing system.

The algorithm within the source code for determining rotational angle is:

```
FormatFloat("#.00",150.0/(data.size()-minIndx)*(maxIndx-minIndx));
```

where `data.size()` is the total number of data points within the data set for the test.

`minIdx` is the data point position where the rotational torque is first applied to the turf after the ground engaging foot is in contact with the turf.

`maxIdx` is the data point position of the maximum data value within the data set.

Therefore the total angle of rotation is divided by the number of data points representing this angle determine the value of degrees per data point (for example, 150 degrees divided by 50 data points result in 3 degrees of rotation per data point). This value is multiplied by the number of data points of rotation until the maximum value is reached. The instruction within the program formats the resultant value with two decimal places for displaying on screen and storage within the data file.

5.5 Conclusion

This chapter has described the design and operation of the components of the turf traction tester. Figure 5.29 shows the complete assembled turf traction testing machine. The external dimensions (excluding the handle) are 1010 mm long, 600 mm wide and 680 mm high; and the total mass including batteries and lifting weights is 108 kg. The mass of the Turf traction testing machine frame disassembled for transport is 52 kg. The final design meets the criteria defined in the system requirements specified in chapter 4.



(a) Original prototype



(b) Final prototype with lifting parallelogram

Figure 5.29 Automated Turf Traction Testing Machine

ERROR ANALYSIS AND CALIBRATION

6.1 Introduction

The turf traction testing device described in this thesis has been designed to provide better accuracy, repeatability and operator safety than other currently used equipment. This chapter describes and quantifies the potential measurement errors and the calibration procedure.

6.2 Sources of Errors and Error Analysis Procedures

The measurement of traction is a physical parameter which defines the amount of resistance the turf surface structure can provide. This turf traction testing device derives a value for traction from the tension in the drive chain using a load cell (Figure 5.24). The errors associated with the design of the turf traction tester include:

- load cell errors,
- errors in the instrumentation system ,
- errors due to the method and mechanics of loading, and
- errors due to calibration.

From previous turf research in Australia (Loch 2003) the maximum traction values for turf species used on sporting fields range between 50 and 90 Nm. Preliminary investigations (Henderson, et al. 2004) indicate that the ideal maximum value for traction for Australian sporting surfaces is 60 Nm. Therefore error analysis of this machine has been quantified for the range of 50 Nm to 100Nm.

The load cell and instrumentation used for measuring and quantifying traction are commercially available and errors associated with each are documented in the manufacturer's specifications and are quantified in section 6.3. Systematic errors, or errors associated with the method of taking measurements, are described in section 6.4. The calibration procedure and errors associated with the calibration process is described in section 6.5.

6.3 Load cell and instrumentation errors

The load cell used is a LOC-AL-100kg ME which is a medium capacity single point aluminium load cell (Appendix B). The sensitivity or output specification is 2mV/V excitation and the specified combined error for this load cell is 0.025% of rated load, i.e. ± 25 g for this load cell.

A Ranger Instruments 2100 industrial digital indicator is used to amplify, scale, digitise, display the signal from the load cell and transmit an ASCII data string to a laptop computer. It is a general purpose digital indicator with specialised weighing functions, for example, live weight measurement, hold and peak hold, totalising and counting.

The accuracy of measurements relate directly with the measurement resolution and errors due to non-linearity, noise, stability and drift of the electronics. The Ranger Instruments 2100 has a quoted resolution of 1 in 30000 (0.003%) or 25 μ V/division (Appendix C). The non-linearity and noise are specified as <20ppm (e.g. <0.002%) and <0.2mVp-p respectively. This equates to a maximum noise error of 0.8mV for an excitation voltage of 8V, therefore the maximum percentage error due to noise at 100Nm is $\pm 0.625\%$ and at 50 Nm is $\pm 1.28\%$. Two thermal stability coefficients are quoted for zero and gain or span of <0.1 μ V/ $^{\circ}$ C and < 8 ppm/ $^{\circ}$ C respectively. This equates to a zero error of 0.0125% and a gain error of 0.016% over a 20 $^{\circ}$ C temperature range.

6.4 Systematic errors

Systematic errors are distortions of the results of measurement which lead to measured values being systematically biased one way or the other. All measurements are prone to systematic error or biasing effect, either produced from the environment, methods of observation or instruments used. These errors are introduced into an experiment such that they always affect the results in the same way.

To derive traction, the forces acting on the chain are measured using the load cell and an idler sprocket (Figure 5.23). The driving force produced by the motor to cause the ground engaging foot to rotate is represented by vector \tilde{v}_1 and the force due to the resistance of the turf surface is represented by vector \tilde{v}_2 (figure 6.1). These force vectors are acting in the one chain, but in opposing directions, the tension in the chain is a direct indicator of the resistance or traction being provided by the turf. As the idler sprocket is free to rotate, $|\tilde{v}_1| = |\tilde{v}_2|$ (assuming there is zero friction), therefore the direction of \tilde{v}_R will bisect the angle between the vectors \tilde{v}_1 and \tilde{v}_2 . The measured traction value is the resultant vector sum \tilde{v}_R of these two vectors.

The drive system was designed so that the relative positioning of the main drive sprocket, the intermediate and idler sprockets in the main drive chain ensures that the resultant vector \tilde{v}_R acts in a direction near to perpendicular to the load cell. Therefore the error due to the resultant vector not being perpendicular to the load cell is the cosine of the angle difference and is compensated for during the calibration of the instrumentation.

Once calibrated the only possible errors relating to the load cell over the operating range would result from changes in the direction of the resultant vector or changes in friction of the bearings. As the drive sprocket positions

are fixed any variations could only result from movement of the idler sprocket during loading. To quantify this, the average amount of deflection was determined by applying 100 Nm to the main drive shaft ten times and measuring the deflection of the load cell using feeler gauges. The average deflection of the load cell at 100kg was 0.45mm. Figure 6.1 and 6.2 shows the change in position of idler sprocket and loading vector angles due to bending of the load cell when loaded with 100kg. This deflection equated to a maximum angle change between vectors \tilde{v}_1 and \tilde{v}_2 of 0.361° (Figure 6.2) therefore the effective change to the resultant force vector \tilde{v}_R is a factor of 5×10^{-6} or an error of 0.0005%.

Another error is due to friction in the bearings in the drive system. It appears as an offset in the recorded data which can be corrected for by subtracting from each data point within each data set during data processing. This offset value is identified by approximately 18 reading that directly precede the sharp rise in traction values as the dog clutch engages.

6.5 Calibration

The instrumentation is based on the measurement of the tension in the drive chain. It uses a load cell as the transducer and a Ranger Instruments digital indicator for signal conditioning, amplification and displaying the data. Therefore calibration is a matter of following the calibration method for Ranger Instruments R2100 digital indicator (Appendix D), for example, measuring and setting the offset to zero for a no load reading and then applying a known calibration load at near maximum capacity to adjust and set the gain. To do this a moment arm and calibration weight is used to apply a known torque (Figure 6.3). The turf traction tester is rolled onto its side so that the loading arm is acting in the vertical plane and utilising gravity to provide the calibration torque. This torque loads the drive chain which then applies a force, via an idler sprocket, perpendicular to the canter lever action

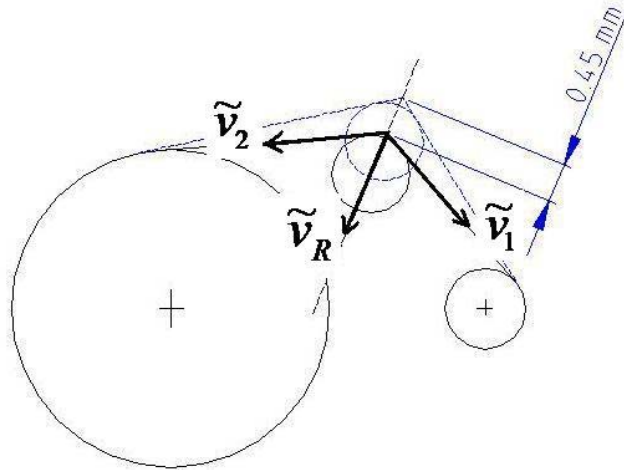


Figure 6.1 Vector diagram of forces showing angle variation of vectors at maximum load

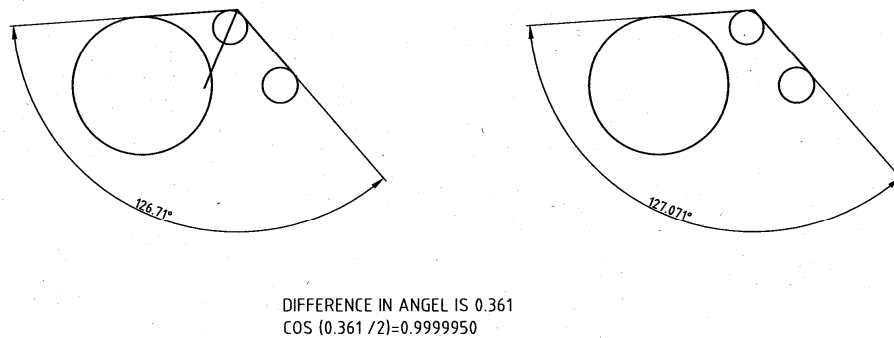


Figure 6.2 Determination of angle change by measuring angle between tangents for change in idler sprocket position.

of the load cell to produce a torque reading. This process is followed by rechecking the zero and intermediate load values to test linearity.



Figure 6.3 Calibration weight and loading arm

The method for applying the calibration loads involves:

- removing the studded foot plate and weights system;
- turning the turf tester onto its side;
- fixing the calibration loading attachment and loading arm (Figures 6.4 and 6.5); and
- applying a calibration weight to the loading arm (Figure 6.3).

The torque value entered for the calibration routine is determined by measuring the moment arm lengths and forces applied by the loading arm itself and the calibration weight. The value of torque is the product of the applied force multiplied by the moment arm length. For example, the moment arm length and force for the loading arm is determined by finding its centre of gravity from its point of balance and measuring the distance from this point to the centre of the main drive shaft. The force is determined by measuring the mass of the loading arm and multiplying by the acceleration due to gravity. The moment arm and force due to the calibration weight is determined the same way. The total torque for the calibration is the sum of these torque components.



Figure 6.4 Calibration loading nut



Figure 6.5 Calibration loading arm attachment

6.6 Conclusion

This chapter has discussed the possible measurement errors and the calibration method.

The absolute maximum quoted errors in the product specifications for both the load cell and instrumentation that affect the measurement accuracy for short term operation are 0.025% and $\pm 1.28\%$ respectively within the operating range specified in section 6.2. The errors relating to creep (load cell) and thermal stability coefficients (both) relate to long term operation and therefore do not affect the reading accuracy over the 10 second period of each test. As an offset is recorded and subtracted from the data during processing these effects can be ignored when comparing different data sets.

The systematic errors discussed in section 6.4 are either insignificant compared to the maximum noise error specifications of the instrumentation or also accounted for during the data analysis as an offset.

From the mechanical design and components used, the anticipated measurement error at full machine capacity of 100 Nm was $\pm 0.63\%$ or a traction error value of ± 0.63 Nm and a maximum error over the specified operating range of $\pm 1.28\%$.

EVALUATION AND PERFORMANCE TESTING

7.1 Introduction

As previously stated, the turf traction testing device was designed to provide better accuracy, repeatability and operator safety than that provided by other equipment in current use. This chapter describes the performance objectives, methodologies and results of the evaluation of the turf traction tester.

7.2 Performance objectives

To determine the ability of this equipment to meet the design objective to measure traction more accurately than existing equipment, three experiments were conducted. The purpose of the experiments was to determine if the turf traction tester could:

- A. detect differences in traction levels for different turf surfaces;
- B. differentiate between turf varieties with a high degree of confidence;
and
- C. detect a difference between sporting surfaces of the same turf variety but having other varying traits.

7.3 Evaluation with respect to detecting variations in traction levels (Performance Objective A)

To determine this equipment's ability to measure traction, tests were conducted of five turf varieties grown on experimental plots at DPI&F's Redlands Research Station. The results were compared with data recorded during research for Sport & Recreation Queensland (Loch 2003) using a similar device to that developed by Canaway & Bell (Canaway & Bell 1986).

The five turf grass species were chosen because previous maximum traction values for these turf varieties spanned the range specified for the design of this equipment. Also the plant physiology differed sufficiently between selected turf varieties so that variations in traction results could be explained by these physiological differences (Loch 2003).

7.3.1 Results

The results of testing five turf varieties are shown in Figure 7.1 and compared with data collected from a report on turf grass (Loch 2003) in Figure 7.2.

7.3.2 Discussion

The turf traction tester produced different traction profiles for different turf varieties (Figure 7.1). These results demonstrate the five data profiles representing the traction values for each turf variety as the device rotates the ground engaging foot through approximately 150 degrees. Turf variety SS2, recording the highest maximum value of 86.4 Nm and El Toro the lowest, with a maximum value of 59.5 Nm.

Figure 7.2 compares the maximum traction readings recorded using the automated turf traction tester under evaluation and the Canaway device described in the Chapter 3. Soil moisture, Clegg Hammer, penetrometer and shear tests were not able to be performed at the time therefore the comparative data in Figure 7.2 can only be used as a guide. However, data collected using the two devices differed by less than 6% for three of the five turf grasses tested and by 9% and 16% for the other two turf varieties. Both devices indicated Aussiblu to have a maximum traction value at least 35% higher than El Toro.

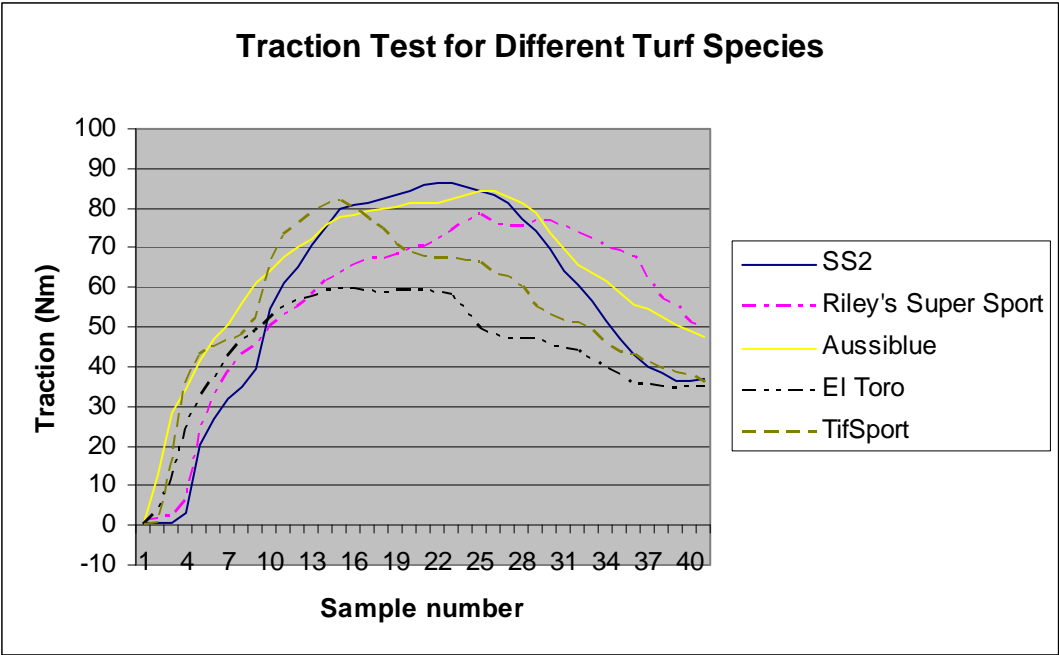


Figure 7.1 Turf traction tests for 5 turf varieties.

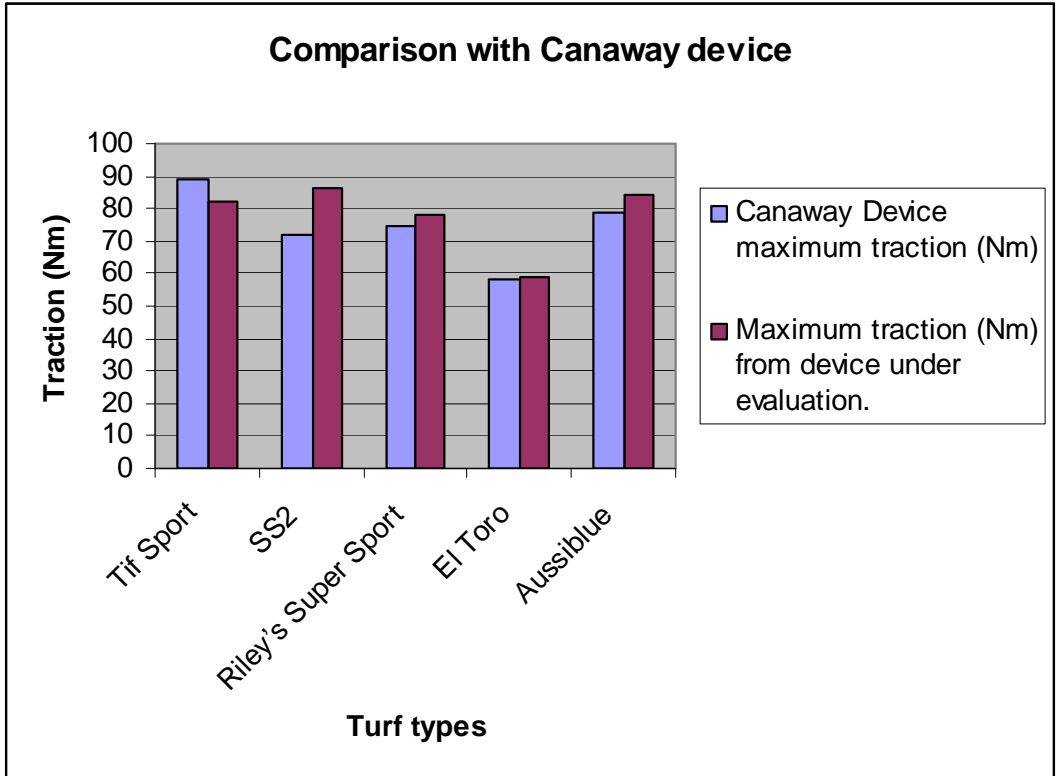


Figure 7.2 Maximum traction results for different turf varieties.

7.3.3 Conclusion (Performance Objective A)

The automated turf traction testing device under evaluation produced results that were comparable with previous data collected using the Canaway device (Canaway & Bell 1986) for measuring traction for different turf species. The discrepancies in Figure 7.2 may be due to natural variability within each turf species or other parameters, for example ground moisture content, or systematic errors in measurement in either or both measuring systems. This test demonstrated that the automated turf traction testing device has some ability to measure the traction property of turf sporting surfaces. The question this raises is to what degree of accuracy and repeatability can this device measure traction.

7.4 Evaluation with respect to detecting turf varieties (Performance Objective B)

The second objective investigates the potential use of this device to differentiate between turf varieties.

7.4.1 Rationale

Seasonal climate, for example temperature, humidity and rainfall, varies between sporting fields across the country and around the world. For example the Australian Football League (AFL), season which is predominately an autumn and winter sport, is played on sporting fields in most Australian states. The winter climate in Victoria is considerably different from that in Queensland and this will affect the growth and physical properties of the turf. To minimise the risk of injury, climate conditions should be taken into consideration for the selection of turf grasses for sporting fields. Therefore research is required to determine the most suitable turf variety which provides the optimum traction levels for each geographic

location. This highlights the need for a turf traction measurement device with the required resolution to discriminate between different turf varieties. The following experiment was conducted to determine whether the equipment described in this thesis has the necessary accuracy and repeatability to enable differentiation of turf varieties.

7.4.2 Method

Data sets were collected from 10 tests performed on each of three turf varieties selected from data collected in section 7.3 which spanned the operational range of the equipment under test. The varieties selected were:

1. Riley's Super Sport;
2. El Toro; and
3. Tif Sport;

grown on experimental plots at DPI&F's Redlands Research Station.

The varieties selected were chosen because the plant physiology differed sufficiently such that a statistically valid difference in traction should be detected if the turf traction tester met the design specification, e.g. to be able to discriminate between turf varieties.

The data sets were analysed using Microsoft Excel and GenStat[®] (a statistical analysis computer program) to determine if the turf traction tester can discriminate between turf varieties. The results are presented in a graph showing all data points, a table of the analysis of variance (ANOVA) and a boxplot (also known as a box-and-whisker diagram) which is a convenient way of graphically representing five statistical values for a numerical data set, for example, the smallest and largest observations, each of the four quartiles (25 percent of data valves) and the median.

The results are shown in Figures 7.3, 7.4 and Table 7.1. All data points from testing three turf varieties with 10 replicates are shown in Figure 7.3.

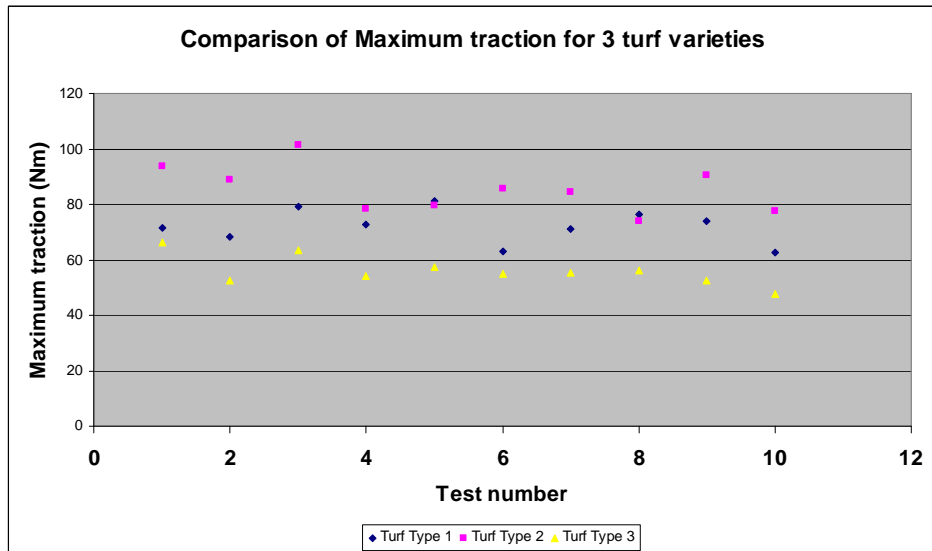


Figure 7.3 Turf traction comparison of 3 turf varieties.

7.4.3 Results

Figure 7.4 is a boxplot giving a graphical representation of the data. Table 7.1 is the analysis of variance output from GenStat®.

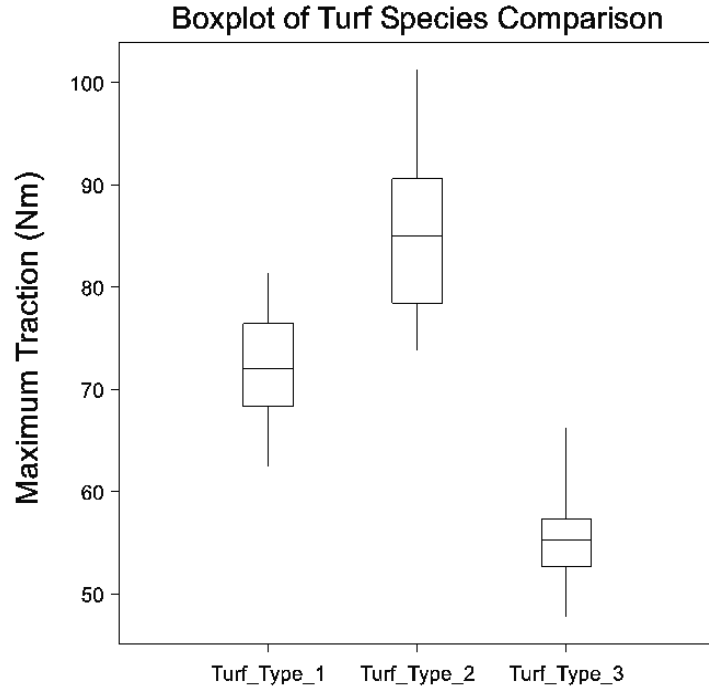


Figure 7.4 Boxplot showing comparason of 3 turf varieties. (explanation of boxplot in section 7.4.2)

7.4.4 Discussion

Figure 7.3 is a graph produced using Microsoft Excel of the maximum values for 30 traction tests from three turf varieties. The data for each turf type is represented by a different colour in the graph and shows that the data falls into three regions, for example, 62 to 81 Nm for turf type 1, 74 to 101 Nm for turf type 2 and 48 to 66 Nm for turf type 3. The boxplot in Figure 7.4 shows that there is little overlap of data for each turf variety indicating that the data may be from three different sources. An ANOVA was performed on the maximum traction data from 30 tests, 10 tests from each of three turf varieties. These results were produced using GenStat[®] and show the means for each data set to be 72.01, 85.34 and 56.07. This analysis also shows the least significant difference (LSD) of 6.25 and the F-test producing a *P* value of <0.001.

7.4.5 Conclusion (Performance Objective B)

The aim of this objective was to determine whether the turf traction tester being assessed can discriminate turf varieties with a high degree of confidence. The experiment described in section 7.3 also assists to assess the degree of repeatability to be expected from a traction testing machine.

The experimentation and analysis to assess the Performance Objective B showed statistically that value of *P* indicates a confidence level of greater than 95% and a least significant difference (LSD) of 6.25. Because the LSD is smaller than the difference between any two mean values indicates that there is a statistically significant difference (at the 95% confidence level) between all three varieties tested and that this device meets this performance objective.

7.5 Evaluation with respect to measuring variability within and between sporting fields (Performance Objective C)

The playing surface of a sporting field may be over 0.5 hectare in area which may vary in compaction, soil type and moisture content. In some instances the turf is over-sown with another turf species as a management practice to change the turf properties. As the turf traction is dependent on ground moisture and mowing height, a device that can measure the traction variability across a sporting field enables management systems to produce a more consistent playing surface. The following experiments to assess Performance Objective C were conducted to determine whether the variability within and between sporting fields could be measured and whether historical information or other surface properties could explain these differences.

7.5.1 Method

Tests were performed at multiple sites on two elite sporting fields (Suncorp and ANZ Stadiums in Brisbane) which have the same turf variety and climatic conditions, and the data analysed using statistical methods. The data sets were referenced geographically using Global Positioning System (GPS) technology or by permanent markings within the sporting field.

The three experiments were:

- Data collected at each stadium at 10 metre intervals along the length of the field (a) 10 metre inside western sideline and (b) parallel to the sideline along the centre line of the field to test variability between sporting fields.
- One hundred evenly distributed measurements across Suncorp Stadium were recorded and analysed to assess the turf traction tester's ability to measure variability within a sporting field.

- Data also collected from both the northern and southern ends of Suncorp Stadium to assess the effect of shading on traction readings.

7.5.2 Results

A summary of data collected from ANZ and Suncorp Stadiums showing averages, maximums, minimums and standard deviations is shown in Table 7.2. Comparative traction results are shown in a histogram (Figure 7.5) and Figure 7.6 is a boxplot providing a graphical representation of the statistical analysis of this data.

Field variability is graphically represented in Figure 7.7 showing contour plots produced using Surfer[®] version 7 from traction data collected at Suncorp Stadium. Figure 7.8 is a GPS referenced representation of the traction data collected at ANZ Stadium. Figure 7.9 shows colour and near infrared (NIR) aerial images collected from the northern end of ANZ Stadium to highlight areas of difference. Figure 7.10 is a bar graph showing traction data collected to investigate the effect of shading at Suncorp Stadium.

Table 7.2 Summary of maximum traction data from Suncorp and ANZ.

	ANZ Stadium [Nm]	Suncorp Stadium [Nm]
Average	63.9	60.3
Standard Deviation	6.1	5.7
Maximum	79.1	69.8
Minimum	50.8	49.3

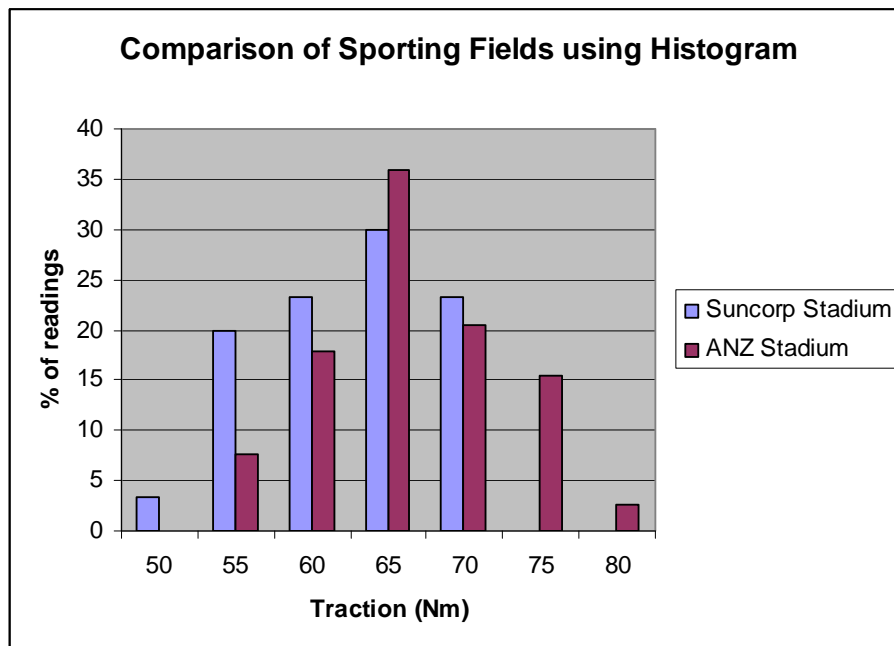


Figure 7.5 Turf traction results from Suncorp and ANZ Stadiums

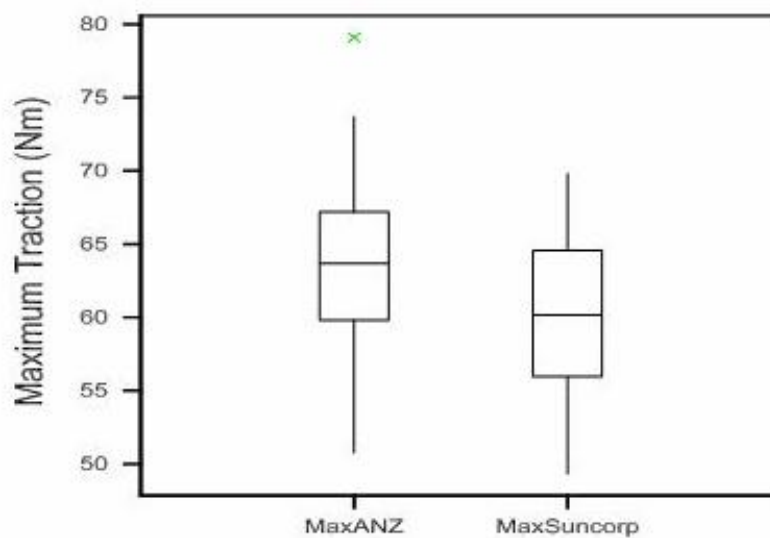


Figure 7.6 Boxplot of data from ANZ and Suncorp Stadiums
(explanation of boxplot in section 7.4.2)

Suncorp Traction Variability (Nm)

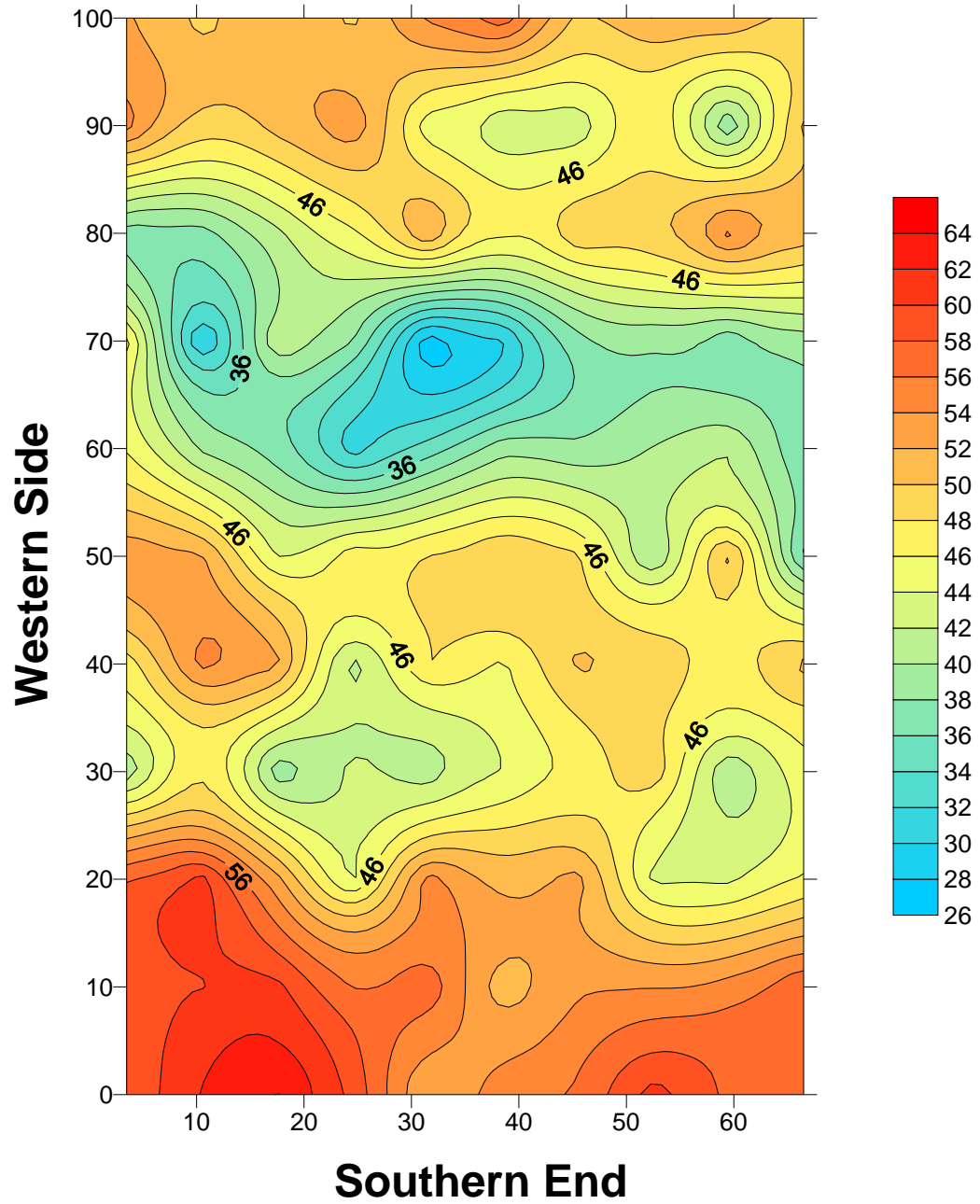


Figure 7.7 Field traction variability of Suncorp Stadium

ANZ Stadium - February 2004

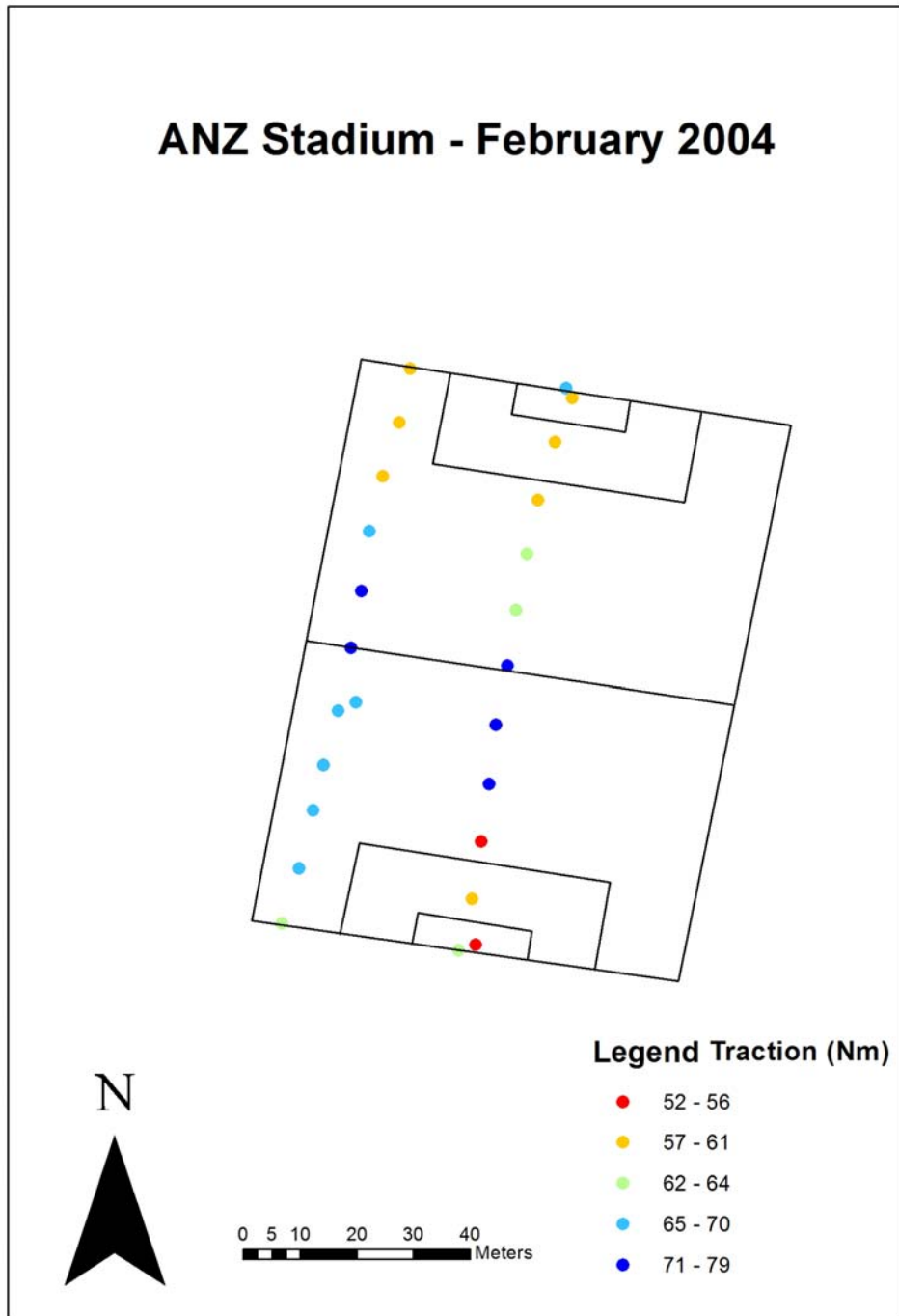
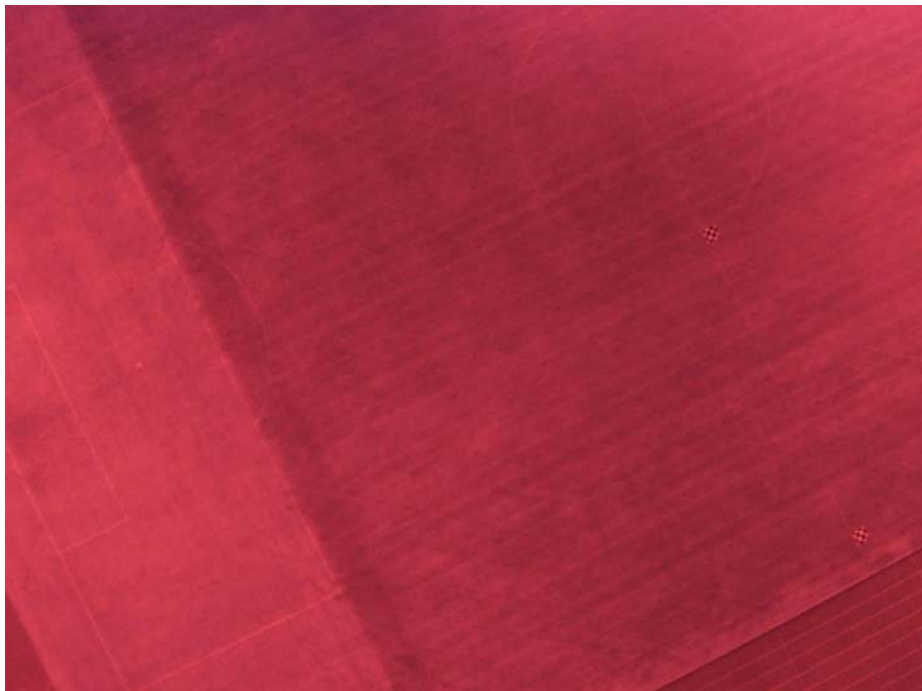


Figure 7.8 Maximum traction data from ANZ Stadium (the field orientation is not directly north-south).



(a)



(b)

**Figure 7.9 Aerial images of northern end of ANZ Stadium
(a) colour and (b) near infrared, in which both images are of the same
area of the sporting surface.**

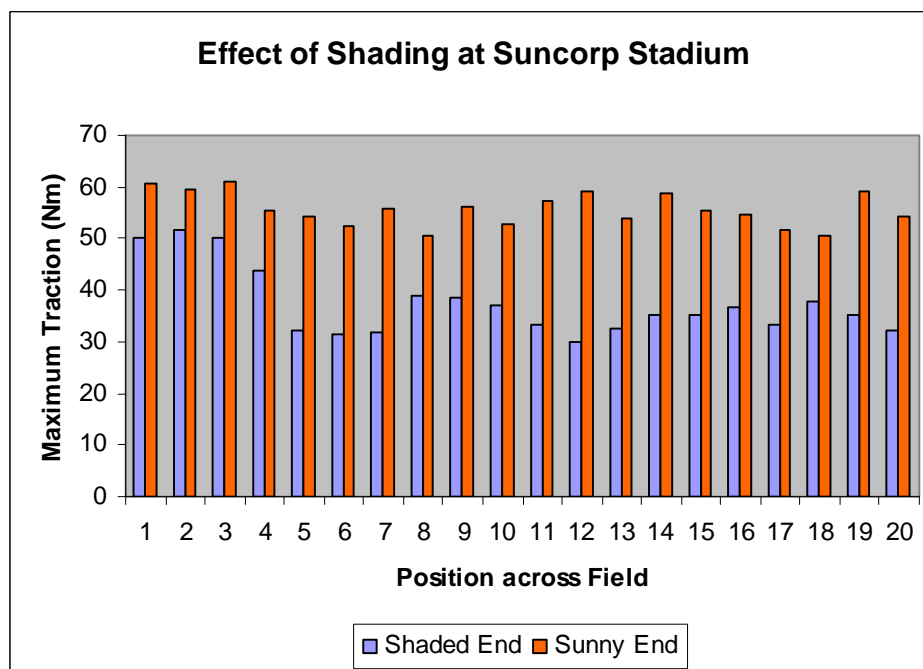


Figure 7.10 Effect of shade on traction at Suncorp Stadium

Table 7.3 Analysis of shading effect on traction from Suncorp Stadium

	Southern end (Sunny) [Nm]	Northern end (Shaded) [Nm]
Average	55.7	37.3
Standard Deviation	3.3	6.6
Maximum	61.0	51.6
Minimum	50.5	29.8

7.5.3 Discussion

To test variability between sporting fields data sets were collected from ANZ Stadium and Suncorp Stadium in February 2004. The turf at Suncorp Stadium was replaced in the preceding year. The sporting fields have the same turf variety but differ in age and management. The results are presented in a box and whisker plot in Figure 7.6 and show the data from ANZ Stadium to be on average higher than Suncorp. The results show 20% of the

readings, from ANZ Stadium, are greater than the maximum reading from Suncorp (Figure 7.5). This is probably due to the turf root systems at Suncorp being less established at the time. Analysis of the two data sets using a T-test in Microsoft Excel gave a probability of 0.015 indicating that the two sets of data are statistically different.

The results of testing geo-referenced multiple sites at ANZ Stadium are shown in Figure 7.8. The data from ANZ Stadium showed an area of high traction crossing the centre of the field and offset by approximately 30 degrees to the half way line. This area is a slight ridge that crosses the field where the water would run off and therefore have lower ground moisture and higher traction.

Traction data from the northern end of the field was found to be much less than the field average. This is because the turf at the northern end was recently planted and the root system was not as established as the rest of the field. Aerial colour and near infrared images in Figure 7.9 were taken at the time of testing verify these results. These images are of the northern goal area and the colour image distinctly shows the grass to be greener while the near infrared image shows this area to be brighter indicating more vigorous growth as would be evident with new turf (Campbell 2002).

Figure 7.7 shows the field variability of traction data at Suncorp Stadium in August 2004, and indicates areas of lower traction at the 30 metre lines (this is probably an effect due to watering practices) and the highest traction at the southern end (is likely due to lower ground moisture from maximum sun exposure). These traction values are less than the readings in the field comparison because of seasonal variability, for example, lower ambient temperatures in August, higher ground moisture and more shading effects.

The effect of shading is shown in Figure 7.10 which clearly demonstrates the data from the sunny or southern end of the field has higher traction than the

shaded or northern end. There is minimal overlap of the data and a T-test showed the probability P to be 9.11×10^{-12} and therefore a highly significant difference between shaded and non-shaded areas.

7.5.4 Conclusion (Performance Objective C)

This evaluation showed evidence that the turf traction tester can differentiate traction properties for the same turf species within one sporting field and between sporting fields that relate to variability of other parameters, for example, mowing height, ground moisture, turf maturity etc.

CONCLUSION

This thesis describes the development of a turf traction measuring device and provides the evidence that demonstrate how this machine meets the objectives of this project. The ability to accurately measure the traction of turf sporting surfaces will allow sporting field curators to optimise surface conditions to minimise injuries while maximising sporting performance.

8.1 Project Conclusions

The project objectives defined in Chapter 1 were to develop a device to measure traction with more accuracy, more repeatability and with greater operational safety than equipment that is currently commercially available. Chapters 2 to 5 describe the background and the design and development of a prototype automated turf traction testing machine to meet these objectives. Chapters 6, 7 and 8 analyse and quantify the ability for this design to meet these objectives.

- **Objective 1:** Develop a device which measures the traction of turf surfaces with better accuracy than commercially available systems to a level of approximately $\pm 1\%$.

Chapter 3 showed that the potential errors for the Canaway and McNitt devices range from 3% to 13%. Error analysis of the prototype described in chapter 5 showed that the dominant error potential is noise with all other error sources being insignificant. The maximum error due to noise at 100 Nm of traction is $\pm 0.66\%$ although this figure increases as the traction decreases due to the

signal to noise ratio. Data presented in the Sure Play report (Henderson et al. 2007) indicate a value of 60Nm as the safe maximum traction level in Australia for sporting surface design and maintenance. In Australia the common problem is too much traction causing injuries, therefore the important range of operational accuracy for this device is between 60 and 100 Nm. My error analysis for this prototype over this range has a combined error of between ± 0.66 and $\pm 1.08\%$. Therefore the objective of developing a turf traction measuring device with improved accuracy of approximately $\pm 1\%$ has been achieved.

- **Objective 2:** Develop a device which measures the traction of turf surfaces with high repeatability.

There are two areas relating to repeatability, the first is repeatable operational procedure and the second is repeatability in measuring and quantifying the value of traction.

The measurement process in the device described in this thesis is mechanised and automated, for example the drop height remains constant for each test, the main drive shaft is vertical during rotation of the ground engaging foot and its rotation speed is constant. This is a large improvement on the manual Cannaway device and addresses the issues raised by McNitt (McNitt et al. 1997).

The instrumentation component in this device has good repeatability as it relies on measuring the tension in the chain, where the moment for the torque measurement (radius of main drive sprocket) remains constant, and the chain tension is measured using a load cell with a specified non-repeatability of 0.02%.

These factors ensure the repeatability of this device and meet the objective of improving the repeatability of traction measurement.

- **Objective 3:** Develop a device which improves the operational safety for turf traction measurements.

The inclusion of a lever in the design eliminates the need for the operator to lift the 46kg mass. To lift the weights the operator applies approximately 12kg force (116N) in a downward direction. The ability to remove the weights for transportation is also a design feature.

The lifting mechanism and removable weights meet the objective of improving the operator safety.

8.2 Further Work & Enhancements

There are a number of other parameters that also affect the quality of the playing surface, therefore a future machine could incorporate other sensors, for example, penetrometer or Clegg Hammer to indicate hardness, and a capacitance probe to measure ground moisture. The instrumentation and control system could also be incorporated into one device to simplify wiring and improve efficiencies such as power requirements.

8.3 Mechanical Optimization

The device described in this thesis is a prototype which was designed to use existing stock and cheap locally available components. In the process of developing a commercial product the physical dimensions of the structure would be optimised using finite element analysis to meet size, strength and rigidity specifications.

8.4 Incorporated Calibration Facility

The calibration method described in section 6.5 is time consuming and introduces friction which is non-existent in the normal operating mode. It requires multiple loading and unloading of weights to ensure friction is not affecting the readings. By incorporating a hydraulic ram to apply a load to the main drive chain and a pressure transducer to provide feedback, a calibration system could be developed which simplifies the procedure and eliminates frictional effects.

8.5 Spatial Mapping Facility

Currently the data is mapped manually which is also time consuming. By incorporating a global positioning system (GPS) receiver, geo-referenced data will automate and simplify the production of contour maps that allow visual quantitative feedback for responsive and appropriate modifications to management practices.

8.6 Conclusion

This device has been used extensively for the past three years to monitor traction levels of sporting fields and evaluating the impact of management practices on sporting surfaces. It has improved the efficiency and reliability of data collection while meeting the objectives of accuracy, repeatability and operational safety.

References:

- Aldous, DE & Chivers, IH 2002, *Sports turf & amenity grasses: a manual for use and identification*, Land Links Press, Melbourne.
- ASTM Standard WK486 “New Test Method for Traction Characteristics of the Athletic Shoe-Sports Surface Interface”
ASTM International, West Conshohocken, PA,
www.astm.org.
- Baker, S 1991, ‘Rootzone composition and the performance of golf greens. 1. Sward characteristics before and after the first year of simulated wear.’ *Journal of the Sports Turf Research Institute*, vol. 67, pp. 14-23.
- Baker, SW & Canaway, PM 1993, ‘Concepts of Playing Quality: Criteria and Measurement’, *International Turfgrass Society Research Journal*, vol. 7, pp. 172-81.
- Bell, MJ & Homes, G 1988, ‘Playing quality standards for level bowling greens.’ *Journal of the Sports Turf Research Institute*, vol. 64, pp. 48-62.
- BS 7044 : Section 2.2. (1990). *Artificial Sports Surfaces. Part 2. Methods of Test. Section 2.2, Methods of Determination of Person/Surface Interaction*. British Standards Institution, London, 8 pp.
- Campbell, JB 2002, *Introduction to Remote Sensing*, Third edn, Taylor & Francis, London
- Canaway, PM 1986, ‘Visual and objective methods of ground cover estimation in turfgrass trials.’ *Journal of the Sports Turf Research Institute*, vol. 62, pp. 215.
- Canaway, PM & Bell, MJ 1986, ‘An Apparatus for Measuring Traction and Friction on Natural and Artificial Surfaces’, *Journal of the Sports Turf Research Institute*, vol. 62, pp. 211-4.
- Cooper, WED 1978, *Electronic Instrumentation and Measurement Techniques*, Second edn, Prentice – Hall International.

- DPI 2004, *Constructing, maintaining and monitoring the condition of non-elite sports fields – a review*, Queensland Department of Primary Industries & Fisheries, Brisbane.
- Dunn, J, Minner, D, Fresenburg, B & Bughrara, S 1994, 'Bermudagrass and Cool-Season Turfgrass Mixtures: Response to Simulated Traffic', *Agronomy Journal*, vol. 86, pp. 10-6.
- Ekstrand, J 1982, 'Soccer injuries and their prevention.' University Medical Dissertation No. 130 thesis, Linkeeping, Sweden.
- Floyd, T 1982, *Digital Fundamentals*, 2 edn, Charles E. Merrill Publishing Company, Columbus.
- Henderson, C, Cooper, L, Bransgrove, K Finlay, G, Jeffrey, N, Power, N, Raine, S & Eberhard, J 2004, *Best management practices for sustainable and safe playing surface of Australian Football League sports fields*, Final Report, Department of Primary Industries and Fisheries, Brisbane.
- Henderson, C, Cooper, L, Bransgrove, K Finlay, G, Jeffrey, N, Power, N, Raine, S & Eberhard, J 2007, *Best management practices for sustainable and safe playing surface of Australian Football League sports fields.*, TU02007, Horticulture Australia Limited (HAL), Brisbane.
- Holmes, G & Bell, M 1986, 'A pilot study of the playing quality of football pitches', *Journal of the Sports Turf Research Institute*, vol 62, pp. 74-91.
- International Standard Organization (ISO), May 2003. Ergonomics – Manual handling. Part 1: Lifting and carrying. ISO 11228-1.
- Loch, D 2003, *Report for Sport and Recreation Queensland on Turfgrass and Light Studies*, Department of Primary Industries & Fisheries, Brisbane.
- Low, J & Reed, A 1996, *Basic biomechanics explained*, Butterworth – Heinemann Ltd.
- Martini, FH 1989, *Fundamentals of Anatomy & Physiology*, Fourth edn, Prentice Hall International.
- McCutchen, WH 2002, Coefficient of Restitution, viewed 21 April 2007, <http://www.racquetresearch.com/coeffici.htm>.

- McNitt, AS 2004, Email from Andrew McNitt. asm4@psu.edu, 24 July 2004.
- McNitt, AS & Petrunak, D 2003, *Evaluation of Playing Surface Characteristics of Various In-Filled Systems*, <http://cropsoil.psu.edu/mcnitt/Infill6.html>.
- McNitt, AS, Waddington, DV & Middour, RO 1996, 'Traction Measurement on Natural Turf', *Safety in American Football*.
- McNitt, AS, Middour, RO & Waddington, DV 1997, 'Development and Evaluation of a Method to Measure Traction on Turfgrass Surfaces', *Journal of Testing and Evaluation*, vol. 25, no. 1, pp. 99-107.
- Mital, A., Nicholson, A.S., and Ayoub, M.M. A guide to manual materials handling (MMH). Second Edition. Taylor & Francis. 1997.
- Mooney, SJ & Baker, SW 2000, 'The effects of grass cutting height and pre-match rolling and watering on football pitch ground cover and playing quality.' *Journal of Turfgrass Science*, vol. 76, pp. 70-7.
- Nigg, B & Yeadon, M 1987, 'Biomechanical aspects of playing surfaces', *Journal of Sports Sciences*, vol. 1, no. 5, pp. 1-20.
- Orchard, J 2002, 'Is there a relationship between ground and climatic conditions and injuries in football?' *Sports Medicine*, vol. 32, no. 7, pp. 419-32.
- Orchard, J 2003, 'The AFL injury report 2002', *Journal of Science and Medicine in Sport*, vol. 6, no. 2, pp. 237-.
- Orchard, J, Seward, H & AFLMOA 2002, *AFL Injury Report 2002*.
- Orchard, J, Seward, H, McGivern, J & Hood, S 1999, 'Rainfall evaporation and the risk of non-contact anterior cruciate ligament injury in the Australian football League', *Medical Journal of Australia*, vol. 170, no. 7, pp. 304-6.
- Orchard, JW & Finch, CF 2002, 'Australia needs to follow New Zealand's lead on sports injuries', *Medical Journal of Australia*, vol. 177, no. 1, pp. 38-9.

- Rogers, J & Waddington, DV 1989, 'The effect of cutting height and verdure on impact absorption and traction characteristics in tall fescue turf', *Journal of the Sports Turf Research Institute*, vol. 65, pp. 80-90.
- Water, TR, Putz-Anderson, V, Garg, A, and Fine, LJ 1993, Revised NIOSH equation for the design and evaluation of manual lifting tasks. *Ergonomics*, 36 (7), 749-776
- Wobschall, D 1987, *Circuit Design for Electronic Instrumentation: Analog and Digital Devices from Sensor to Display*, Second edn, McGraw-Hill Inc.

Appendix A

Borland C++ program for data presentation, storage and analysis:

```
//-----  
  
#include <vcl.h>  
#pragma hdrstop  
  
#include "traction.h"  
  
#include <math.h>  
  
#include <vector>  
using namespace std;  
  
//-----  
  
#pragma package(smart_init)  
#pragma link "VaClasses"  
#pragma link "VaComm"  
#pragma resource "*.dfm"  
TForm1 *Form1;  
  
//-----  
  
__fastcall TForm1::TForm1(TComponent* Owner)  
: TForm(Owner)  
{  
    fileNameString =  
        currentTime.FormatString("ddmmhhnn").c_str();  
    fileNameString += "_turf.csv";  
    DisplayFile->Caption = "Output File: " +  
        fileNameString;  
    Timer1->Enabled = true;  
}  
  
//-----
```

```

void __fastcall
    TForm1::ChangeFileNameButtonClick(TObject
        *Sender)
    {
        if(!OpenDialog1->Execute()) return;
        fileNameString = OpenDialog1->FileName;
        DisplayFile->Caption = "Output File: " +
            fileNameString;
    }

//-----

void __fastcall
    TForm1::ChangeCommsConfigClick(TObject
        *Sender)
    {
        FormComms->ShowModal();
    }

//-----

void __fastcall TForm1::ExitButtonClick(TObject
    *Sender)
    {
        VaComm1->Close();
        Close();
    }

//-----

void __fastcall TForm1::Timer1Timer(TObject
    *Sender)
    {
        if(Buffer.Length() == BuffLen && BuffLen)
            {
                ProcessBuffer();
                Buffer = "";
                BuffLen = 0;
            }
        else BuffLen = Buffer.Length();
    }

//-----

```

```

void __fastcall TForm1::ProcessBuffer(void)
{
    Buffer =
        StringReplace(Buffer, "\x03\x02", ",", TReplaceFlags() << rfReplaceAll);
    Buffer = StringReplace(Buffer, "
", "", TReplaceFlags() << rfReplaceAll);
    TStringList *run = new TStringList;
    run->CommaText = Buffer;
    Buffer = Now();
    vector <float> data;
    for(int i=0;i < run->Count;i++)
    {
        double f = fabs(atof(run->Strings[i].c_str()));
        data.push_back(f);
        Buffer = Buffer + "," + String(f);
    }
    delete run;

    float maximum = 0;
    unsigned maxIndx = 0;
    for(unsigned i=0;i < data.size();i++)
    {
        if(data[i] > maximum)
        {
            maximum = data[i];
            maxIndx = i;
        }
    }
    unsigned minIndx;
    for(unsigned i=maxIndx;i > 1;i--)
    {
        if((data[i] < data[i-1] || data[i] == 0) &&
        data[i] < 5)
        {
            minIndx = i;
            data[i] = 0;
            break;
        }
    }
    Chart->Series[0]->Clear();

    for(unsigned i=minIndx;i < maxIndx + 20;i++)

```

```

        Chart->Series[0]->AddXY(150.0/(data.size() -
minIndx) * (i-minIndx),data[i]);

MaxLabel->Caption = "Maximum Value = " +
    FormatFloat("#.00",data[maxIndx]) + " Nm";
AngleLabel->Caption = "Rotation Angle = " +
    FormatFloat("#.00",150.0/(data.size() -
minIndx) * (maxIndx - minIndx)) + " Deg";
Analysis = FormatFloat("#.00",data[maxIndx]) +
    "," +
    FormatFloat("#.00",150.0/(data.size() -
minIndx) * (maxIndx - minIndx));
TimeLabel->Caption = "Test Time ";
TimeLabel->Caption +=
    currentTime.FormatString("ddmmhhnn").c_str();
if(data[maxIndx] > 90) Beep();
Memo->Lines->Add(Buffer);
Memo->Lines->Add(Analysis);
Memo->Lines->SaveToFile(fileNameString);
}

//-----

void __fastcall TForm1::ReceiveCharacters(TObject
*Sender, int Count)
{
    Buffer = Buffer + VaComm1->ReadText();
}

//-----

```

Appendix B

Load Cell Specifications: (reproduced from information supplied by Scale Components Pty. Ltd.)

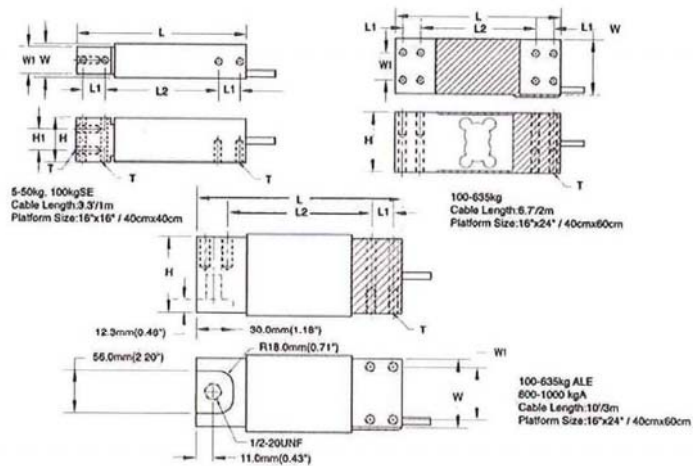
Table B1. Specifications for Load Cell

Standard Capacity	5, 7, 10, 15, 20, 30, 50, 100SE, 100, 100ALE, 150, 150ALE, 250 250ALE, 300, 300ALE, 500, 500ALE, 635, 635ALE, 800A, 1000A *1		
Recommended Excitation	10 V AC/DC	Compensated Temp. Range	-10°C to +40°C
Maximum Excitation	15 V AC/DC	Operating Temp. Range	-20°C to +60°C
Output at Rated Load	2 mV/V±10%	Zero Balance	±3%
Combined Error	0.025%	Input Resistance	410±10Ω
Non Repeatability	0.02%	Output Resistance	350± 3Ω
Creep (20 minutes)	0.03%	Insulation Resistance (50VDC)	>5000 MΩ
Zero Return (20 minutes)	0.03%	Deflection at Rated Load	<1mm
Temp. Effect/10°C on Span	0.015%	Safe Overload	150%
Temp. Effect/10°C on Zero	0.026%	Ultimate Overload	200%

*1: SE: Small Envelope. LE: Large Envelope. A: American Standard Thread.

Table B2. Dimensions of Load Cell

Dimensions



Capacity		L	L1	L2	W	W1	H	H1	T
5/ 7/ 10/ 15/ 20/ 30/ 50/ 100SE	(mm)	150.0	19.0	100.0	30.0	24.0	39.5	19.0	M6x1.0
	(inch)	5.91	0.75	3.94	1.18	0.94	1.56	0.75	
100/ 150/ 250/ 300/ 500/ 635	(mm)	174.0	19.0	122.0	60.0	30.0	65.0	---	M8x1.25
	(inch)	6.85	0.75	4.80	2.36	1.18	2.56	---	
100ALE/ 150ALE/ 250ALE/ 300ALE/ 500ALE/ 635ALE/ 800A/ 1000A	(mm)	191.0	25.0	125.0	76.2	60.0	75.0	---	5/16- 18UNC
	(inch)	7.52	0.98	4.92	3.00	2.36	2.95	---	

Appendix C

Ranger 2100 Specifications: (reproduced from
<http://www.australiascales.com.au/files/2100-700-150.pdf>)

Table C1. Specifications for Ranger 2100 Digital Indicator

PERFORMANCE	
Approvals	NSC and OIML Approved for 6,000 divisions @ 1.0 μ V per division, C-Tick and CE.
Display	Backlit alphanumeric LCD with six 27mm high digits
Backlight	LED backlight with adjustable brightness
Display resolution	Up to 30,000 divisions, minimum of 0.25 μ V/division
Count-by	1, 2, 5, 10, 20, 50, 100
Zero cancellation	+ / - 2.0mV/V
Span adjustment	0.1mV/V to 3.0mV/V full scale
Stability/Drift	Zero: < 0.1 μ V/ $^{\circ}$ C, Span < 10ppm/ $^{\circ}$ C, Linearity < 20ppm, Noise < 0.05 μ V p-p
Operating Environment	Temperature -10 to +50 $^{\circ}$ C, Humidity < 90% non condensing
DIGITAL	
Setup and calibration.	Full digital with visual prompting in plain messages
Memory retention	Full non-volatile operation
Digital filter	Averaging from 1 to 100 consecutive readings
Zero range	Adjustable from +/- 2% to +/-20% of full capacity
A/D CONVERTER	
Type	24 bit Sigma Delta
Resolution	8,388,608 internal counts.
A/D Sync Filter	Fixed 25Hz, FIR filter > 80dB
LOAD CELLS	
Excitation	8 volts for up to 8 x 350 ohm load cells (6 wire + shield)
SERIAL COMMS (Software Option 0224)	
Serial output	Single RS-232 with 15kV static protection. Data can be configured for automatic transmit, network or printer drive
POWER INPUT	
Standard	2100 12VDC (500mA+ depending on load cells and backlight)
Variants	2100/S 2100 fitted with 0329 stainless steel housing
	2100/DC 2100 fitted with 12-24VDC power input and 0329 s/s housing
	2100/AC 2100 fitted with 110-240VAC power input and 0329 s/s housing
	2100/B 2100 fitted with a re-chargeable 12 Volt battery and 0329 s/s housing
	2100/EX 2100/EX for hazardous areas
DIMENSIONS	
Body size	189mm (L) x 99 mm (H) x 23 mm (D)
Panel cutout	Flush mounted with cable holes drilled separately (template provided)
FEATURES	
Standard Features	Five point linearity correction and assignable function key for operator use
	Totalising, counting, hold/peak-hold, live-weight, intelligent batching software
	3 remote inputs and lb/kg switching fitted as standard
	Battery backed clock and calendar fitted as standard
OPTIONS	
Software Options	0224 RS-232 serial output and 0225 3 O/C outputs with check-weighing software
Hardware	Panel mounts, desk/wall brackets, plug packs, output modules, etc are available

Appendix D

Ranger 2100 Calibration Procedure: (reproduced from Rinstrum - 2100 Digital Indicator Reference Manual Rev 2.6)

9. Calibration

The calibration of the 2100 indicator is fully digital. The calibration results are stored in permanent memory for use each time the unit is powered up.

Note: Some of the digital setup steps can affect calibration. The BUILD and OPTIONS settings MUST be configured before calibration is attempted.

To perform a calibration, when in Full Setup select the CAL Group using the <GRP> key.

The calibration programme will automatically prevent the 2100 from being calibrated into an application outside of its specification. If an attempt is made to calibrate the 2100 outside of the permitted range, an error message will display and the calibration will be abandoned. Refer to Error Messages page 59.

The 2100 has a wide-range amplifier. The non-trade calibration range of the instrument extends well beyond the Trade approved range.

Note: It should not be assumed that just because the 2100 has successfully calibrated a scale, that the scale is correct for trade use. Always check the scale build against the approval specification.

9.1. Performing a Digital Calibration with Test Weights

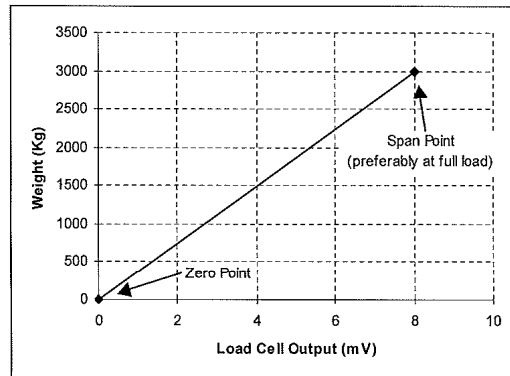


Figure 10: Chart - Zero and Span Points to Interpolate Weight from Load Cell

The Zero setting (CAL: ZERO) specifies a gross zero point for the scale. The Span setting (CAL: SPAN) specifies a second point (preferably close to full scale) used to convert the A/D readings into weighing units (eg. kg). Select either of the Zero (CAL: ZERO) or Span (CAL: SPAN) calibration items. It is important that an initial Zero calibration is performed before any SPAN calibrations. The chart shown here demonstrates how the 2100 uses the zero and span points to interpolate a weight reading from the load cell reading.

Note: Calibration points (Zero, Span and Linearisation) must be spaced by at least 2% of full scale from each other.

To perform a linearisation, a calibration of the zero and span points must have been performed. Both the zero and full scale calibration points are used in the linearisation of the scale base. These two points are assumed to be accurately set and thus have no linearisation error.

A maximum of five linearisation points can be set independently between zero and full scale. Unused or unwanted points may also be cleared. The maximum correction that can be applied using a linearisation point is + / - 2%.

9.2.1. ED.LIN (Edit Linearisation Points)

<ul style="list-style-type: none"> • Press the <OK> key to view the list of linearisation points currently in use.
<ul style="list-style-type: none"> • Press the <SEL> key to step through the list of points. Each point is shown as Ln.ppp where n is the point number (1 to 5), and ppp is the approximate percentage of full scale where the linearisation is applied. For example, L1.050 indicates that linearisation point one is active and was entered at about 50% of full scale. Unused linearisation points are shown with a row of dashes (eg. L2. ---).
<ul style="list-style-type: none"> • Press <OK> to change the linearisation point selected or press <ITM> to exit without making any changes.
<ul style="list-style-type: none"> • After pressing <OK>, the current weight reading is displayed. Add the calibration test mass to the scale. The closer the test mass is to the point of maximum error in linearity the more effective will be the correction. Press <OK> to enter a corrected weight value for this point or <ITM> to exit without making changes.
<ul style="list-style-type: none"> • Use the <SEL> and <EDT> keys to enter the correct value of the calibration weight being used.
<ul style="list-style-type: none"> • Press the <OK> key to trigger the Linearisation routine. When the process is complete the display will show the weight to allow the new weight reading to be checked before returning to the menus. Press <ITM> to leave the routine or <OK> to repeat the operation.

9.2.2. CLR.LIN (Clear Linearisation)

<ul style="list-style-type: none"> • Press the <OK> key to view the list of linearisation points currently in use.
<ul style="list-style-type: none"> • Press the <SEL> key to step through the list of points. Each point is shown as Ln.ppp where n is the point number (1 to 5), and ppp is the approximate percentage of full scale where the linearisation is applied.
<ul style="list-style-type: none"> • For example, L1.050 designates that linearisation point one is active and was entered at about 50% of full scale. Unused linearisation points are shown with a row of dashes (eg. L2. ---).
<ul style="list-style-type: none"> • Press <OK> to clear the linearisation point selected or press <ITM> to exit without making any changes.
<ul style="list-style-type: none"> • Once <OK> has been pressed, the linearisation point will be cleared, and the display will return to CLR.LIN.

Note: All linearisation points are cleared by restoring the default calibration of the instrument. The zero and span settings are also cleared by this process.

To perform a linearisation, a calibration of the zero and span points must have been performed. Both the zero and full scale calibration points are used in the linearisation of the scale base. These two points are assumed to be accurately set and thus have no linearisation error.

A maximum of five linearisation points can be set independently between zero and full scale. Unused or unwanted points may also be cleared. The maximum correction that can be applied using a linearisation point is + / - 2%.

9.2.1. ED.LIN (Edit Linearisation Points)

<ul style="list-style-type: none"> • Press the <OK> key to view the list of linearisation points currently in use.
<ul style="list-style-type: none"> • Press the <SEL> key to step through the list of points. Each point is shown as Ln.ppp where n is the point number (1 to 5), and ppp is the approximate percentage of full scale where the linearisation is applied. For example, L1.050 indicates that linearisation point one is active and was entered at about 50% of full scale. Unused linearisation points are shown with a row of dashes (eg. L2. - - -).
<ul style="list-style-type: none"> • Press <OK> to change the linearisation point selected or press <ITM> to exit without making any changes.
<ul style="list-style-type: none"> • After pressing <OK>, the current weight reading is displayed. Add the calibration test mass to the scale. The closer the test mass is to the point of maximum error in linearity the more effective will be the correction. Press <OK> to enter a corrected weight value for this point or <ITM> to exit without making changes.
<ul style="list-style-type: none"> • Use the <SEL> and <EDT> keys to enter the correct value of the calibration weight being used.
<ul style="list-style-type: none"> • Press the <OK> key to trigger the Linearisation routine. When the process is complete the display will show the weight to allow the new weight reading to be checked before returning to the menus. Press <ITM> to leave the routine or <OK> to repeat the operation.

9.2.2. CLR.LIN (Clear Linearisation)

<ul style="list-style-type: none"> • Press the <OK> key to view the list of linearisation points currently in use.
<ul style="list-style-type: none"> • Press the <SEL> key to step through the list of points. Each point is shown as Ln.ppp where n is the point number (1 to 5), and ppp is the approximate percentage of full scale where the linearisation is applied.
<ul style="list-style-type: none"> • For example, L1.050 designates that linearisation point one is active and was entered at about 50% of full scale. Unused linearisation points are shown with a row of dashes (eg. L2. ---).
<ul style="list-style-type: none"> • Press <OK> to clear the linearisation point selected or press <ITM> to exit without making any changes.
<ul style="list-style-type: none"> • Once <OK> has been pressed, the linearisation point will be cleared, and the display will return to CLR.LIN.

Note: All linearisation points are cleared by restoring the default calibration of the instrument. The zero and span settings are also cleared by this process.